Aussois, 2015

Hydraulic fracture

B.A. Schrefler

Thanks to E. Milanese, J.F. Molinari, P. Rizzato, J.M.R. Huyghe, S. Secchi, L. Simoni

Department of Civil, Environmental and Architectural Engineering, University of Padova
International Center for Mechanical Sciences CISM, Udine

Layout

- Peculiarities of fracturing in saturated porous media and physical evidence
- Meso-mechanical investigations (work in progress)
- SGFEM with space and time adaptivity
- XFEM Peel test and hydraulic fracturing
- Conclusions

Introduction

Mechanical fracture

Fracture lips are stress free

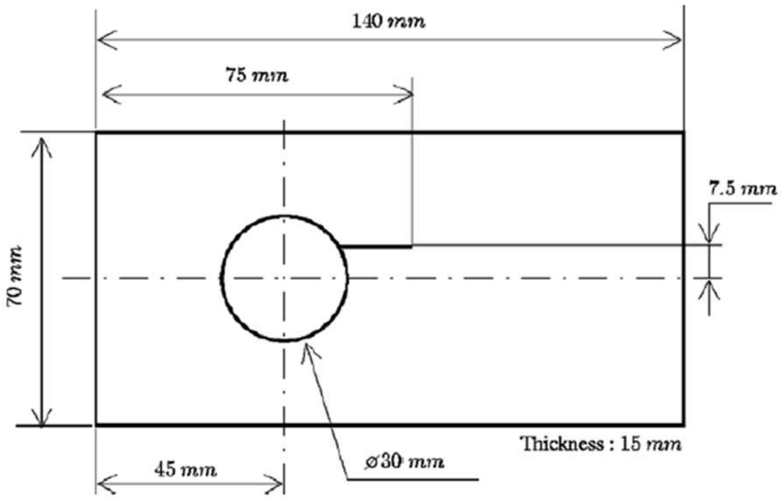

Fig. 8. Geometry of the PMMA specimen tested.

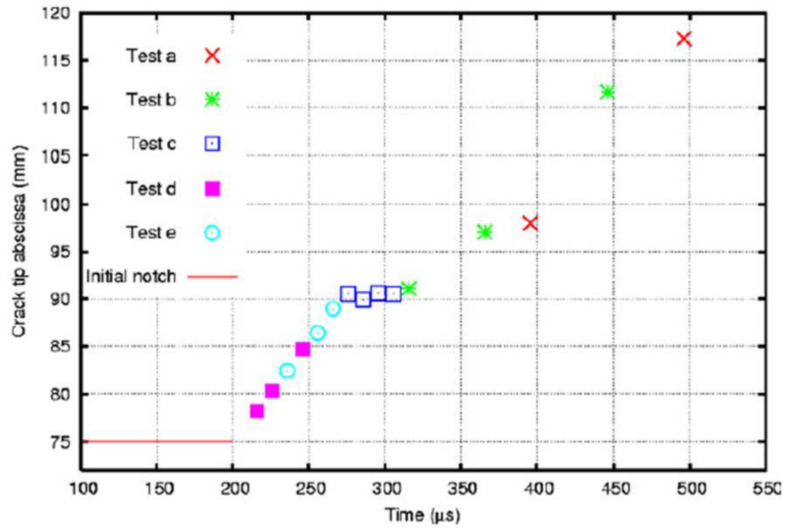

Fig. 9. Experimental horizontal crack propagation history.

In solid mechanics crack propagation is addressed but time comes into play mainly for dynamic fracturing;

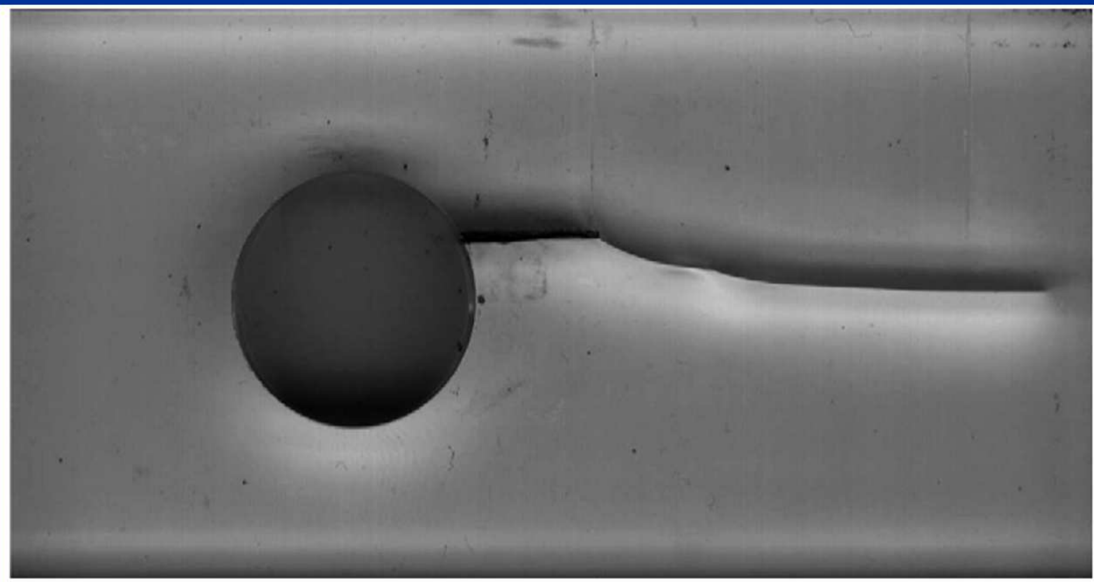

Fig. 10. The experimental crack's final path.

COHESIVE FRACTURE IN A THERMOELASTIC MEDIUM

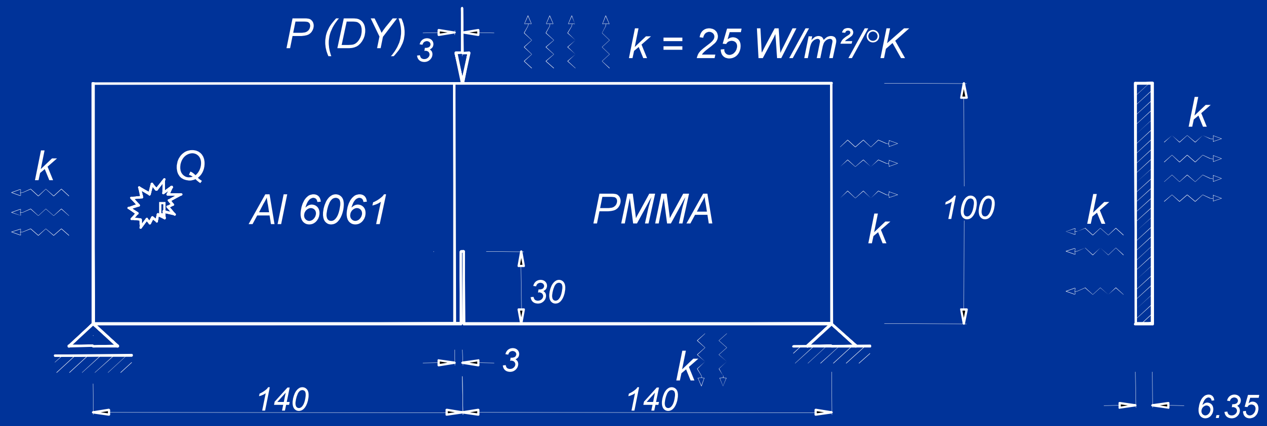

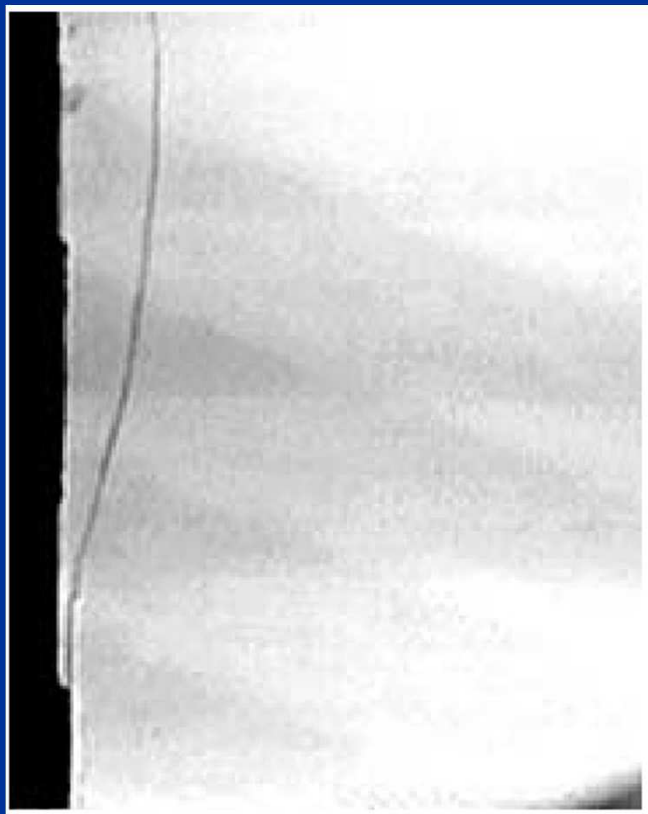

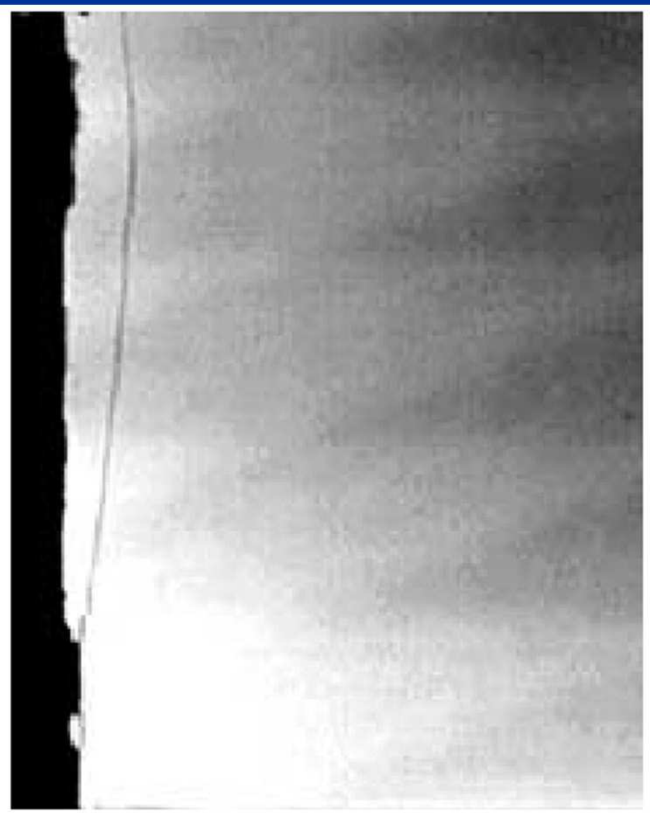

Hydraulic fracture

- Fracture lips in presence of fluids in the fracture and in the domain are not stress free
- Interaction between crack tip advancement speed and fluid velocity (crack and domain); time matters

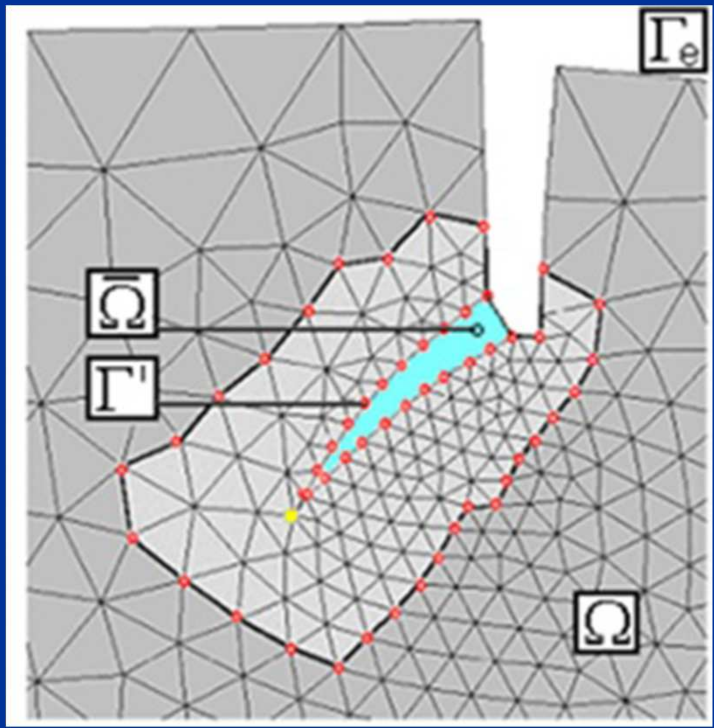

Fracture propagation in saturated porous media

Stepwise advancement and pressure fluctuations also at macroscopic level
experimental evidence

Experimental evidence : fracking

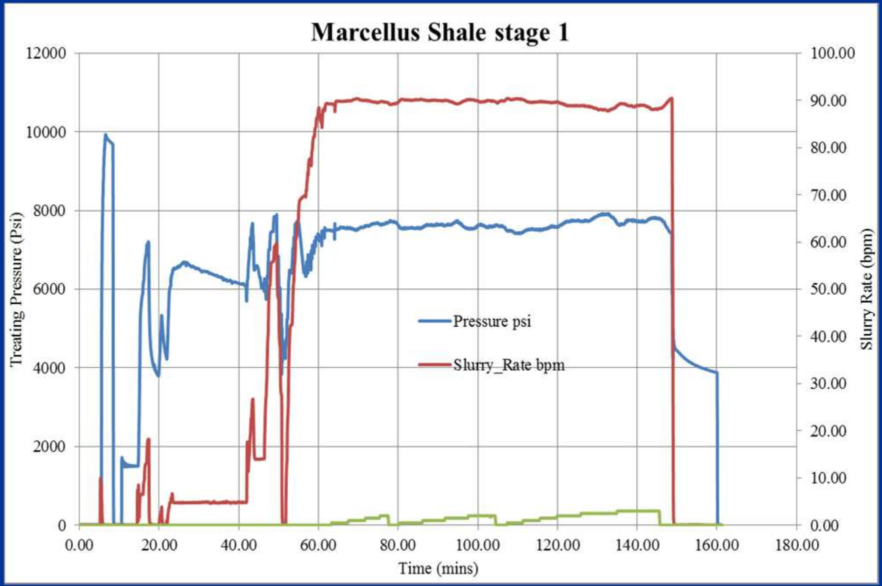

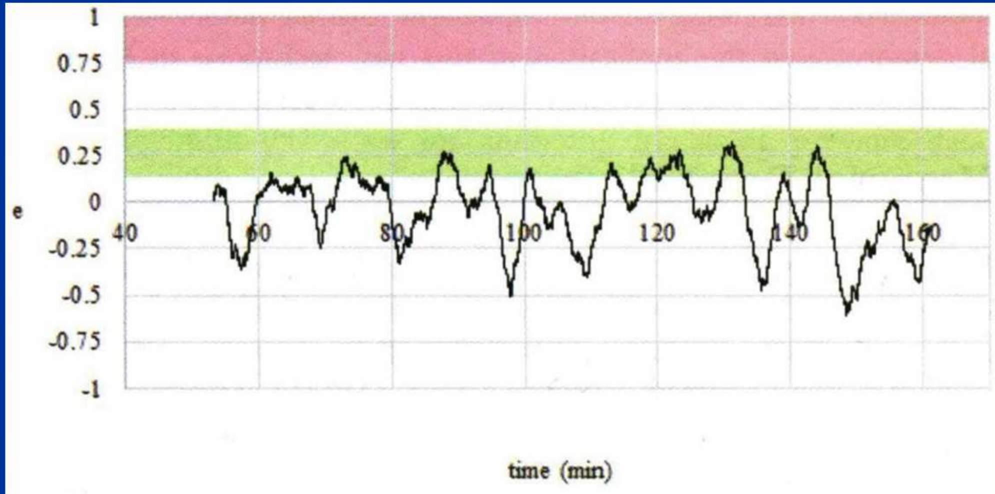

Figure 2. Fracture Growth Exponent Plot for Stage 1 of Marcellus Shale Case

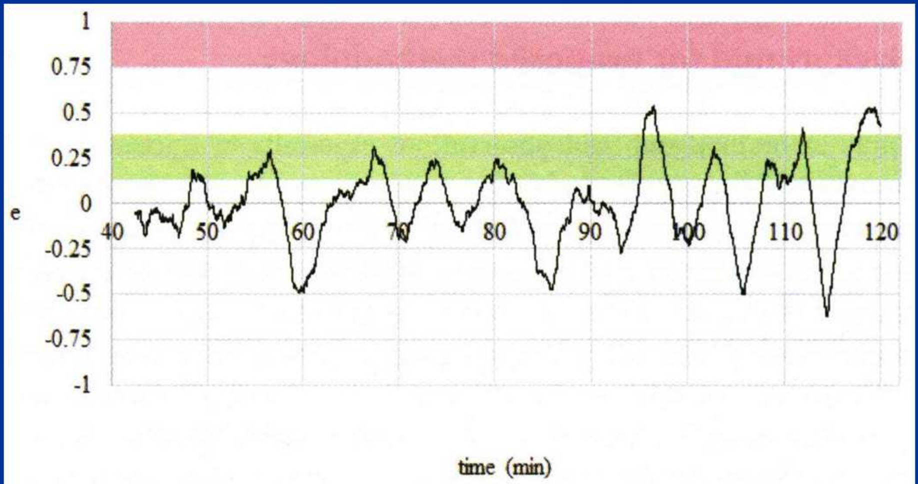

Figure 3. Pressure-Time Data for Stage 2 of Marcellus Shale Case

Intermittent advancement at constant injection rate

Soliman et al , 2014

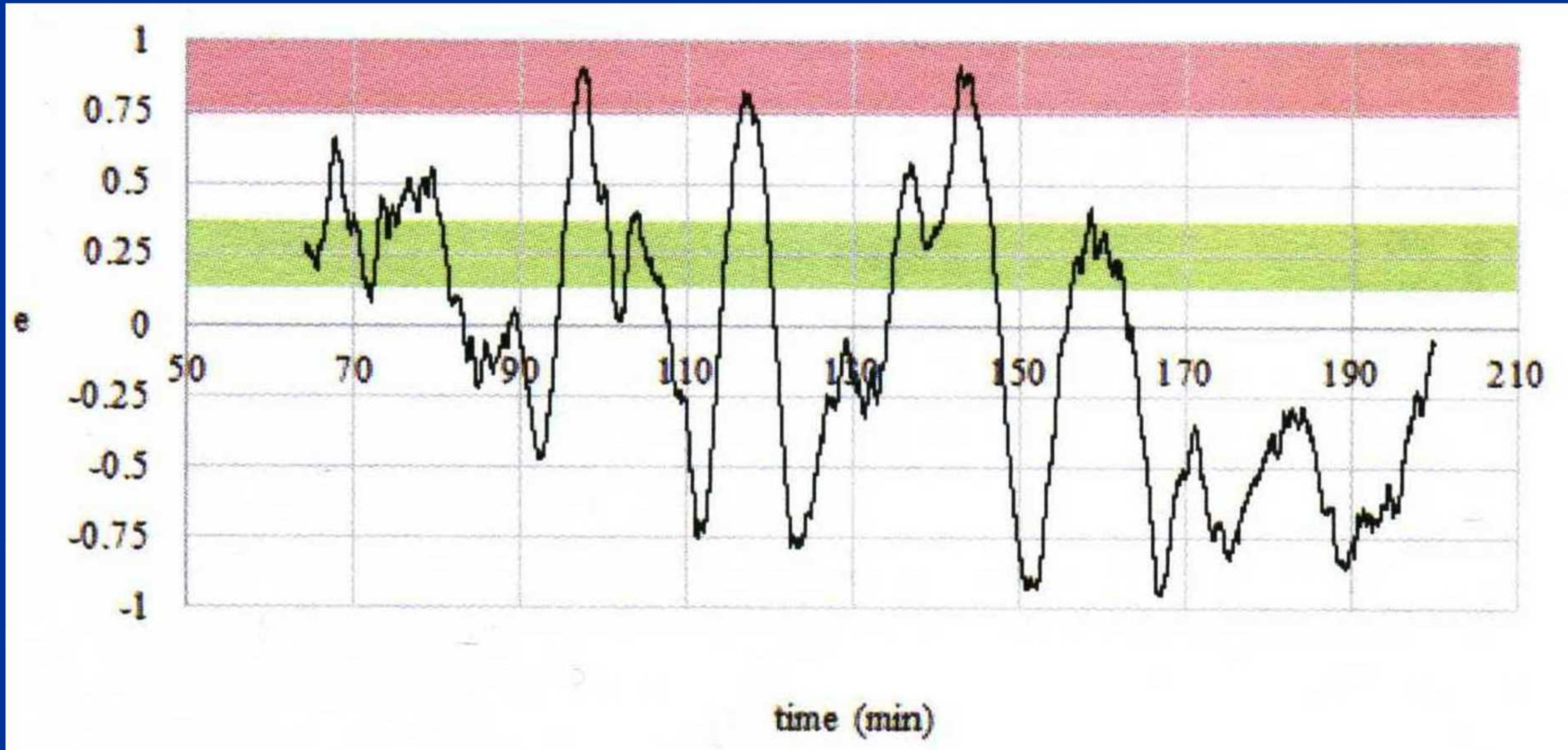

Eagle Ford

*"Identifying these alternating **periods of dilation and growth in length** would help to diagnose problems and identify potential sand-out very early in the treatment."*

Soliman et al , 2014

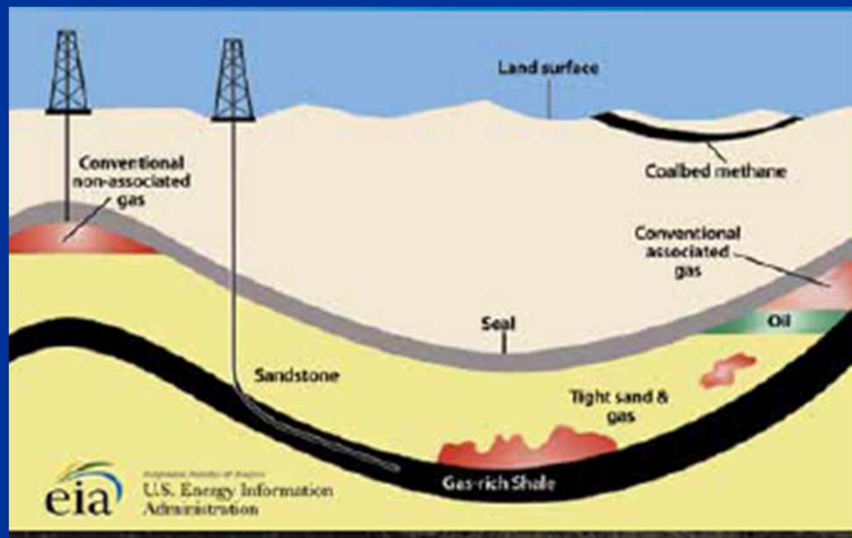

Explanation for the behaviour put forward

$$p(t) = \alpha t^{e}$$

Perking-Kern (1961), Nolte-Smith (1981)

*Crack width is essentially controlled by **fluid pressure drop** in the fracture. Hence, **wellbore pressure fluctuations** demonstrate fracture **intermittent advancing.***

*"**e**" represents at the same time the exponent of the time pressure profile and the fracture growth.*
- negative e: there is a large decrease of pressure corresponding to the well crossing permeable and fractured formations;
- e in the range of 0.13-0.30 crack propagation (green zone in Figure)
- e in the range of 0.75-1.0 crack screening off, i.e. tip arrest, among other (pink zone in the figures).

*The minor fluctuations are linked to intermittent advancement due to "**mini-periods of propagation intermingled with periods of dilation**"*

Soliman et al , 2014

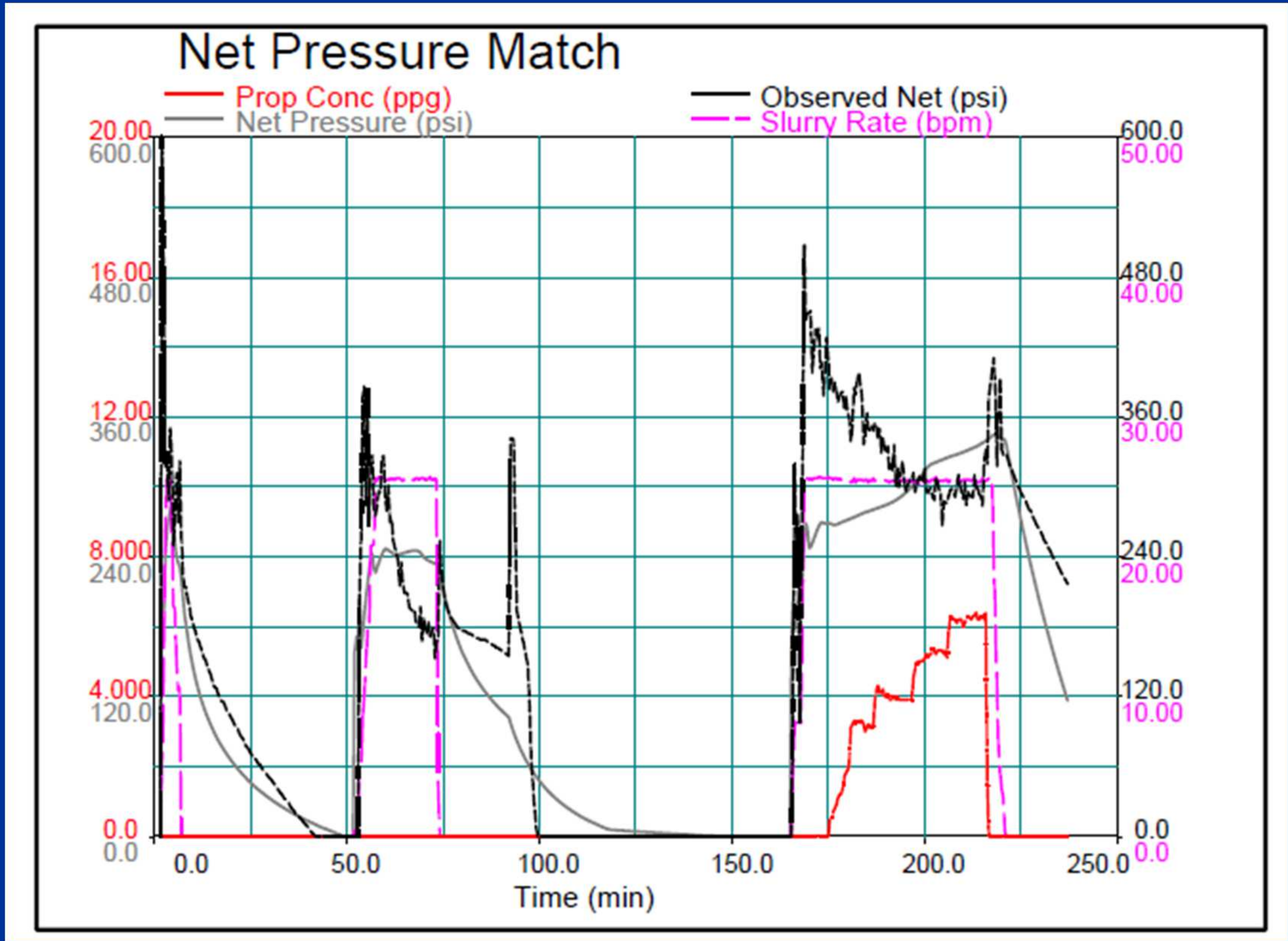

Figure 16: Net pressure match for a treatment in coal that showed very strong containment from mapping with an aspect ratio of 20. The observed net pressure (from wellhead data) is seen to be falling while pumping clean fluid.

C.J. de Pater, SPE, 2015

Experimental evidence : mechanical load

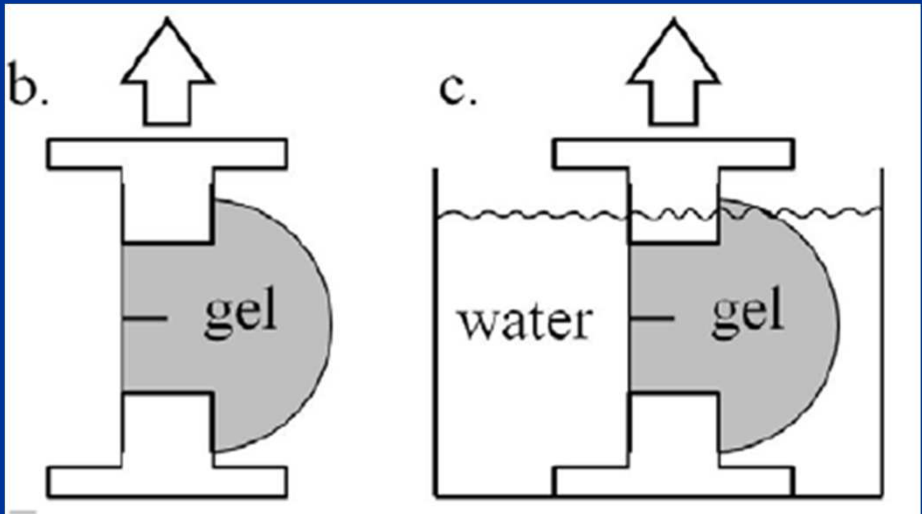

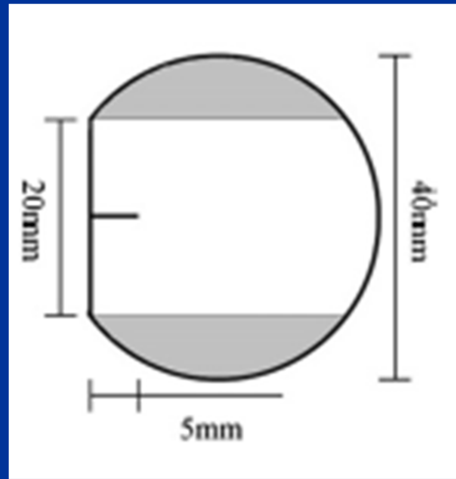

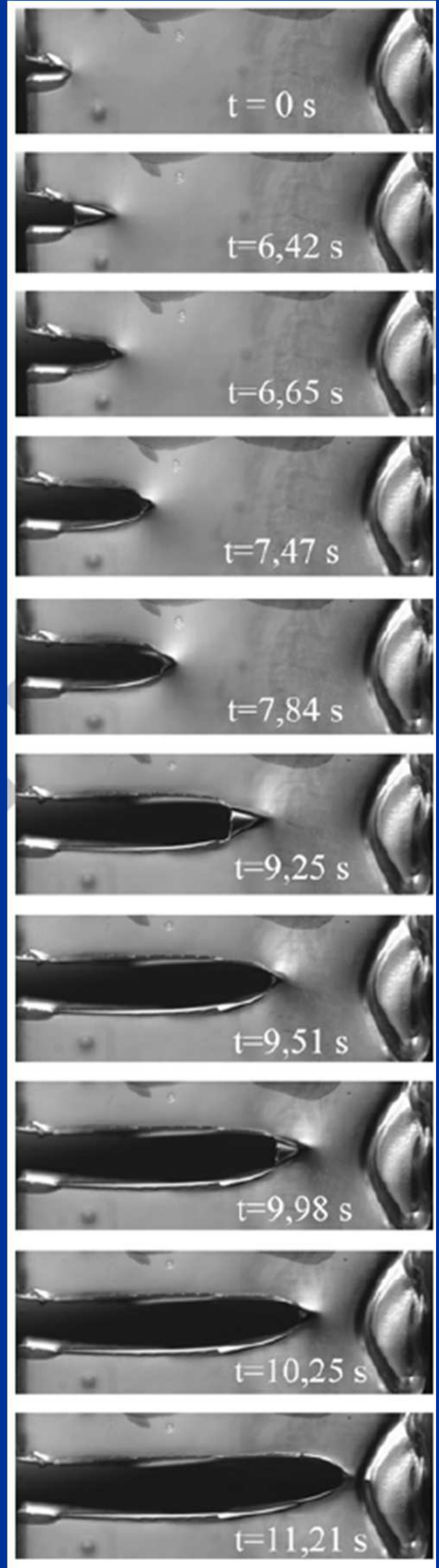

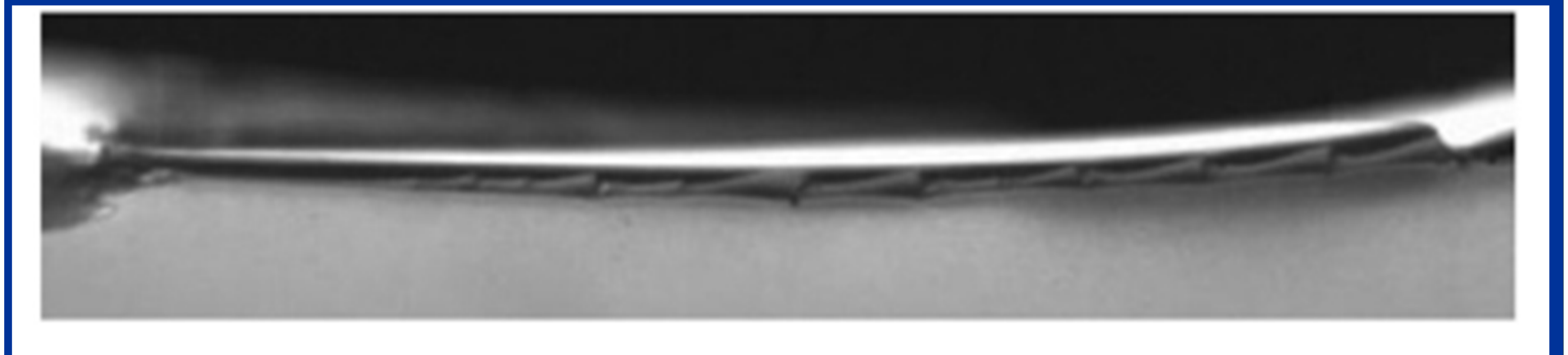

Saturated hydrogel immersed in water:
stepwise crack advancement

Pizzocolo, Huyghe , Ito, JFM 2012

Explanation for the behaviour put forward

Based on the fact that the pause duration ΔT between advancements, the length of the advancement steps Δx, the stiffness of the medium E and the hydraulic permeability k were approximately related by the ***consolidation*** *formula of Terzaghi and Peck (1967) the authors "predicted a tri-axial stress state at the crack tip of a Mode I crack. The stress state was first carried by the fluid, which resulted in* ***reduced pressure*** *and attraction of fluid towards the crack tip. The most conductive source of fluid to feed this stream is the fluid residing in the crack itself. Hence fluid was sucked from the crack into the crack tip, resulting in progressive transfer of the tensile stress from the fluid to the effective stress of the solid. As this happens, the yield strength of the solid is exceeded resulting in further propagation of the crack".*

Pizzocolo, Huyghe , Ito, JFM 2012

Meso-scale analysis
Disordered media

Tzschichholz and Herrmann (1995)

2D beam homogeneous and heterogeneous lattice model

- *Impermeable fracture, constant injection rate*
- *Drop of pressure in time and oscillations on short time scales.*
- *Linear pressure increase in the time intervals of quiescence (due to loading procedure)*

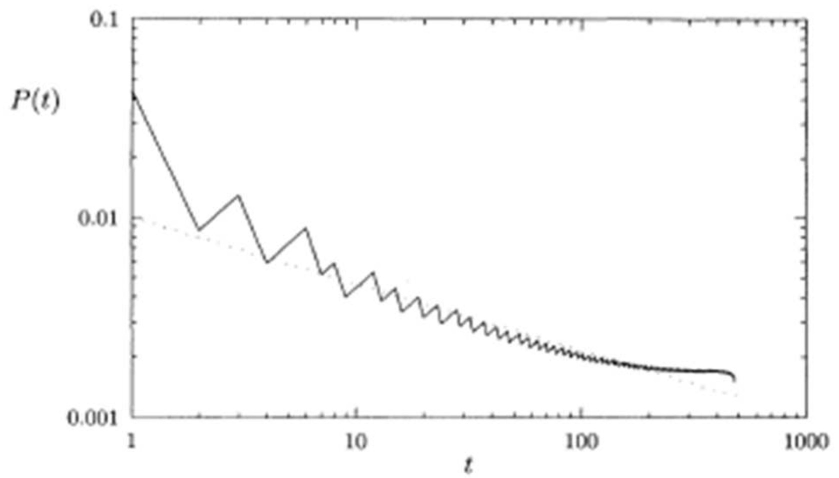

FIG. 1. Log-log plot of the pressure P inside the crack versus time t for homogeneous cohesion ($r \to +\infty$) of strength $\langle f_{coh} \rangle = 0.01$. Points at subsequent time steps are connected by straight lines. The dotted line corresponds to a slope of $-1/3$ as predicted by continuum mechanics. The linear lattice size is $L = 150$.

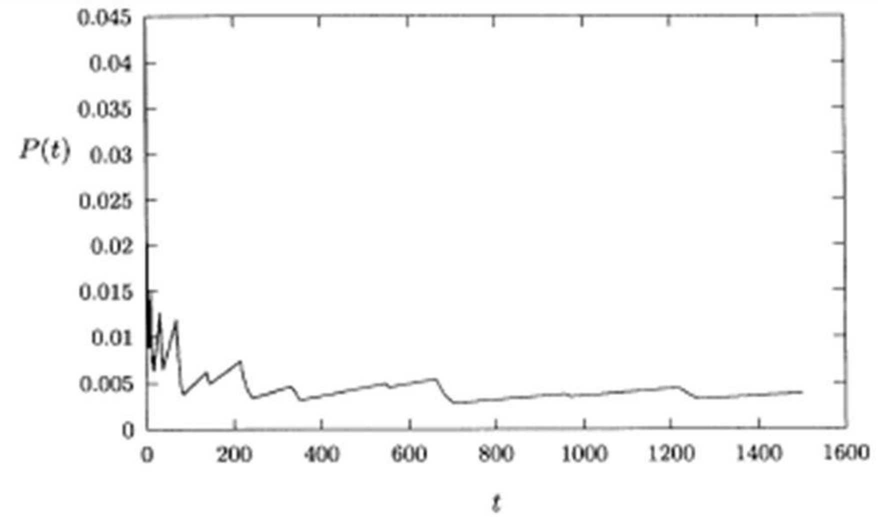

FIG. 7. Linear plot of the pressure P inside the crack versus time t. The pressure was obtained from the simulation corresponding to Fig. 5.

- *Discontinuous breaking process in time with* ***temporal clustering*** *of the breaking events : "bursts" .*

- *Bursts* ***unevenly distributed in time****, relatively often for small times and rarer later – avalanche behaviour*

- *Resemblance with* ***magnitude records of earthquakes*** *or acoustic emission records from laboratory experiments.*

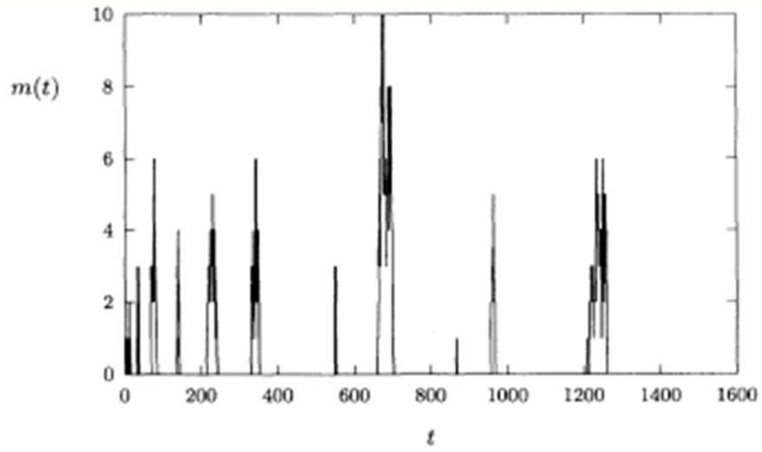

FIG. 5. Record of the breaking sequence in time corresponding to the crack displayed in Fig. 3. In this plot we have defined the magnitude $m(t)$ as the number of simultanously broken beams at a given unit time interval. The simulation stopped after 1500 time steps. Note the temporal clustering of breaking events and the large time intervals of quiescence.

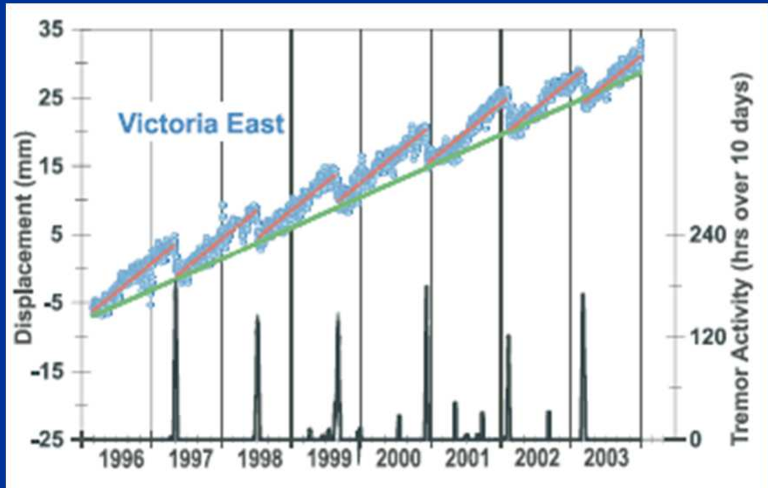

SLOW SLIP EVENTS AND SEISMIC TREMOR AT CIRCUM-PACIFIC SUBDUCTION ZONES

Assumptions

- *Pressure distribution acts perpendicular along the entire inner crack surface and is spatially constant.*
- *Crack opening volume V, corresponds to the total amount of injected incompressible fluid*
  $V(t) = \Delta V t, \quad \Delta V = const.$
- *The "fluid" pressures are calculated from the crack surface displacement field (influence functions)*
- *Only beams along the surface of the inner hole can break. In that way only one single crack is generated.*

- *No results for crack* ***tip advancement***
- ***No flow***

Tzschichholz and Herrmann 1995

Explanation for the behaviour put forward

At the beginning high pressures are needed to push the fluid into the crack. The crack is enlarged and the pressure drops because the enlarged crack can now be opened much more easily than before. The pressure goes down although additional fluid has been added to the crack in the time step. If the pressure drops too much the stresses at the crack tip fall below their cohesion value and the crack can not grow at the next time step. By injecting more fluid into the crack the pressure increases linearly in time until the cohesion forces can be overcome again.

Impermeable fracture

Tzschichholz and Herrmann (1995)

Our model

Consolidation type model (Biot theory, overlapping domains) with the solid phase substituted by a truss lattice of equivalent stiffness (mechanical model)

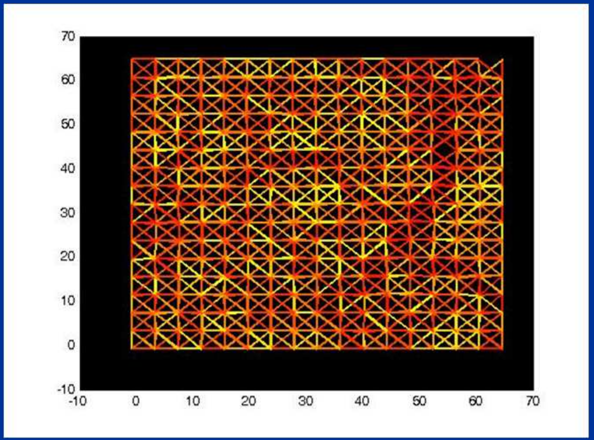

The fluid is incompressible, and follows Darcy's law; «permeable fracture»

E. Milanese, Ed-multifield, Secchi-Schrefler, 2000

$$\begin{bmatrix} \mathbf{0} & \mathbf{0} \\ \tilde{\mathbf{Q}}^{\mathrm{T}} & \mathbf{S} \end{bmatrix} \begin{Bmatrix} \dot{\overline{\mathbf{u}}} \\ \dot{\overline{\mathbf{p}}} \end{Bmatrix} + \begin{bmatrix} \mathbf{K} & -\tilde{\mathbf{Q}} \\ \mathbf{0} & \mathbf{H} \end{bmatrix} \begin{Bmatrix} \overline{\mathbf{u}} \\ \overline{\mathbf{p}} \end{Bmatrix} = \begin{Bmatrix} \mathbf{f}^{(1)} \\ \mathbf{f}^{(2)} \end{Bmatrix}$$

Mechanical Model

Model definition

Bonds parameters:

- Vertical, horizontal and diagonal bonds
- **Isotropic** behavior
- Initial Young modulus: E = 100 Mpa
- After damage: $E^* = (1-D)E$, $D = 0.1$
- Maximum times damaged: 30 ($E^* = 4.24$ MPa)
- Initial threshold: pick among uniform random distribution [0 1] MPa
- After damage new threshold is drawn from a uniform random distr. [0 1]

- **Biaxial tensile strain** driven simulation
- Lattice sizes: **16**/32/(64)
- Lattice side length: 64
- Step increment: 1/5000 (size dependent?)

Enrico Milanese, 2014

Validation: Consolidation test

- Sample: 700m high, 200mm wide
- Coupled mesh: plane elements with 9 nodes for displacements, 4 nodes for pressure
- Stiffness matrix: defined by truss grid simulating 9 node plain stress elements
- Coupling matrix: shape function from 9 node plane element
- Displacement BC: fixed bottom, no lateral expansion
- Pressure BC: zero pressure on top
- External forces on top: -80N on side nodes, -100N on central node
- Time interval: 1000s (≈16 min)
- Total time: 31536 s (1 year)

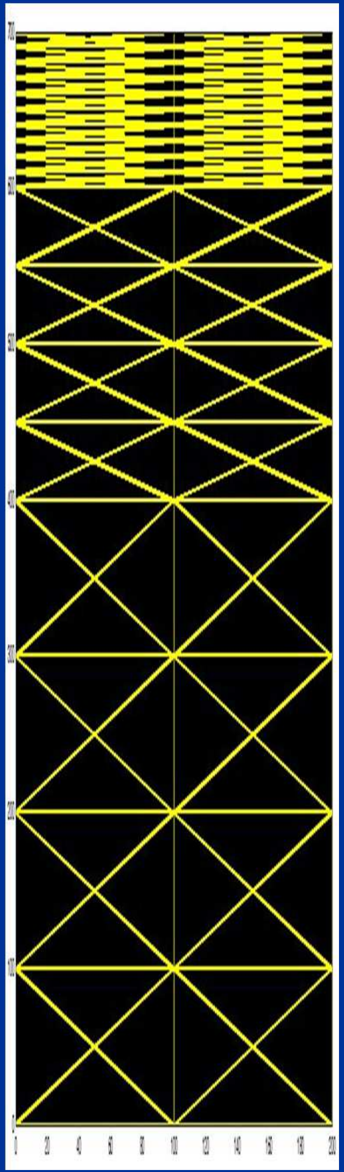

- *Pressure distribution is almost rectangular after the first step (black line). It drops as time increases (red line=116 days, magenta line=232 days)*

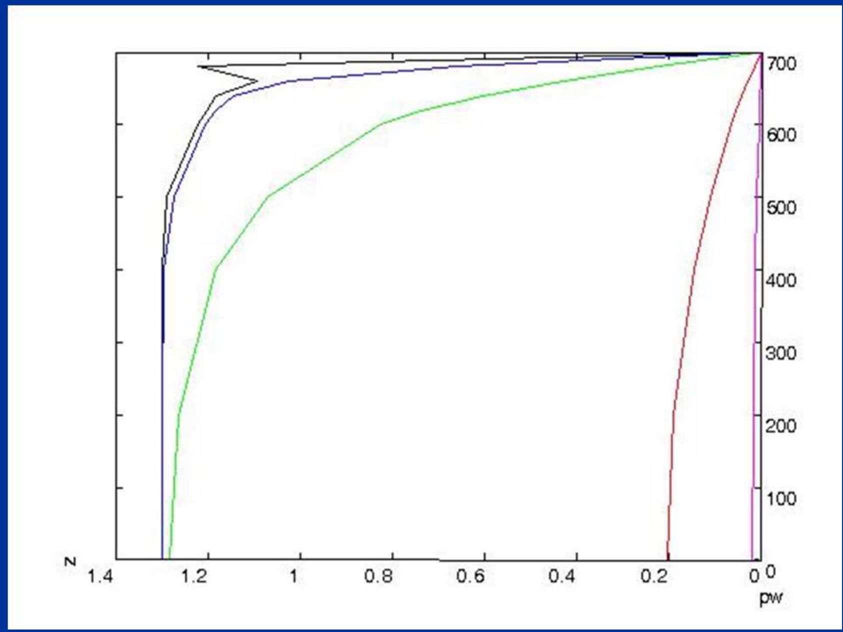

- *Common assumption in 1D consolidation: total stress is constant.*

This implies that:

$$\frac{\partial \varepsilon}{\partial t} = -m_v \frac{\partial \sigma'_{zz}}{\partial t} = -m_v \left(\frac{\partial \sigma_{zz}}{\partial t} - \alpha \frac{\partial p}{\partial t} \right)$$

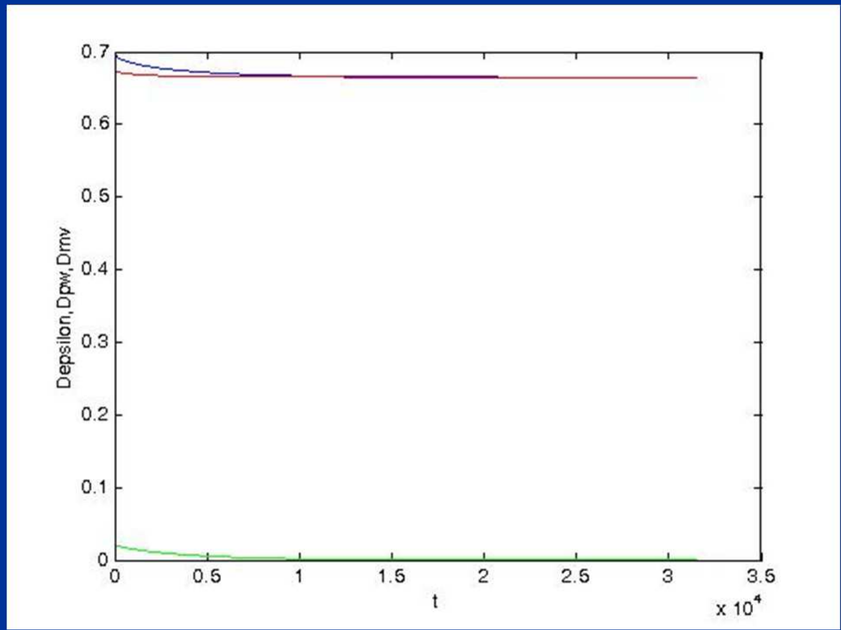

Blue line: strain variation
Green line: pressure variation
Small difference only at early stage (red line)

- *Settlement is linear up to 60% of final value if plotted with squared time, as observed by Taylor (1948)*

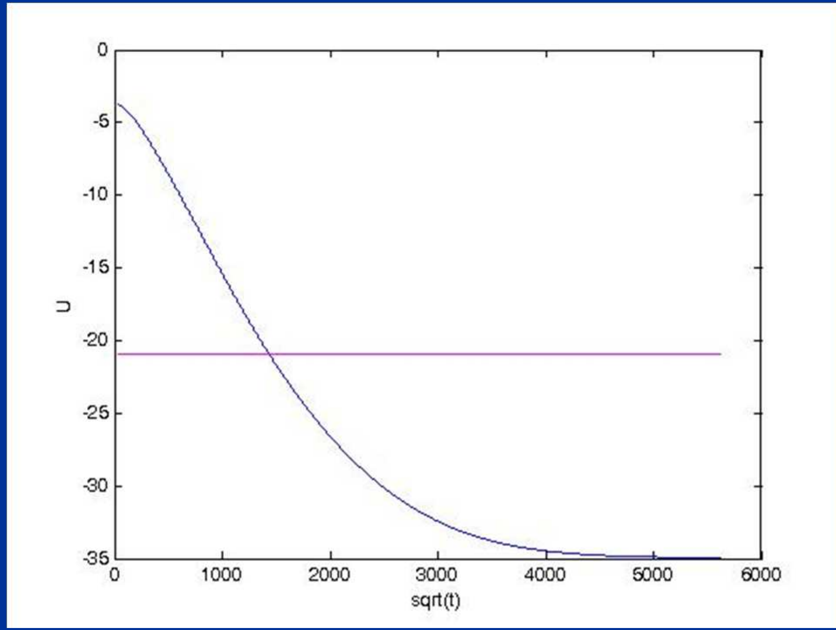

- *As Verruijt (2014) states: the consolidation is practically terminated for $T_v = c_v t / h^2 = 2$ (T_v dimensionless time)*

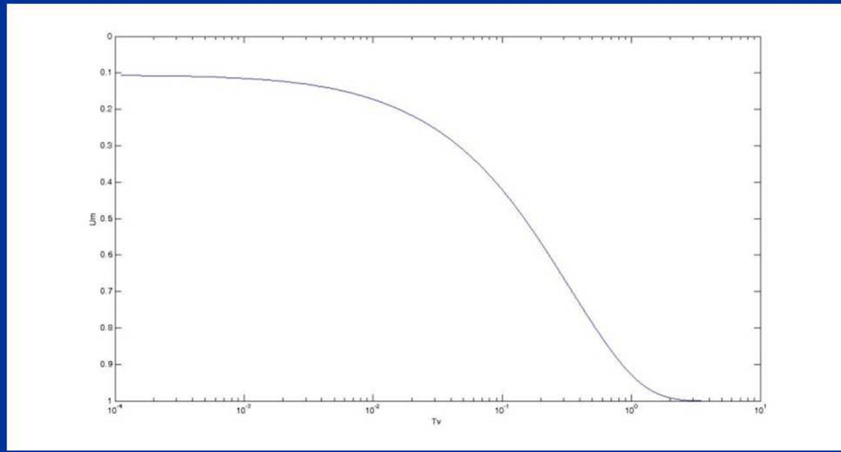

Literature – fuse model, no fluid

SOC in microfracturing

Zapperi S., A. Vespignani, H. E. Stanley, *Nature*, 388, 658-660 (1997)

- Mesoscopic scale, tilted lattice, strain driven experiment
- Hooke law: $\sigma_{\alpha\beta} = C_{\alpha\beta\gamma\delta}\,\epsilon_{\gamma\delta}$
- Modified Hooke tensor for damage: $\tilde{C} = (1-D)\,C = aC$
- Equivalent electrical problem $\sigma \rightarrow I \quad \epsilon \rightarrow V \quad C \rightarrow \rho$
- Random damage at early stage is set
- Breaking rule: each resistor (bond) has a random failure threshold I_c and when reached *damage a* is imposed (C is reduced); new higher threshold may be assigned or bond is removed
- After bond failure voltage increase is stopped and rearrangements occur, then voltage is applied again and so on until macroscopic crack

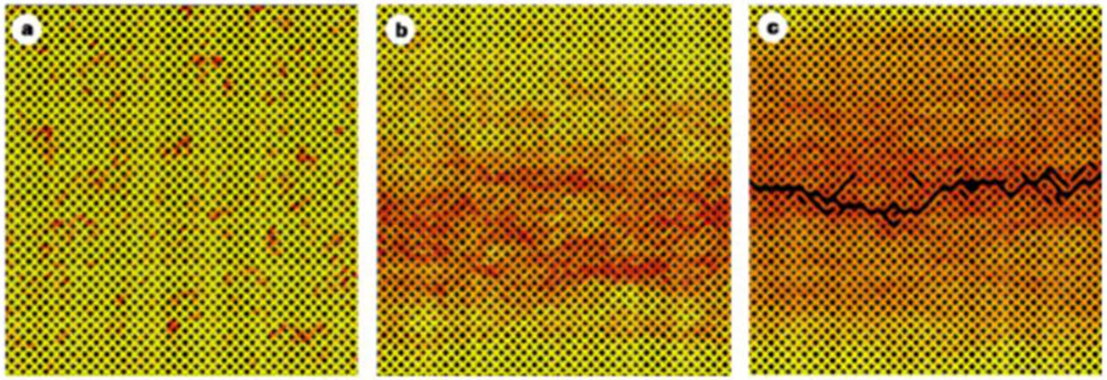

EPFL LSMS

Enrico Milanese, 2014

Literature – fuse model, no fluid

SOC in microfracturing

Zapperi S., A. Vespignani, H. E. Stanley, *Nature*, 388, 658-660 (1997)

Self-Organized Criticality behavior:

- No tuning parameter, external drive (voltage increase) has a much slower timescale than fracture propagation
- Macroscopically plastic behavior: steady state
- Avalanche size probability distribution follows power-law distribution:

$$P(s) \sim s^{-\tau} \qquad \tau = 1.19 \pm 0.01$$

- P(s) cut-off scales with system size: scale-free activity
- Current (stress) decreases as sandpile columns height
- Similar power-law distribution for time duration of each avalanche and energy bursts

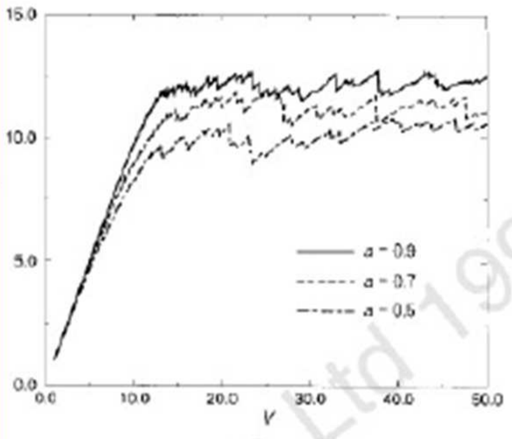

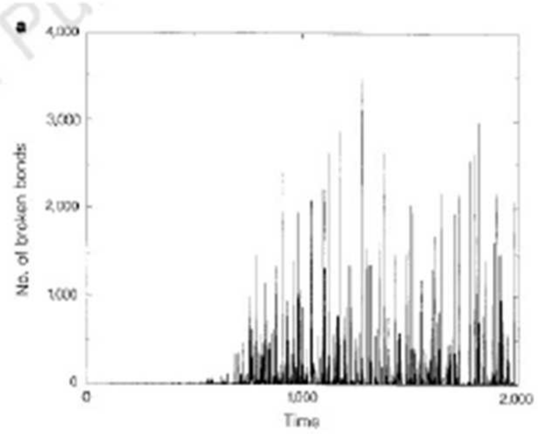

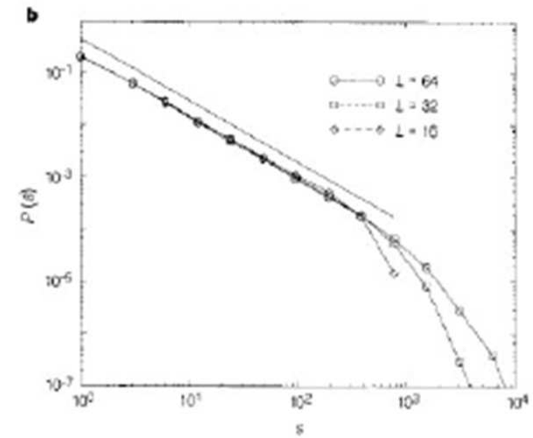

Truss model with and without fluid

- *20.000 avalanches are collected for the steady state analysis; about 55000 for the elastic and plastic domain*
- *About 60 to 70 single runs are carried out for this; 300-400 avalanches per single run*
- *The probability distribution function P(s) of the avalanche sizes in the steady-state is calculated*
- *To best represent the probability distribution, logarithmic binning is chosen: the abscissa (20.000 avalanches obtained from n analyses) is subdivided in 10, 100 and 10.000 parts (logarithmically) and the number of avalanches in the respective intervals is collected. 10.000 bins means that every dimension of the avalanche is taken into account separately.*

No fluid

Mechanical Model

One analysis behavior

Size: L = 16

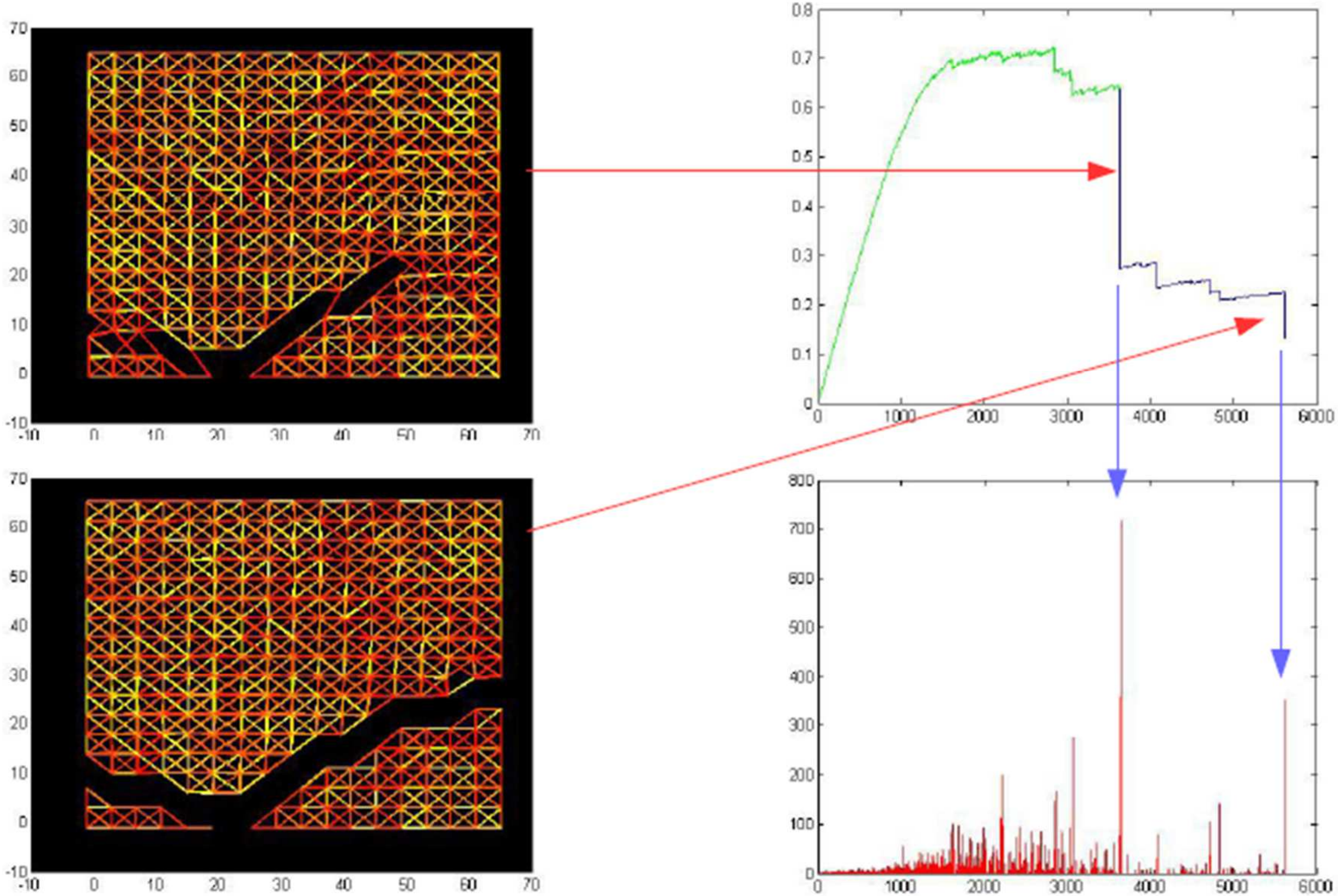

Enrico Milanese, 2014

No fluid

Mechanical Model

Logarithmic spaced bins: steady state avalanches

Using logarithmic spaced bins

- Around 20.000 avalanches in the steady state are gathered
- τ value range: 1.19~1.21

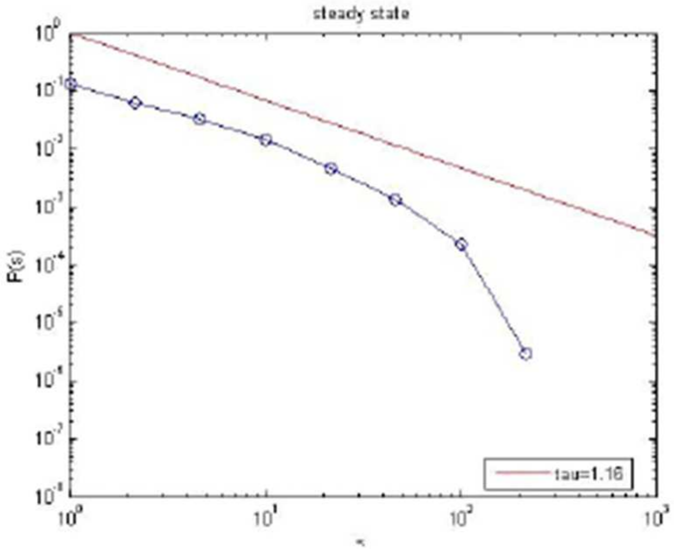

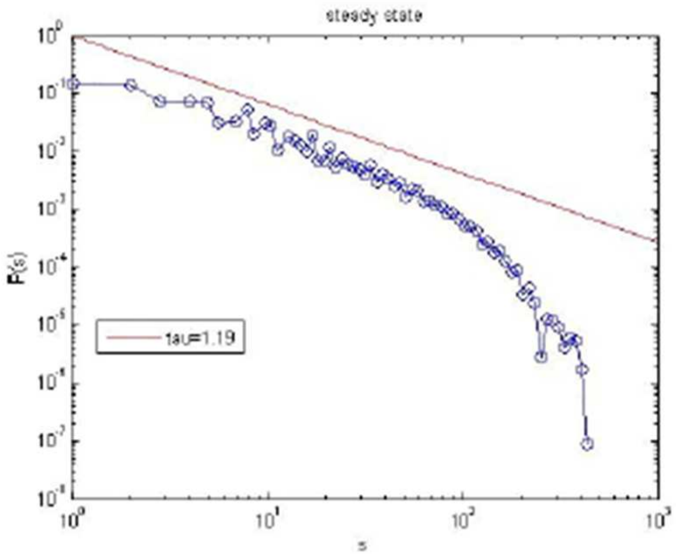

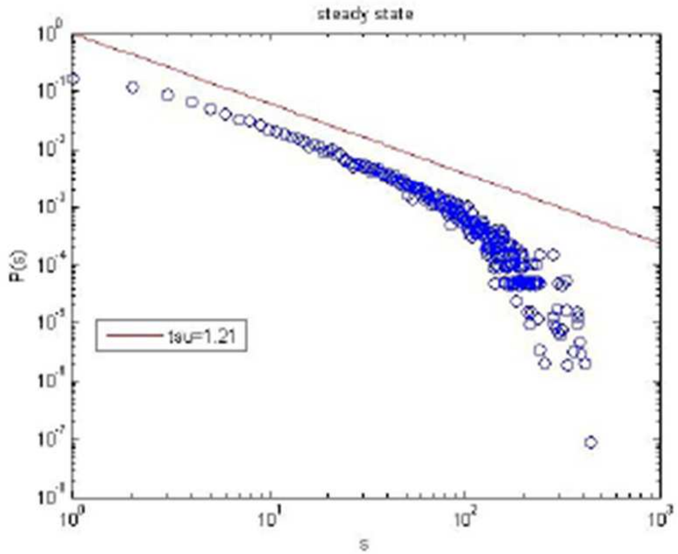

No fluid

Mechanical Model

Logarithmic spaced bins: all avalanches

Using logarithmic spaced bins

- around 55.000 avalanches gathered
- τ value range: 1.53~1.58

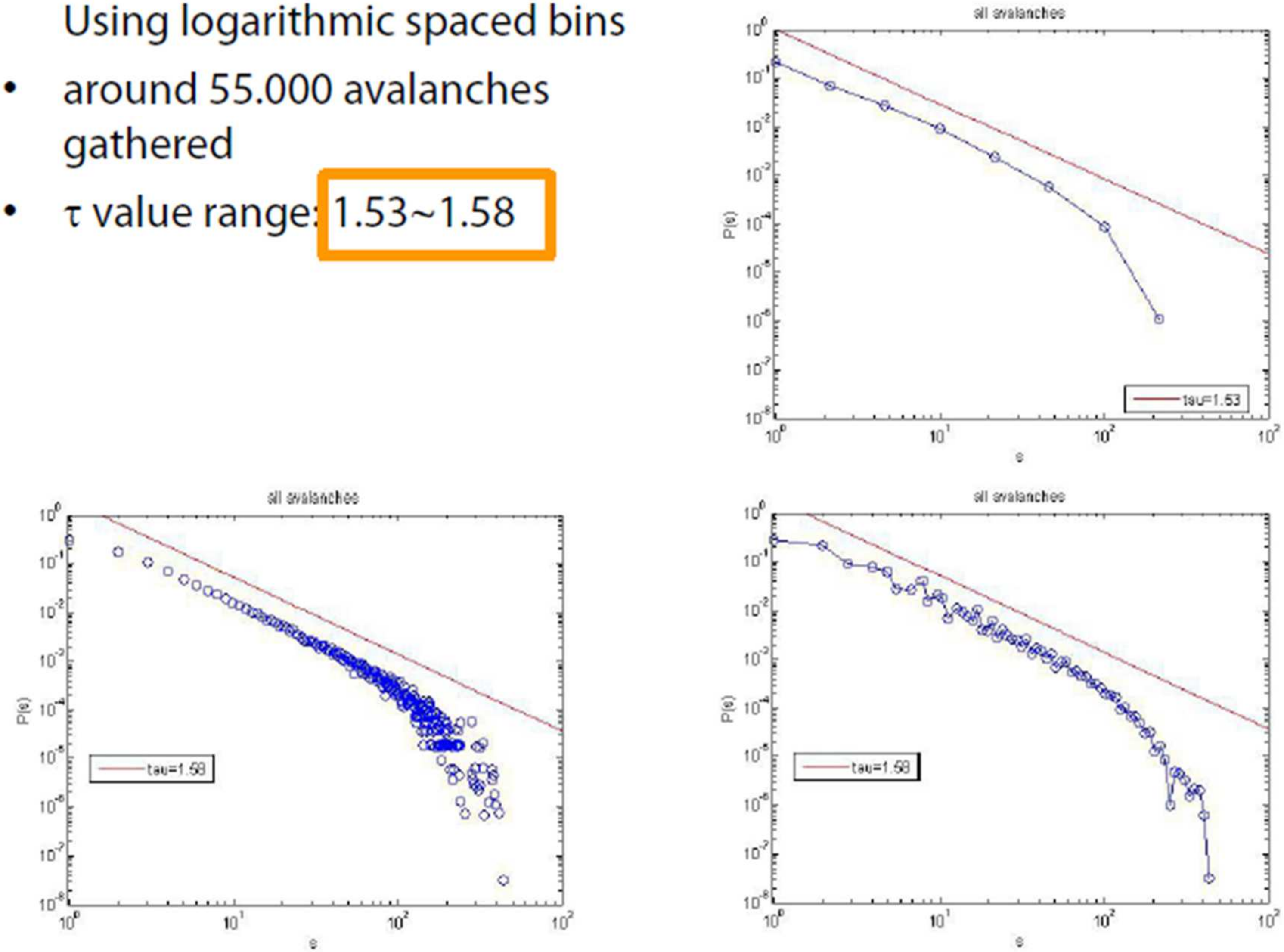

No fluid

Conclusions

What I have found

- Steady state (plasticity behavior) for both fuse and mechanical models
- **Different stress drop** at failure between fuse and mechanical models
- **Power-law behavior** for both fuse and mechanical models
- Scale-free behavior for both models
- "**Loading-free**" behavior for both fuse and mechanical models
- Bigger size problems need slower increment, thus requiring more computational effort

Further work

- Dynamics, hydraulic fracturing

Enrico Milanese, 2014

With fluid – displacements specified

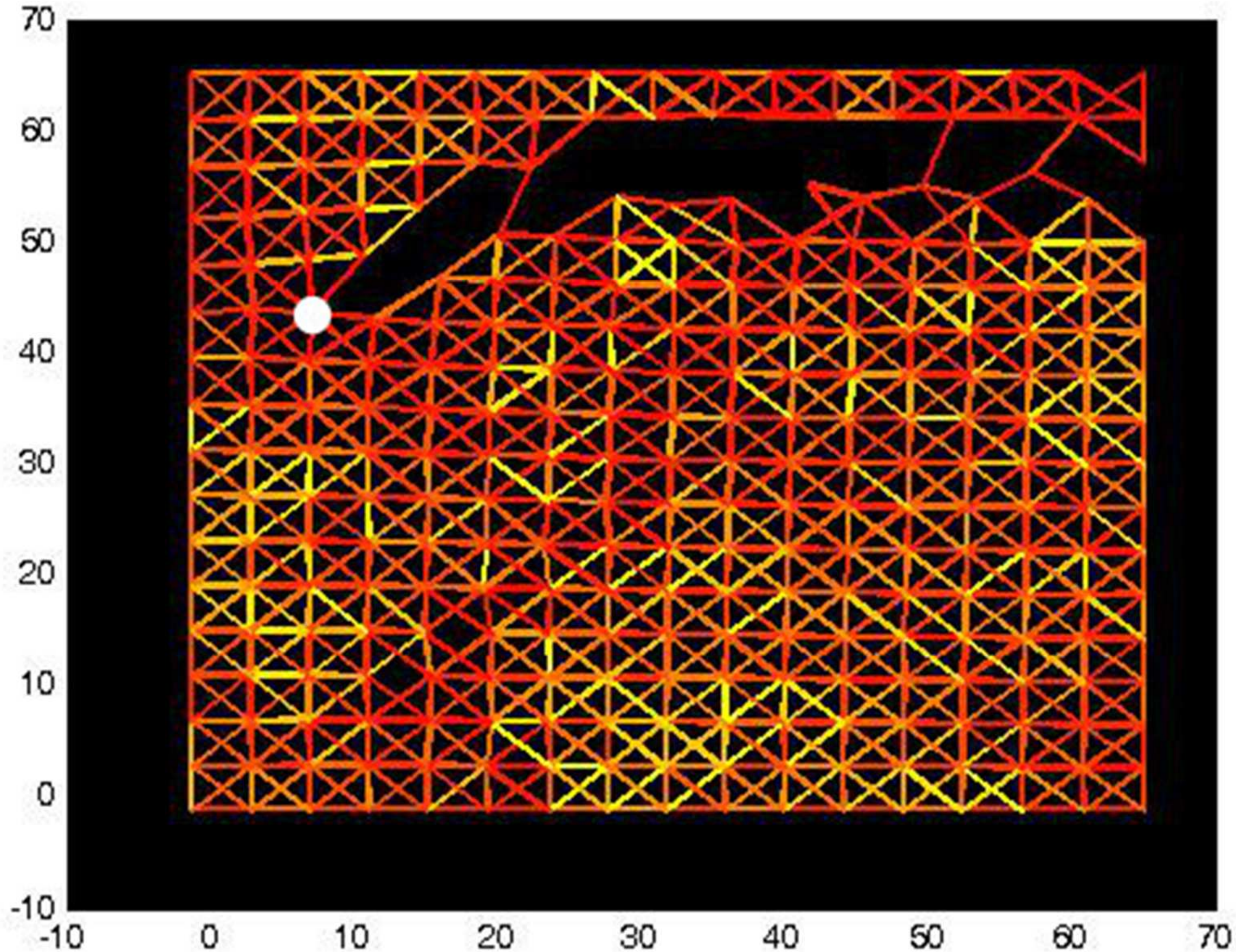

Stepwise advancement

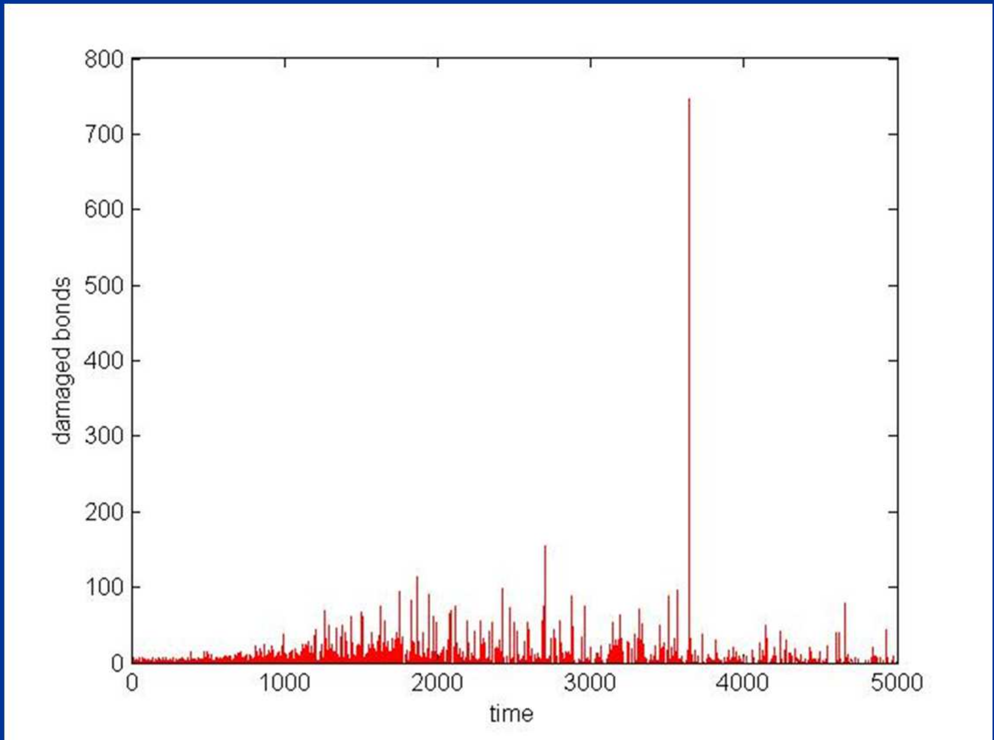

Avalanches for a single run

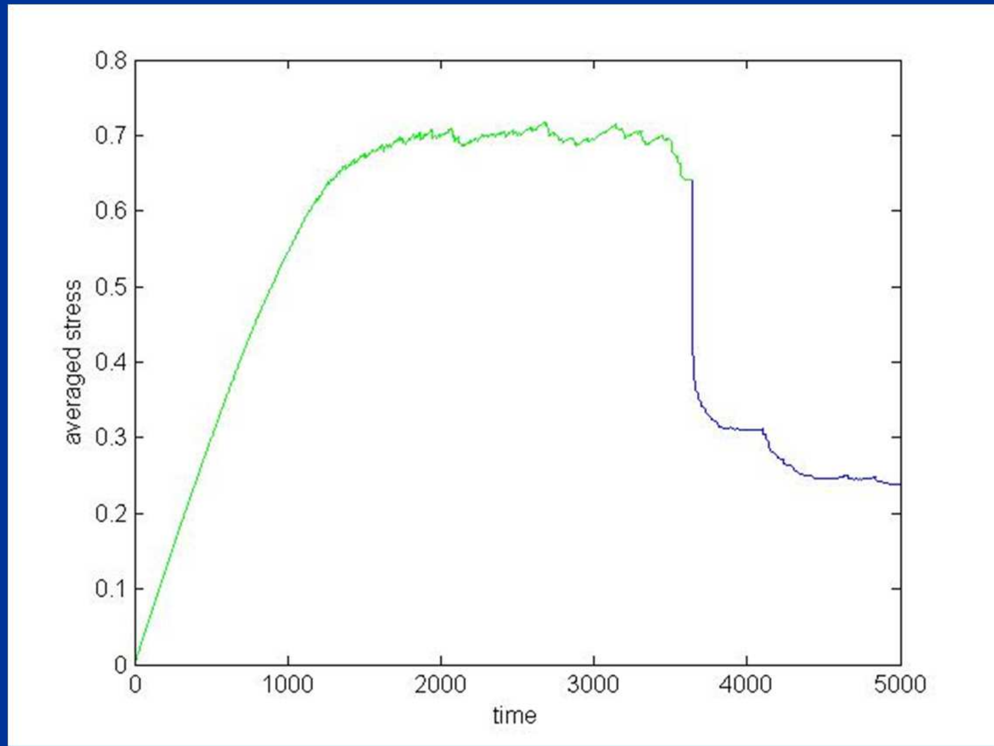

Plasticity type behaviour

Pressure fluctuations at «tip»

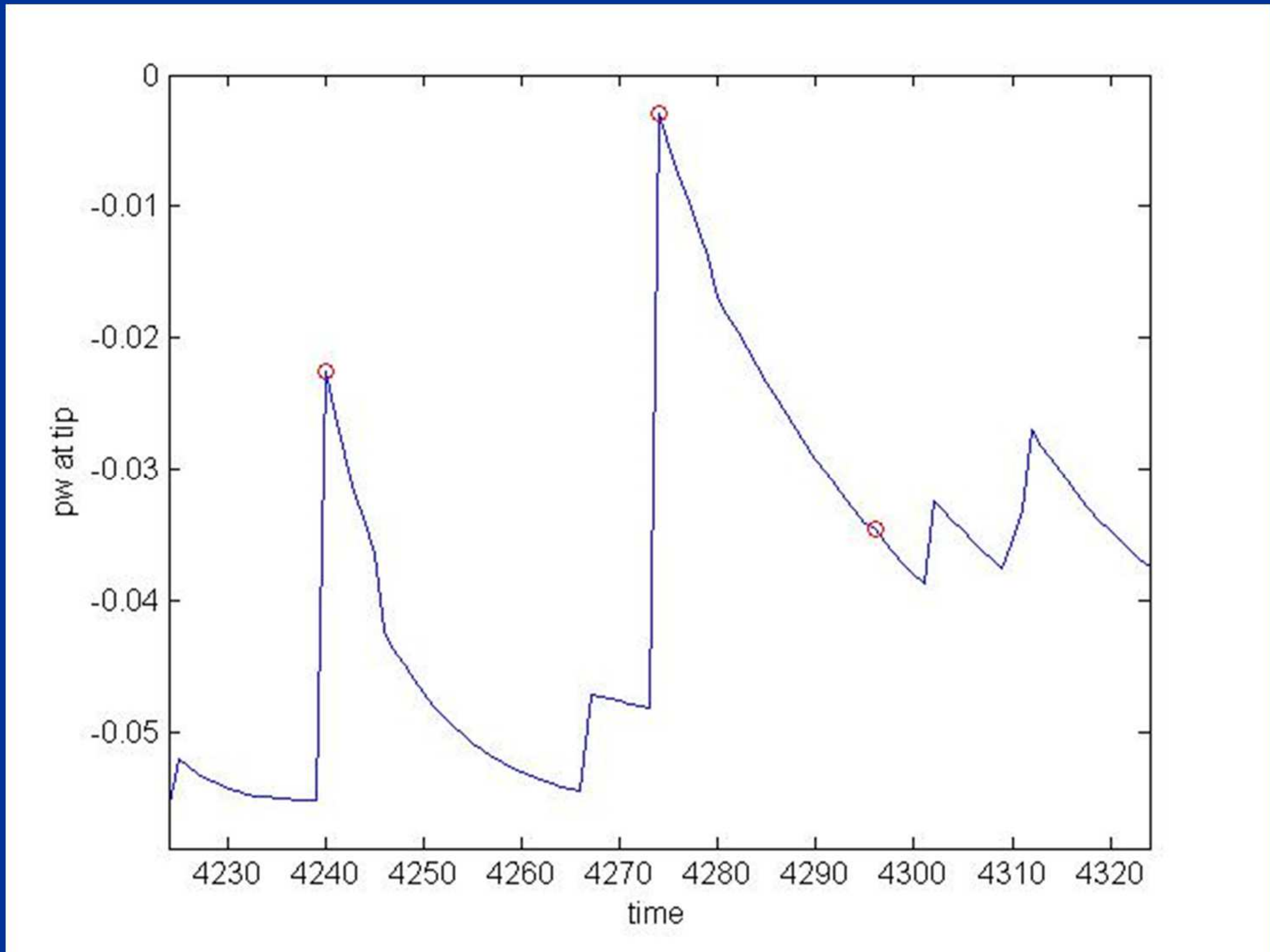

Pressure rise

With fluid – displacements specified homogeneous medium

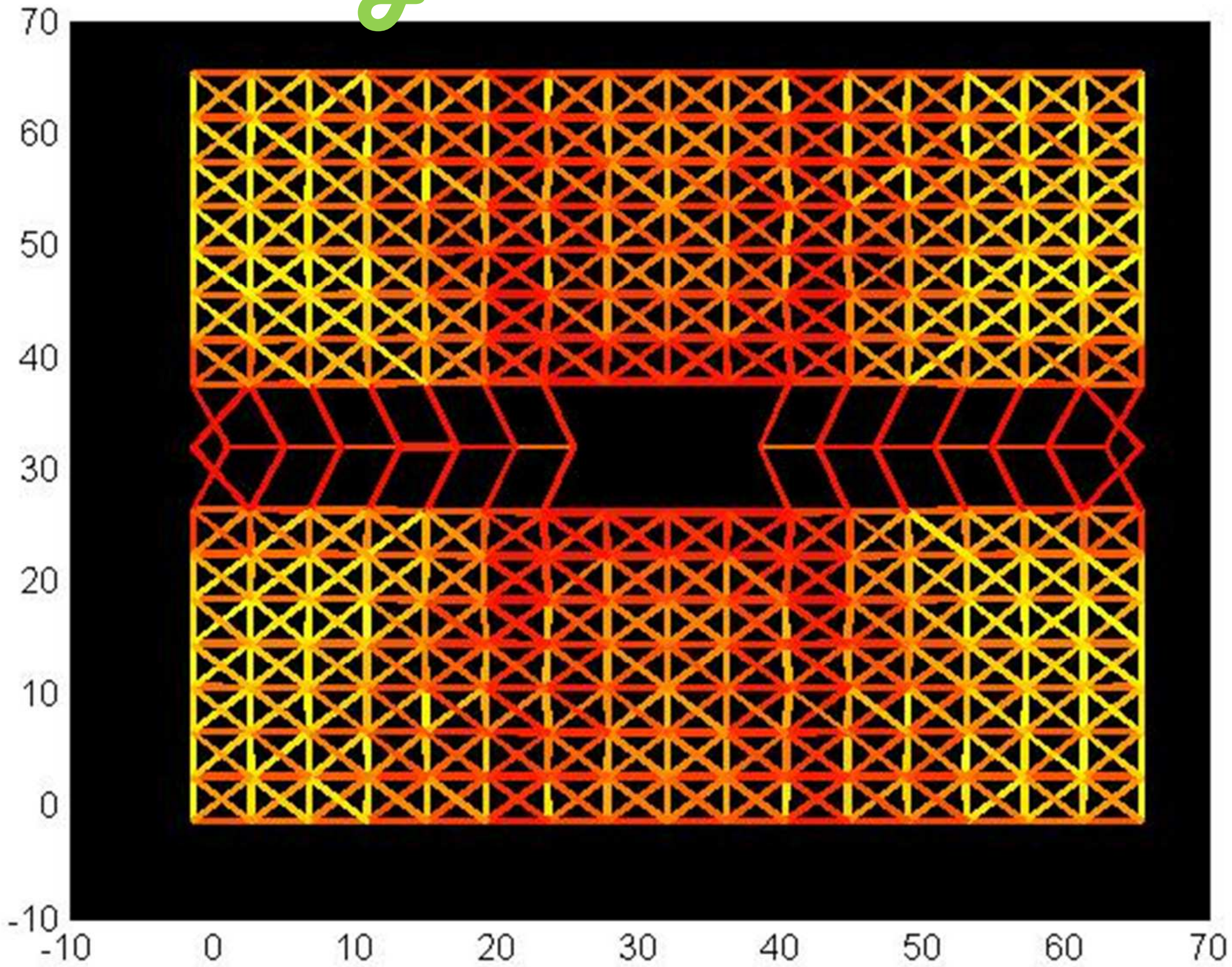

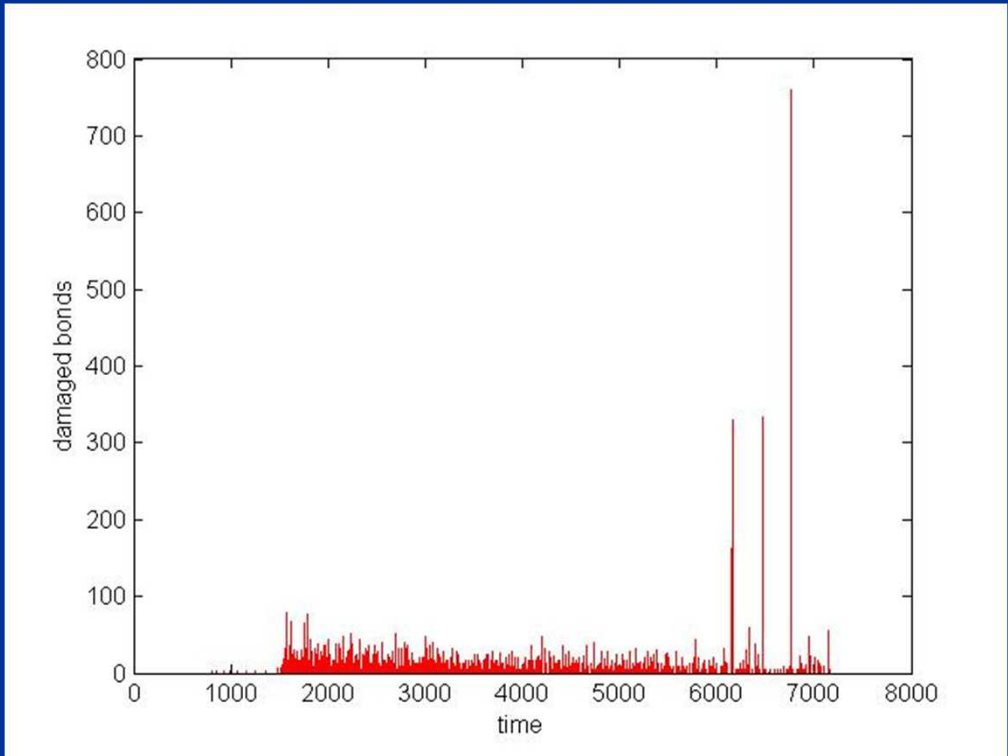

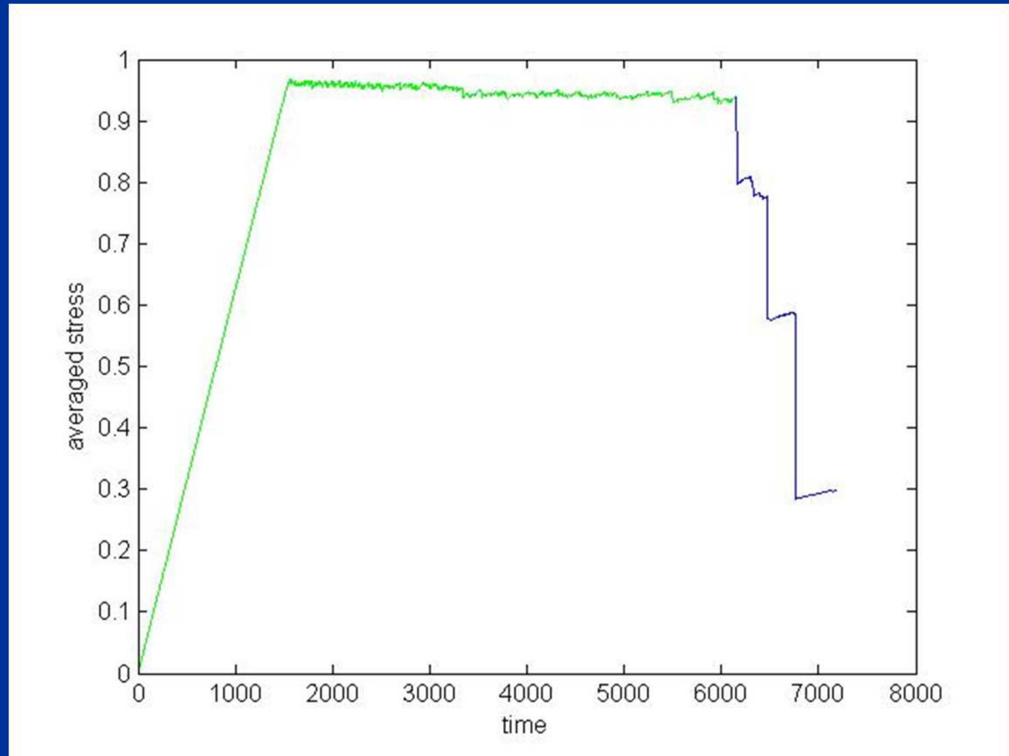

Avalanches for a single run
Advancements still unevenly distributed in time and ***irregular step size***

Elastic-perfectly plastic behaviour

Flow assigned in the centre

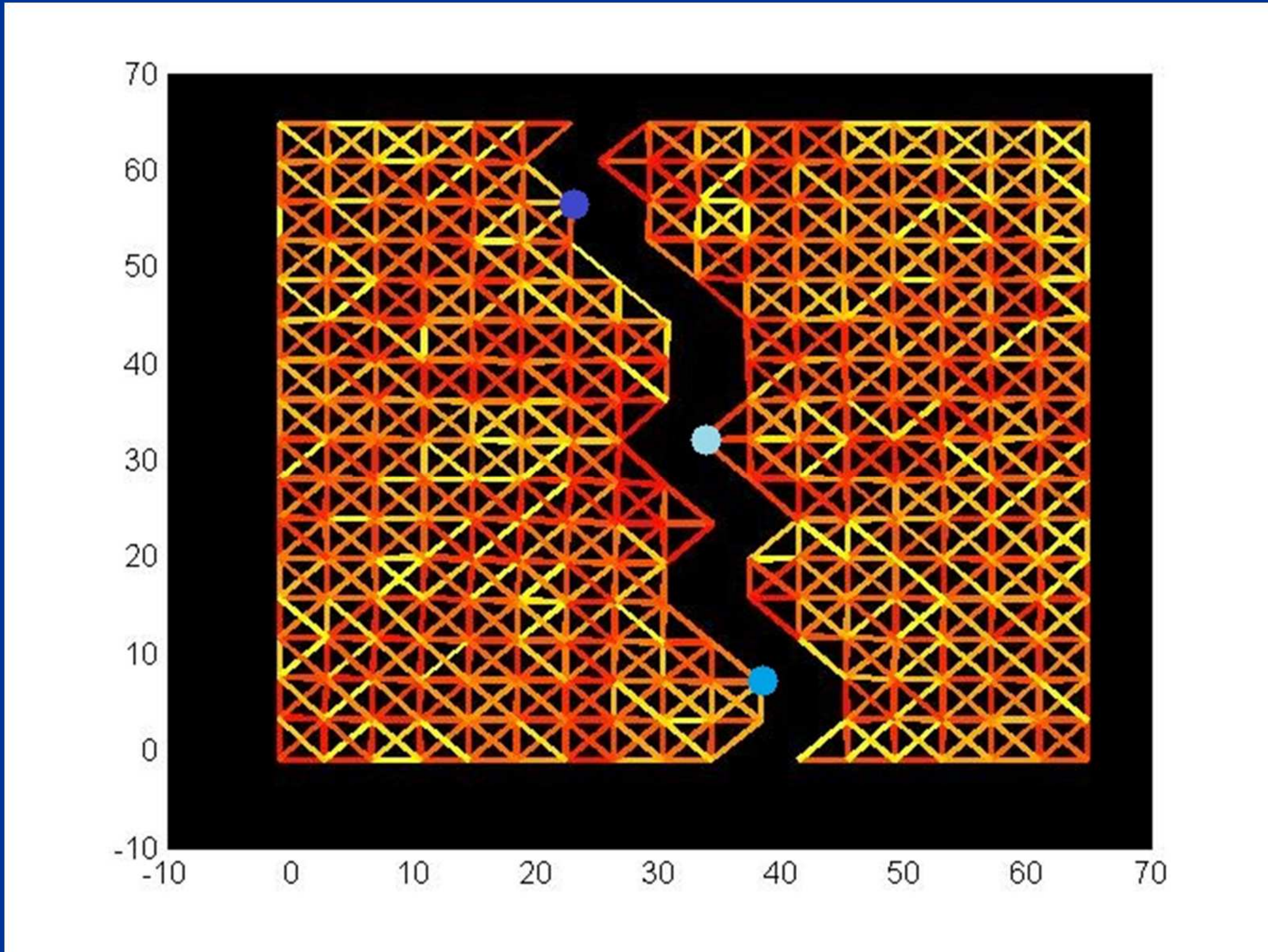

Stepwise advancement

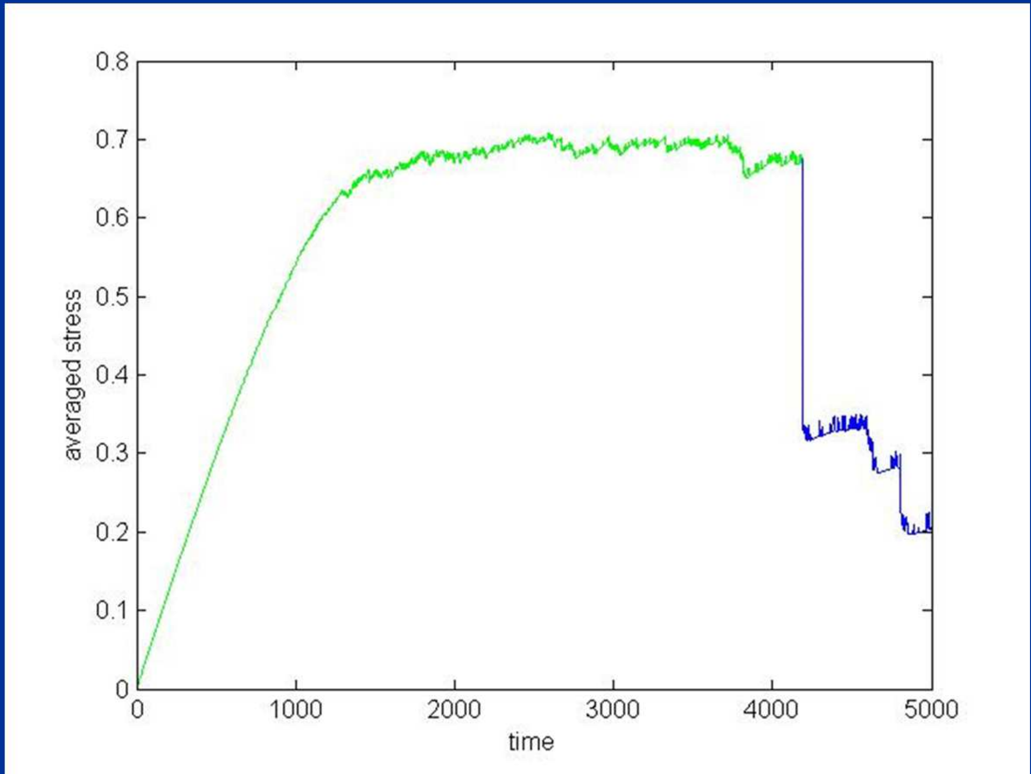

Plasticity type behavior

Avalanches for a single run

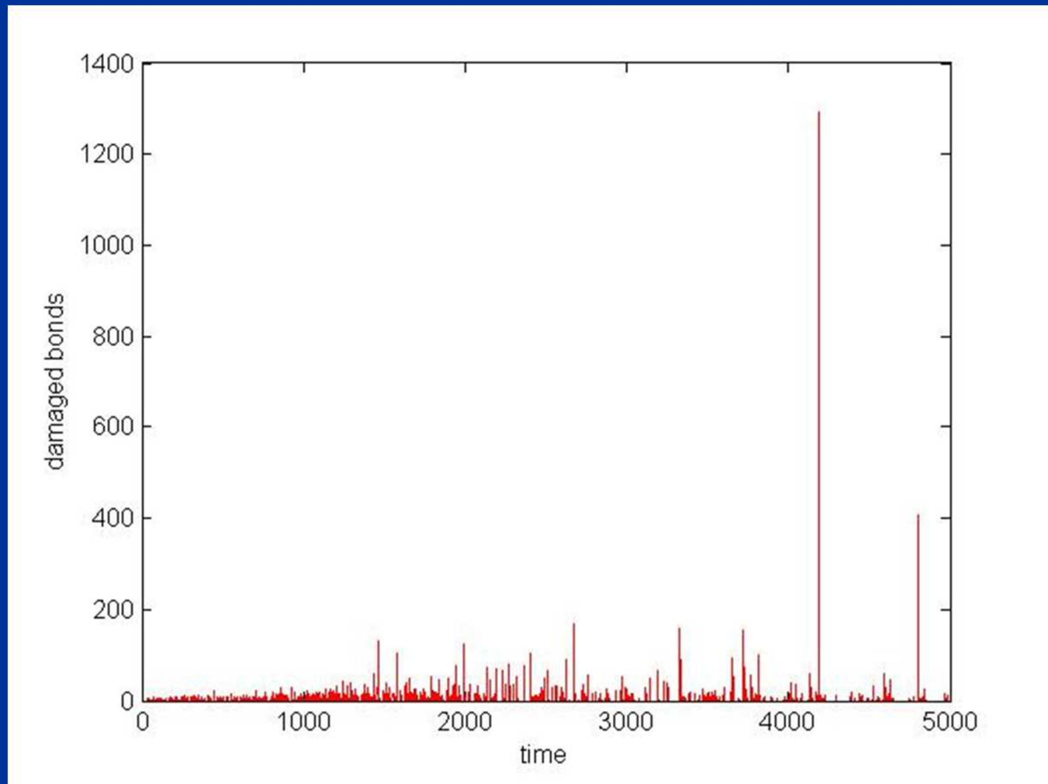

Pressure fluctuations at «tip»

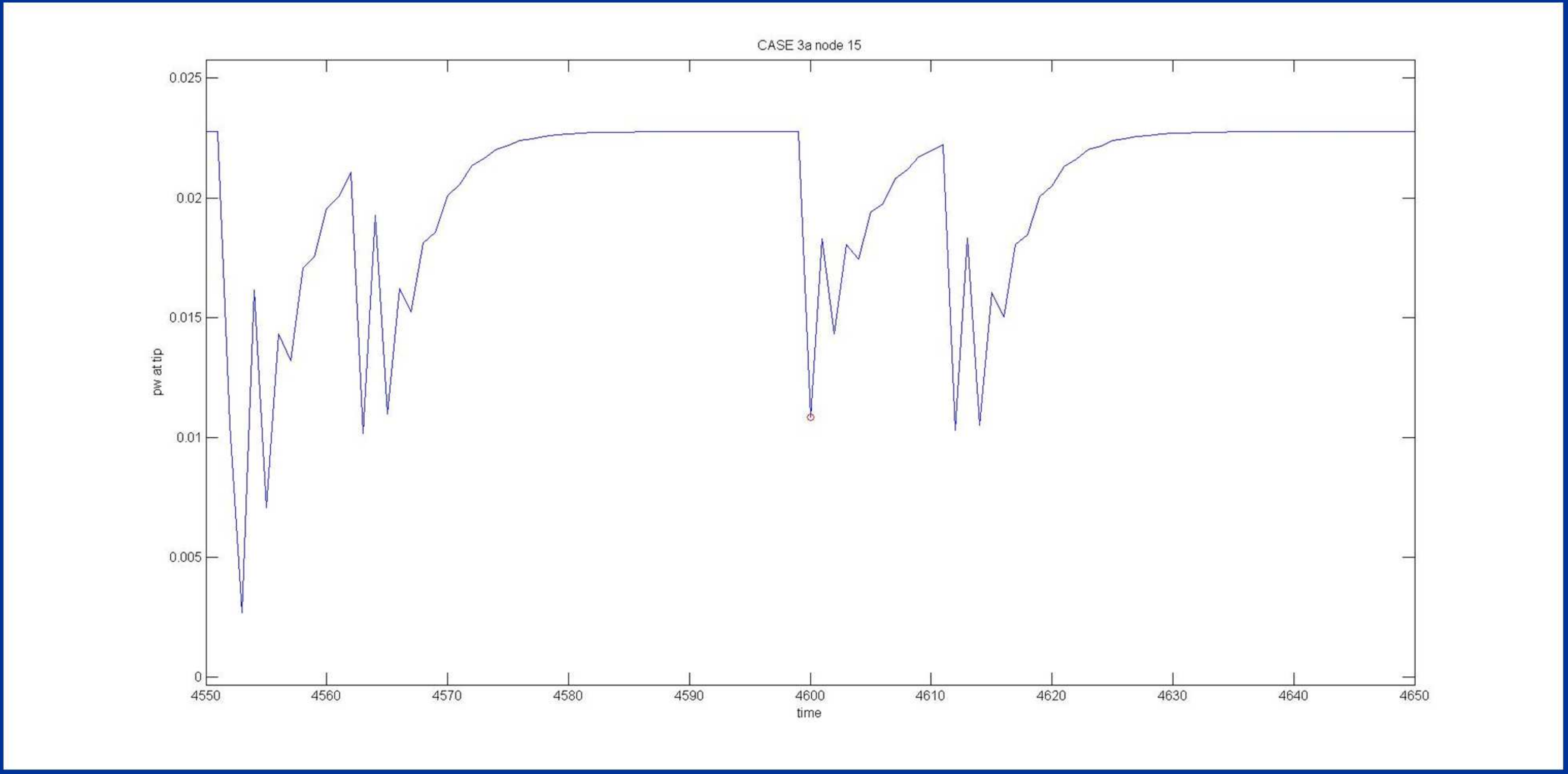

Pressure drop

Why pressure rise or drop?

Mechanical load f (1) – prevailing scenario:

If a load (or displacement b.c. due to advancing fracture) is applied the fluid takes initially almost all because it is much less compressible than the solid skeleton and discharges the solid (stress split of Terzaghi, which acts instantaneously). Then through the coupling (volumetric strain) with the fluid, the pressure dissipates and the solid is reloaded. Hence we have a pressure ***RISE*** *upon rupture.*

stresses and pressures out of phase

Flow specified f (2) – prevailing scenario:

The flow effect is transmitted to the solid through the pressure coupling term in the effective stress. The solid is loaded and upon rupture produces a sudden increase of the volumetric strain. This in turn produces a drop in pressure. Hence pressure ***DROP*** *upon rupture.*

stresses and pressures in phase

Stepsize irregular also for homogeneous media

Can such a behaviour* be **predicted** by FE Methods?

* Pressure fluctuation, stepwise advancement

Solutions for hydraulic fracturing

1. Boone and Ingraffea (1990) (linear fracture mechanics , interface elements, fluid leakage in the medium surrounding the fracture and moving crack depending on the applied loads and material properties)

2. Carter et al., (2000) (fully 3D hydraulic fracture model (LEFM) which neglects the fluid continuity equation in the medium surrounding the fracture)

3. Réthoré et al., (2007, 2008) Kraaijeveldt et al.(2013) Rizzato (2014) (XFEM for hydraulic fracturing in a 2D setting)

4. Carrier and Granet (2012) Interface elements, cohesive model

5. Mohammadnejad T, Khoei AR (2013) (extension of the model of Réthoré et al., (2008) to three-phase porous media)

6. Irzal et al., (2013) (PUFEM with cohesive fracture and large deformation)

7. Wheeler (2014), Miehe, Markert (Phase field models)

8. Schrefler et al. (2006) and Secchi and Schrefler (2012) (SGFE + unstructured, automatic mesh generation & mesh refinement, 2D and 3D)

SGFEM *with remeshing*

with S. Secchi, L. Simoni, P. Rizzato

POROUS MEDIA MECHANICS WITH COHESIVE FRACTURE MODEL

Governing equations

Linear Momentum Balance for the Mixture

$$\int_\Omega \delta\varepsilon_{ij}\, c_{ijrs}\,\varepsilon_{rs}\, d\Omega - \int_\Omega \rho\, \delta u_i g_i\, d\Omega - \int_\Omega \delta\varepsilon_{ij}\, \overline{\alpha}\,\delta_{ij}\, p\, d\Omega$$

Coupling with pressure

$$-\int_\Omega \delta\varepsilon_{ij}\, c_{ijrs} \frac{\alpha_s}{3} \delta_{rs}\, T d\Omega$$

Temperature coupling

$$-\int_{\Gamma_e} \delta u_i t_i\, d\Gamma - \int_{\Gamma'} \delta u_i c_i\, d\Gamma' = 0$$

Cohesive tractions

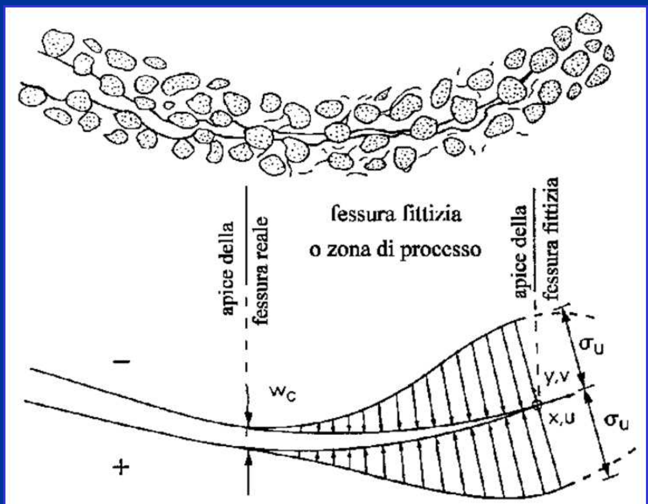

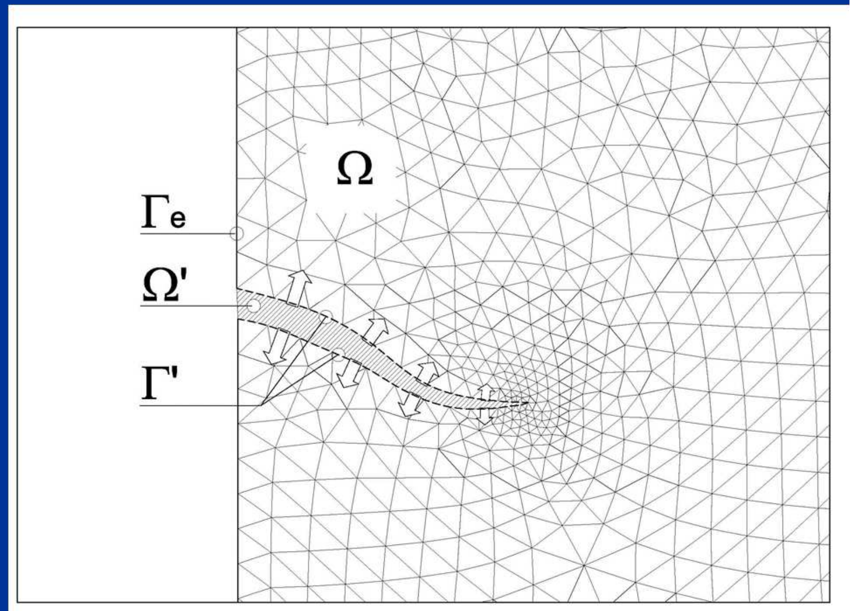

Porous media mechanics with cohesive fracture model

Mass balance for water in the domain

$$\int_\Omega \delta p\left\{\left(\frac{\overline{\alpha} - n}{K_s}+\frac{n}{K_w}\right)\frac{\partial p}{\partial t}+\overline{\alpha}\, v^s_{i,i} - \left[\left(\overline{\alpha} - n\right)\alpha_s + n\alpha_w\right]\frac{\partial T}{\partial t}+\left[\frac{k_{ij}}{\mu_w}\left(- p_{,j}+\rho_w g_j\right)\right]_{,i}\right\}d\Omega$$

$$- \int_\Omega \left(\delta p\right)_{,i}\left[\frac{k_{ij}}{\mu_w}\left(- p_{,j}+\rho_w g_j\right)\right]d\Omega + \int_{\Gamma_e}\delta p\, q_w\, d\Gamma + \int_{\Gamma'}\delta p\,\overline{q}_w\, d\Gamma' = 0$$

b.c. included + integr. by parts

Effective stress principle (p: compression positive)

$$\sigma'_{ij} = c_{ijrs}\left(\varepsilon_{rs} - \delta_{rs}\varepsilon_T\right) - \overline{\alpha}\, p\,\delta_{ij}, \qquad \varepsilon_T = \frac{\alpha}{3}\, T$$

Coupling

$\overline{\alpha} = 1 - K/Ks$ Biot's coefficient

α Thermal expansion coeff.

Mass balance equation within the crack

$$\int_{\Omega'} \delta p \left\{ \frac{n}{K_w}\frac{\partial p}{\partial t} + \frac{\partial w}{\partial t} - n\,\alpha_w \frac{\partial T}{\partial t} \right\} d\Omega'$$

$$- \int_{\Omega'} (\delta p)_{,i} \left[\frac{w^2}{12\mu_w}\left(-p_{,j} + \rho_w g_j\right)\right] d\Omega' + \int_{\Gamma'} \delta p\, \bar{q}_w \, d\Gamma' = 0$$

Coupling (thermal)

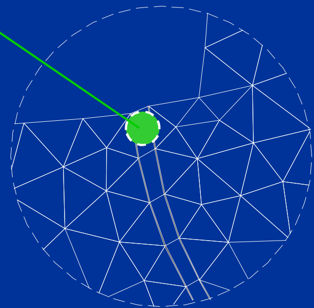

Poiseuille Coupling (displ.)

Energy balance

$$\int_\Omega \delta T \rho C_v \dot{T}\, d\Omega + \int_\Gamma \delta T q_i^{conv}\, d\Gamma + \int_\Gamma \delta T q_i\, d\Gamma = \int_\Omega \delta T_{,i}\, q_{,i}\, d\Omega + \int_\Omega \delta T s\, d\Omega$$

Dirichlet and Neumann b.c. including convective term: $q_i^{conv} = h\left(T - T_\infty\right) n_i$

Heat generation. fracture coupling term

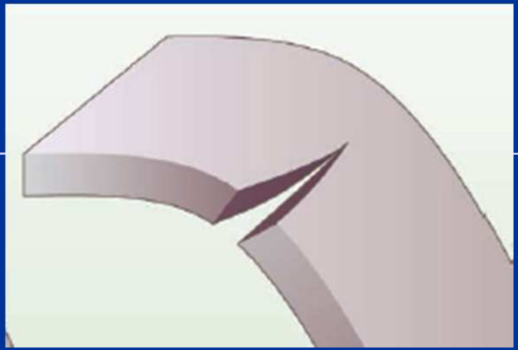

Solid phase: cohesive fracture model

Mode I crack opening

DUGDALE/BARENBLATT Model

$$\sigma = \sigma_0 \left(1 - \frac{\delta_{\sigma 1}}{\delta_{\sigma cr}} \right) \frac{\delta_\sigma}{\delta_{\sigma 1}}$$

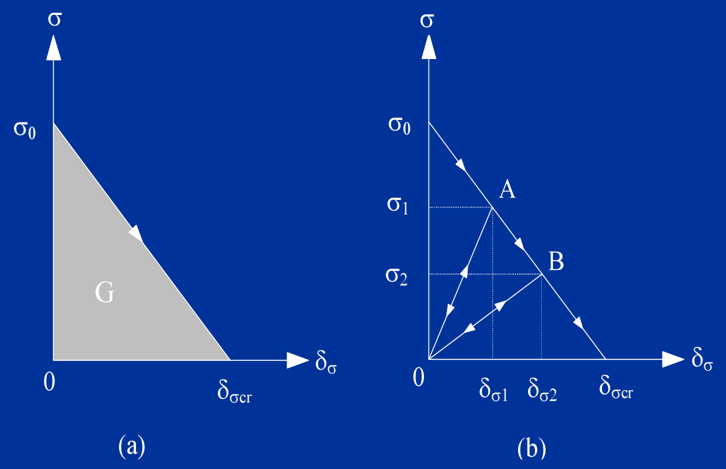

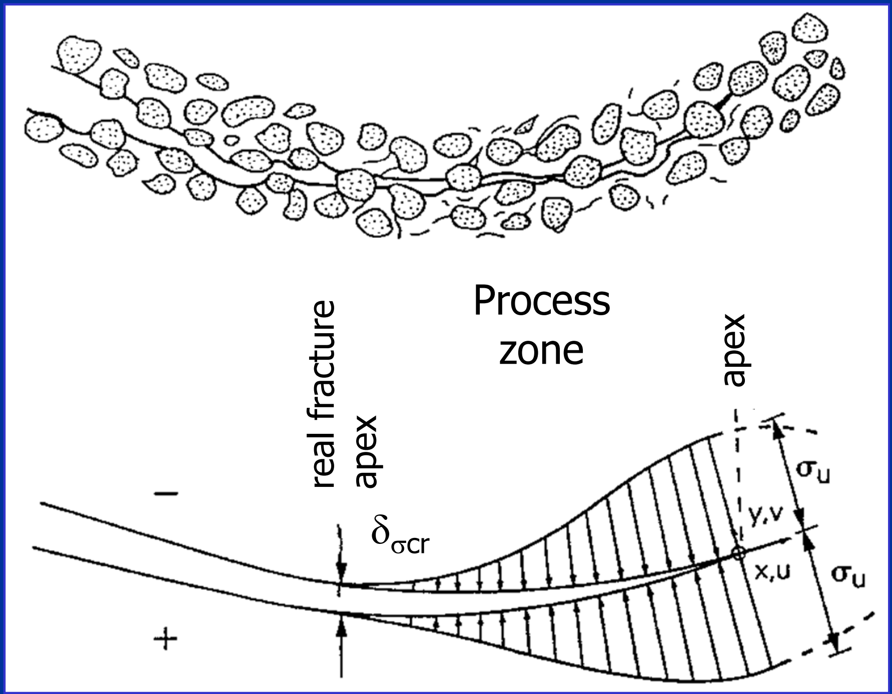

(a) Fracture energy and
(b) Loading/unloading law for each material

Solid phase: cohesive fracture model

Mode II crack opening

$$\tau = \tau_0 \left(1 - \frac{|\delta_{\tau 1}|}{\delta_{\tau cr}} \right) \frac{\delta_\tau}{|\delta_{\tau 1}|}$$

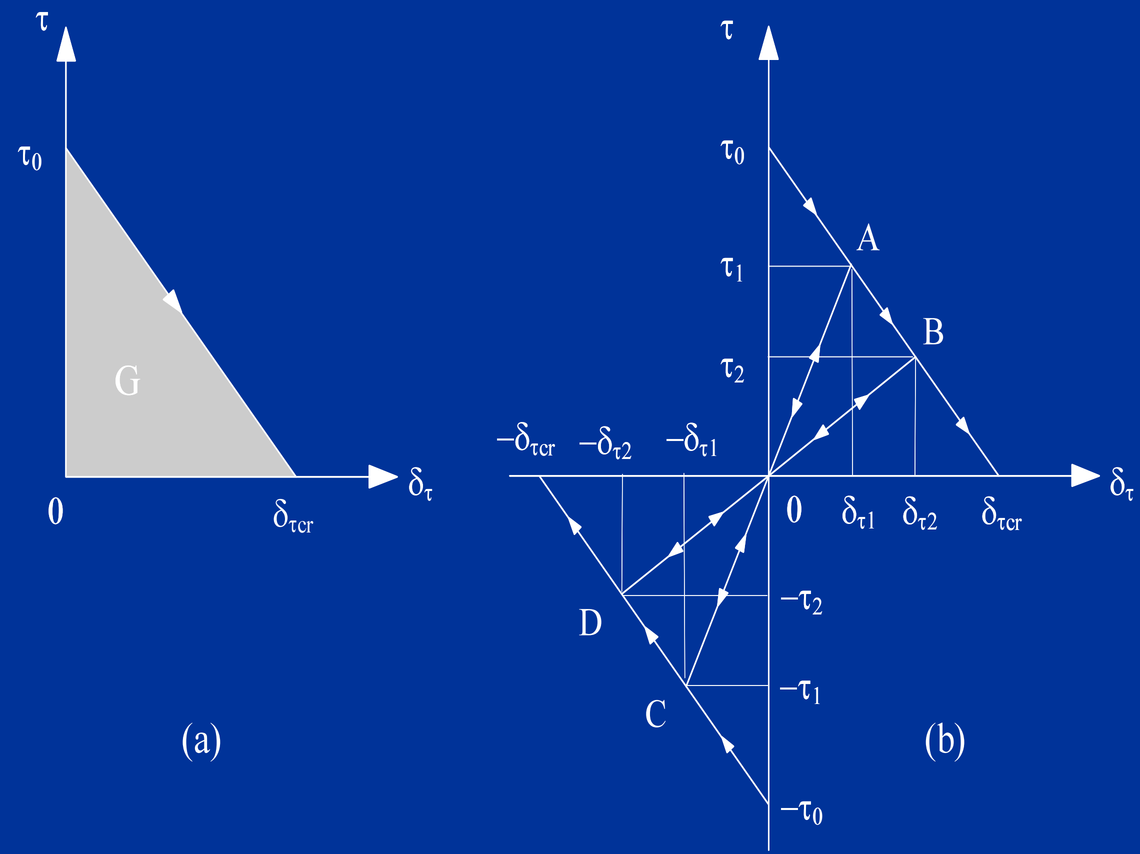

Fracture energy (a) and (b) loading unloading law for the interface and mixed mode

Solid phase: cohesive fracture model

Mixed Mode crack opening

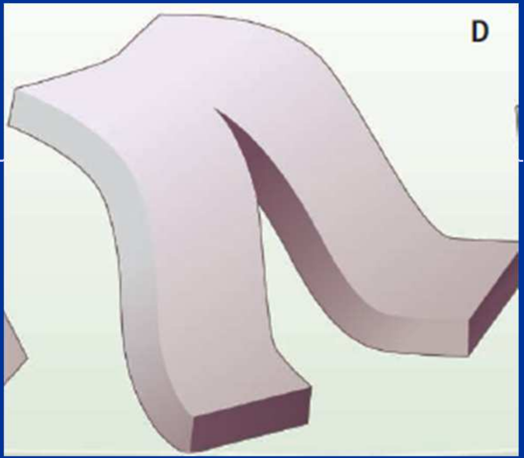

Cohesive law (***Margolin; Ortiz***)

- Equivalent traction t

$$\underline{t} = \frac{t}{\delta}\left(\beta^2 \underline{\delta}_s + \underline{\delta}_n\right)$$

$$t = \sqrt{\beta^{-2}\left|\boldsymbol{t}_s\right|^2 + t_n^2}$$

- Effective opening displacement δ

$$\delta = \sqrt{\beta^2 \delta_s^2 + \delta_n^2}$$

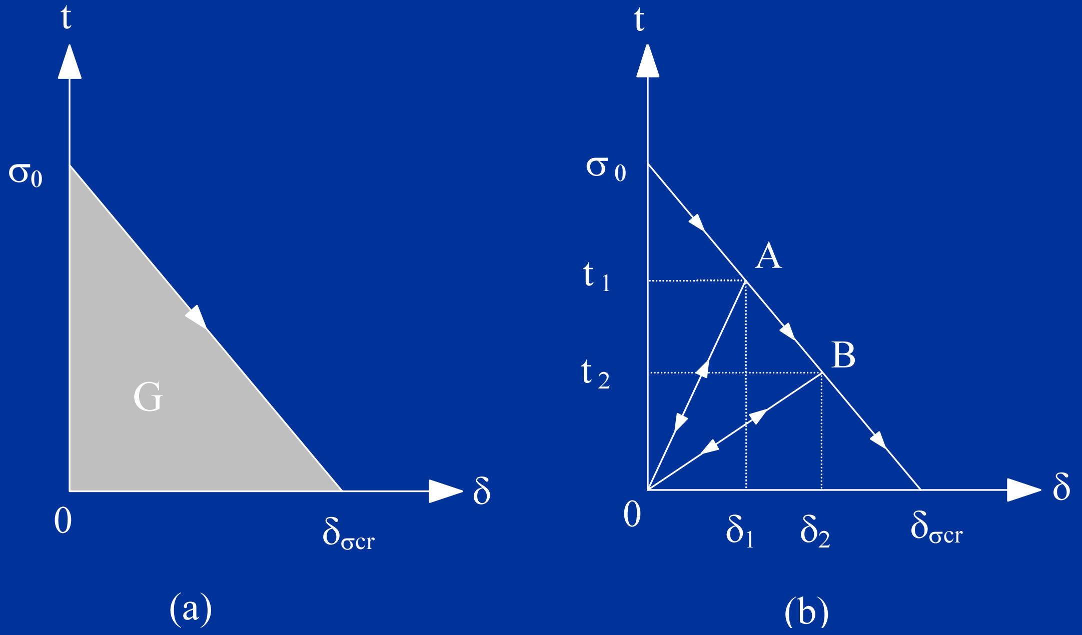

Fracture energy (a) and loading-unloading law (b) in terms of effective opening and traction

DISCRETIZED GOVERNING EQUATIONS - SGFE

Space discretization

$$\begin{bmatrix} \mathbf{K} & \mathbf{C}_{sg} & \mathbf{C}_{sT} \\ \mathbf{C}_{sg}^{T} & \mathbf{S} & \mathbf{C}_{pT} \\ \mathbf{0} & \mathbf{0} & \mathbf{P} \end{bmatrix} \begin{bmatrix} \dot{\mathbf{d}} \\ \dot{\mathbf{p}} \\ \dot{\mathbf{T}} \end{bmatrix} + \begin{bmatrix} \mathbf{0} & \mathbf{0} & \mathbf{0} \\ \mathbf{0} & \mathbf{H}_{p} & \mathbf{0} \\ \mathbf{0} & \mathbf{0} & \mathbf{H}_{th} \end{bmatrix} \begin{bmatrix} \mathbf{d} \\ \mathbf{p} \\ \mathbf{T} \end{bmatrix} = \begin{bmatrix} \dot{\mathbf{F}} \\ \mathbf{0} \\ \mathbf{0} \end{bmatrix} + \begin{bmatrix} \mathbf{0} \\ \mathbf{G}_{p} \\ \mathbf{G}_{th} \end{bmatrix}$$

$$\mathbf{K} = \int_{\Omega_E} \mathbf{B}^T \mathbf{D}\, \mathbf{B}\, dV \qquad \mathbf{C}_{sg} = -\int_{\Omega_E} \mathbf{B}^T \overline{\alpha} \mathbf{m}\, \mathbf{N}^p\, dV \qquad \mathbf{G}_{th} = -\int_{\Gamma_E} \mathbf{N}^{th^T} q^e\, d\Gamma - \int_{\Omega_E} \mathbf{N}^{th^T} s\, dV$$

$$\mathbf{C}_{sT} = \int_{\Omega_E} \mathbf{B}^T \mathbf{D}\, \mathbf{m} \frac{\alpha_s}{3} \mathbf{N}^{th} dV \qquad \mathbf{S} = -\int_{\Omega_E} \mathbf{N}^{p^T} \left(\frac{\overline{\alpha} - n}{K_s} + \frac{n}{K_w} \right) \mathbf{N}^p\, dV \qquad \mathbf{H}_p = -\int_{\Omega_E} \left(\nabla \mathbf{N}^p \right)^T \frac{\mathbf{k}}{\mu_w} \nabla \mathbf{N}^p\, dV$$

$$\mathbf{C}_{pT} = \int_{\Omega_E} \mathbf{N}^{p^T} \left((\overline{\alpha} - n)\alpha_s + n\alpha_s \right) \mathbf{N}^{th}\, dV \qquad \mathbf{P} = \int_{\Omega_E} \mathbf{N}^{th^T} \left[(1-n)\rho_s C_s + n\rho_w C_w \right] \mathbf{N}^{th}\, dV$$

Cohesive forces

$$\dot{\mathbf{F}} = \int_{\Omega_E} \mathbf{N}^T \dot{\mathbf{f}}\, dV + \int_{\Gamma_E} \mathbf{N}^T \dot{\mathbf{t}}\, d\Gamma + \boxed{\int_{\Gamma_{E\,crack}} \mathbf{N}^T \dot{\mathbf{c}}\, d\Gamma} \qquad \mathbf{H}_{th} = \int_{\Omega_E} \left(\nabla \mathbf{N}^{th} \right)^T \lambda \nabla \mathbf{N}^{th}\, dV - \int_{\Omega_E} \left(\nabla \mathbf{N}^{th} \right)^T \rho_w C_w\, \mathbf{q}\, \mathbf{N}^{th}\, dV$$

$$\mathbf{G}_p = \int_{\Omega_E} \mathbf{N}^{p^T} q_E\, dV + \int_{\Gamma_E} \mathbf{N}^{p^T} q^\Gamma\, d\Gamma + \sum \mathbf{N}^{p^T} Q - \int_{\Omega_E} \left(\nabla \mathbf{N}^p \right)^T \frac{\mathbf{k}}{\mu_w} \nabla \left(\rho_w\, \mathbf{g}\, h \right) dV$$

2D & 3 D Crack nucleation

- **Maximum principal tensile stress criterion**
- Advancing fracture & **remeshing**
- Boundary conditions modifications
- Coulomb friction

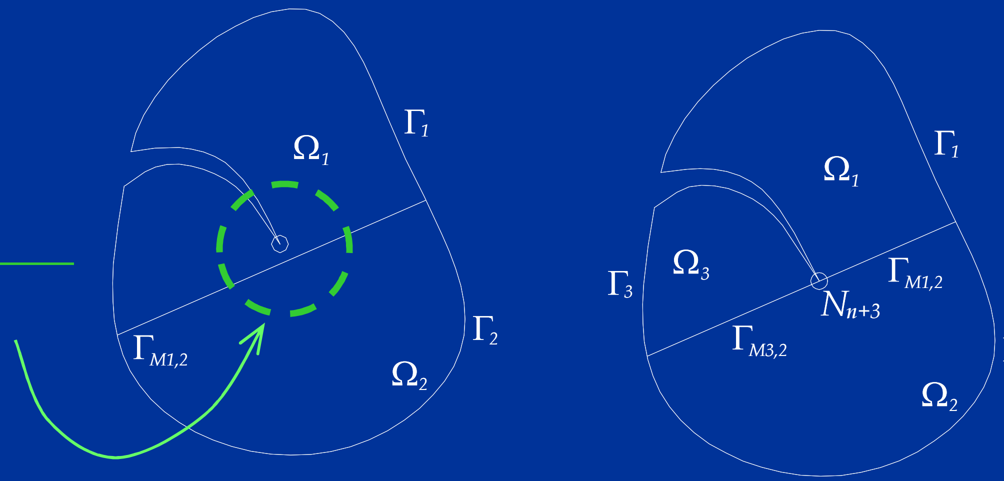

Nucleation: new nodes are created

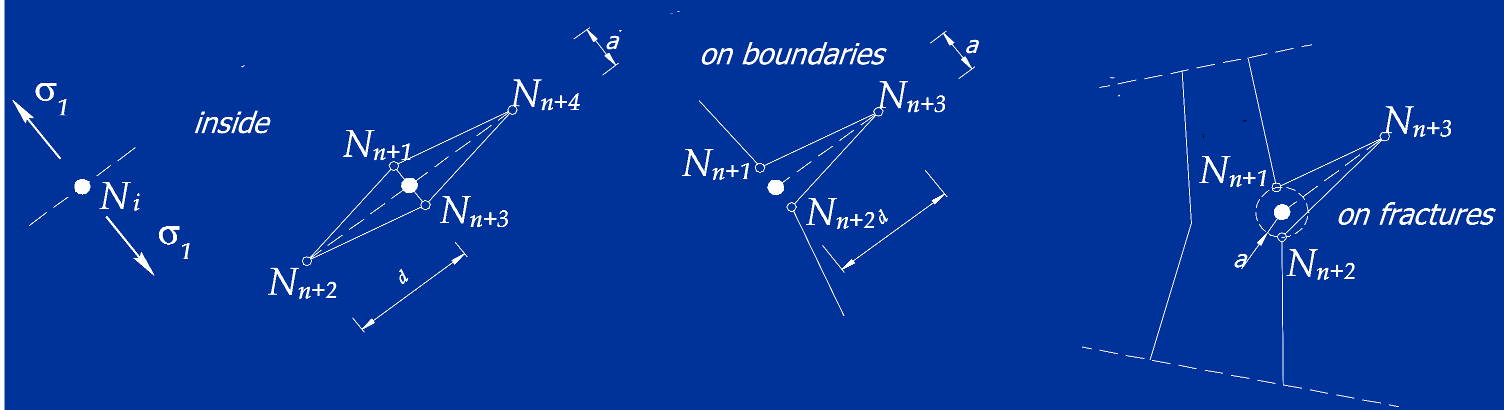

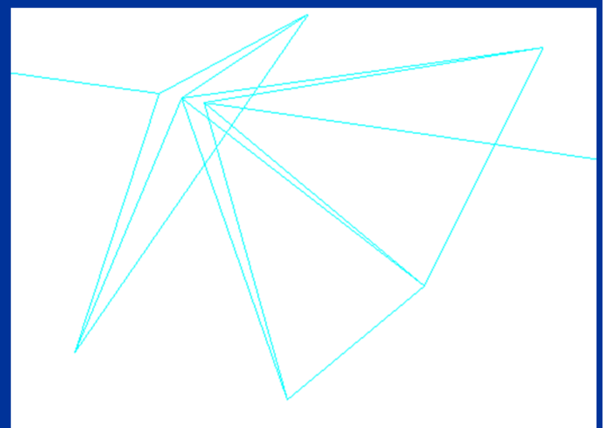

2D & 3 D Crack advancement

Nucleation types:

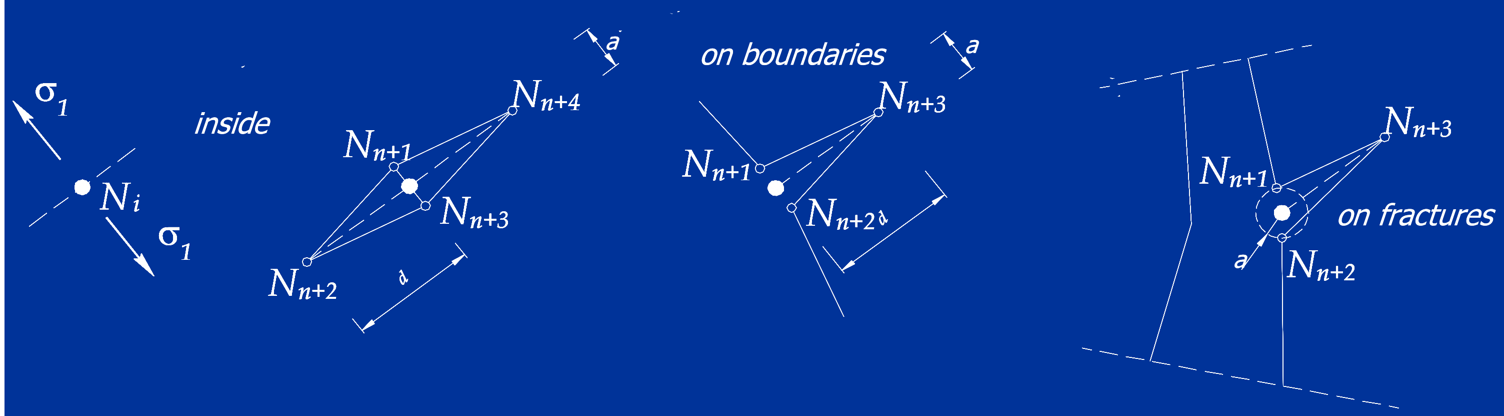

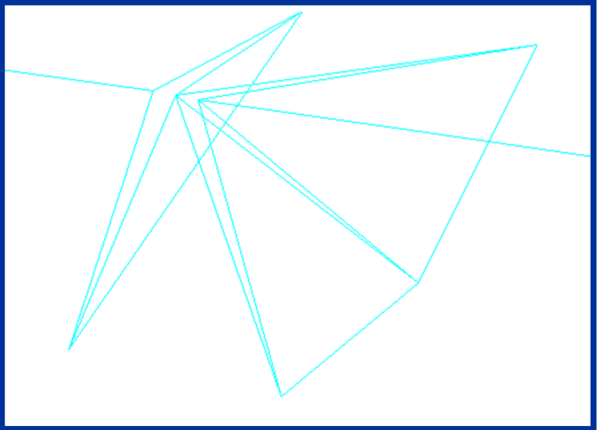

In **2D** the fracture follows directly the direction normal to the maximum principal tensile stress while in **3D** the fracture follows the face of the element around the fracture tip which is closest to the normal direction of the maximum principal tensile stress; the fracture tip (front) becomes a curve in space

Crack tip advancement – time stepping

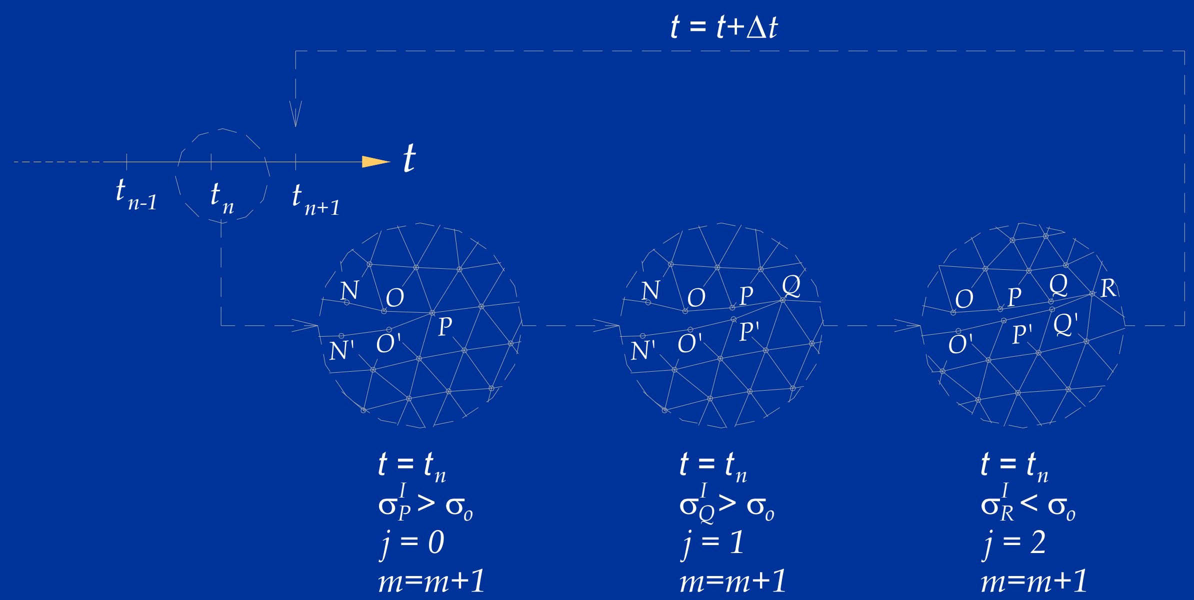

At each time station t_n **j successive front advancements** are possible **within the same time step** (in 2D and 3D) until the Rankine criterion is satisfied (**no interference between crack tip advancement algorithm and time stepping**) : jumps allowed within a time step

Remeshing strategy

Projection of vector V_n

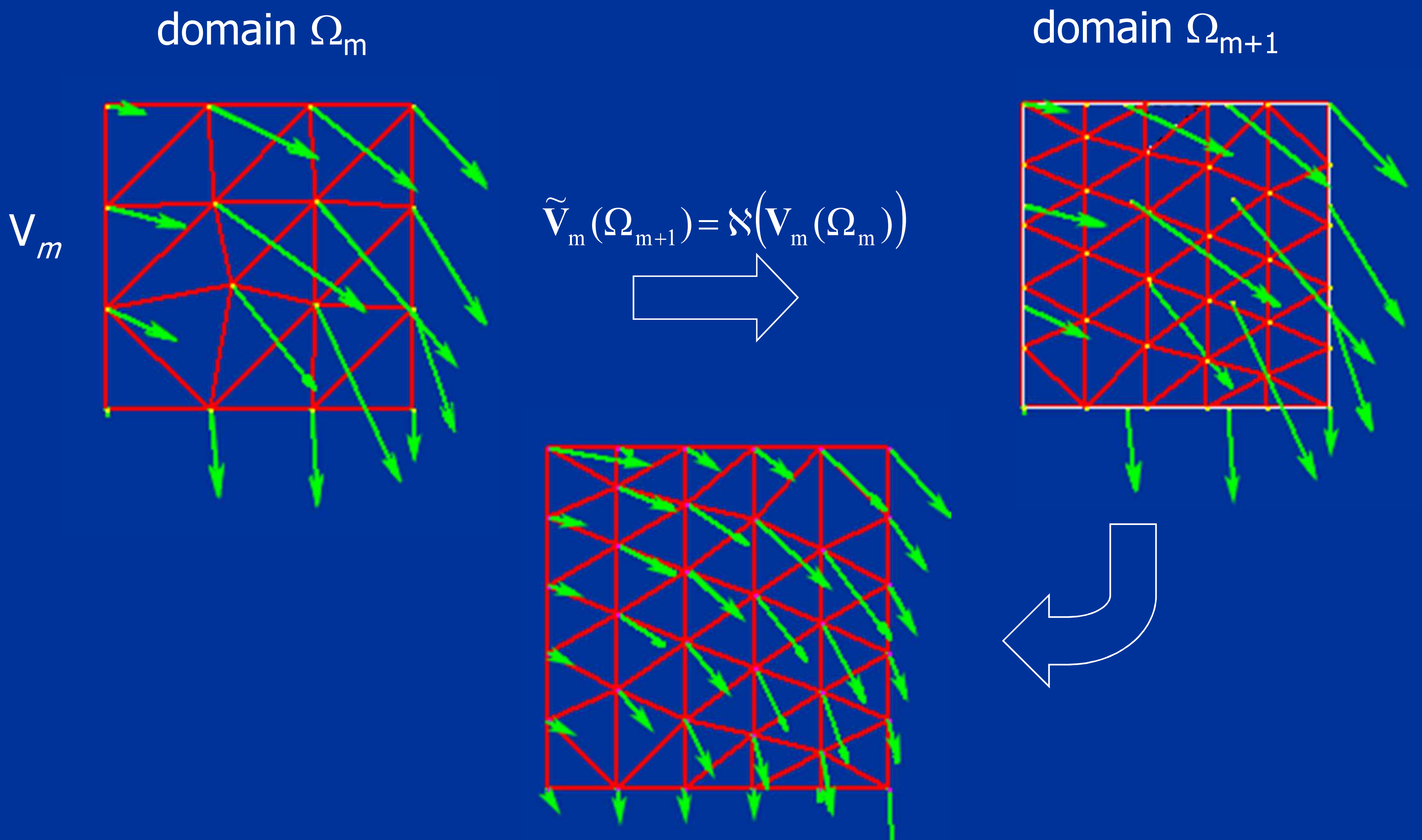

General algorithm: adaptivity in time and space

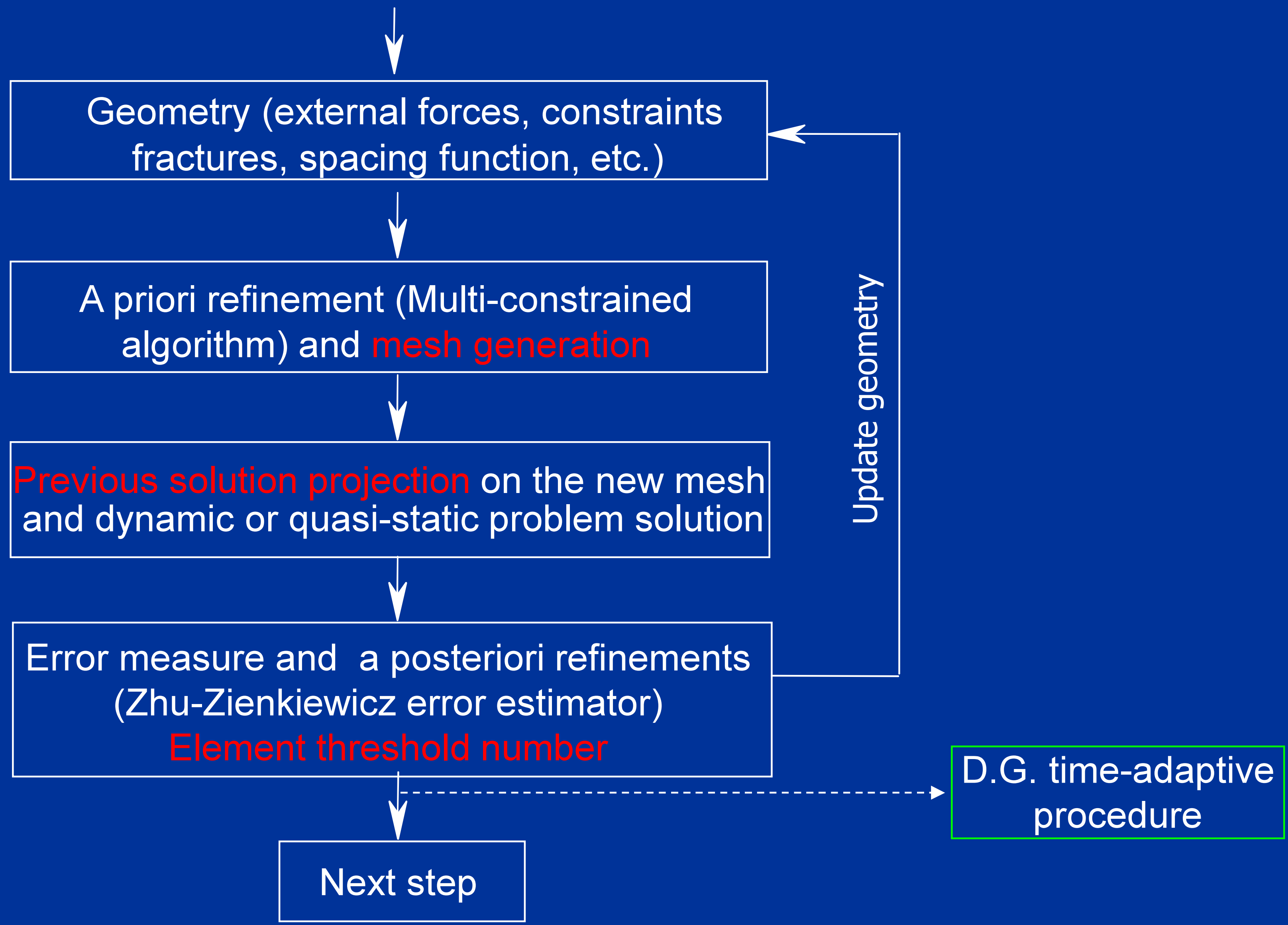

Element threshold number algorithm

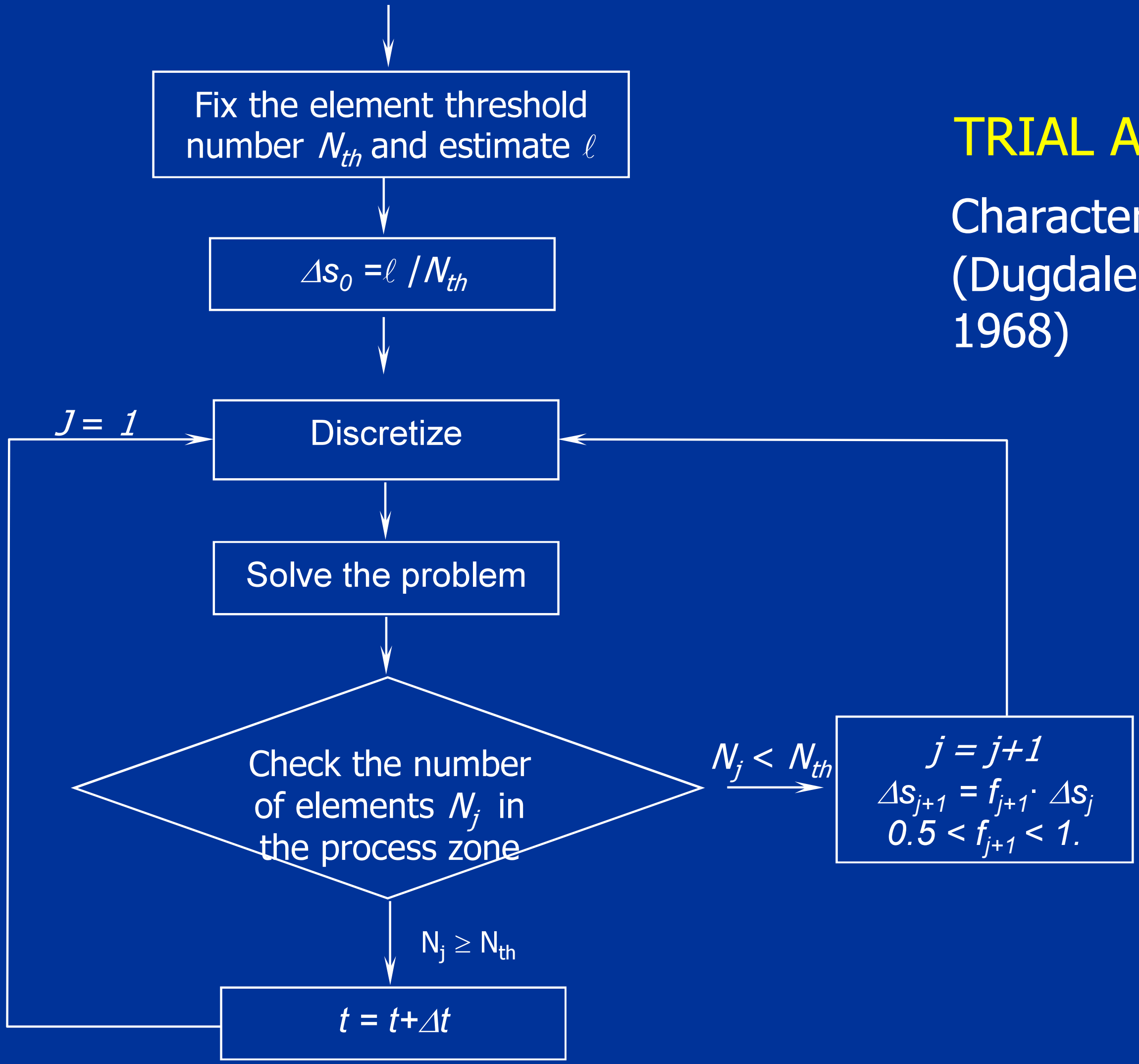

TRIAL ADVANCING STEP

Characteristic cohesive zone size ℓ (Dugdale, 1960; Barenblatt, 1962; Rice, 1968)

$$\text{e.g.:}\ \ell = \frac{\pi E G_c}{8(1-\nu^2)\sigma_0^2}$$

$$\Delta s_{trial} = \frac{\ell}{N_{min}}$$

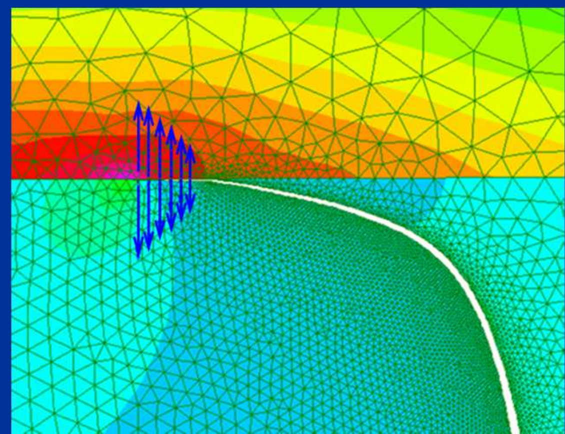

Hydraulic fracturing

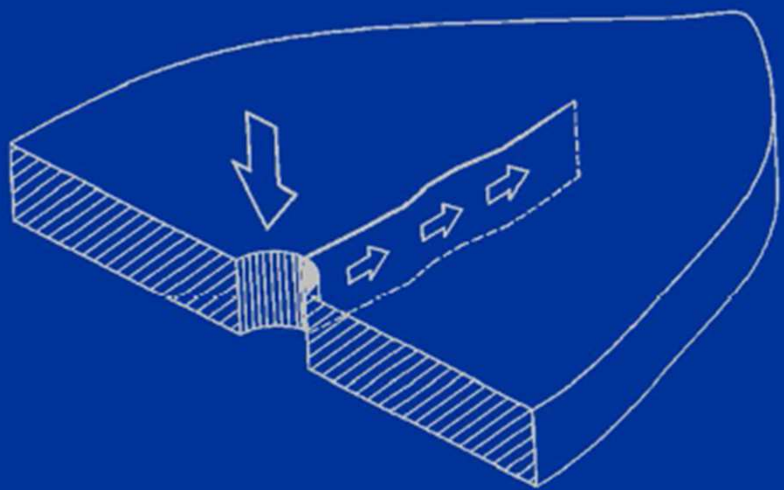

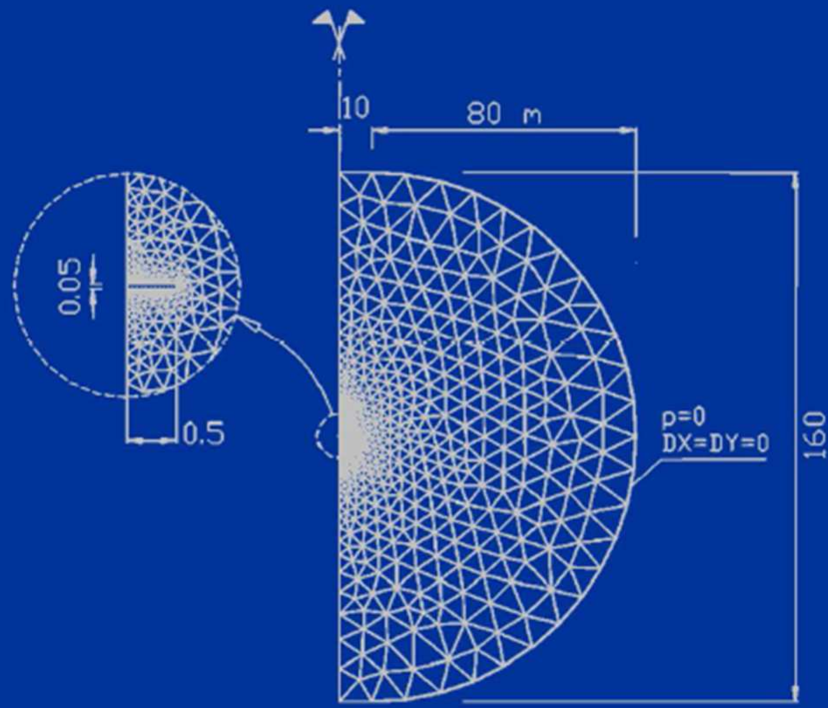

Permeability coefficient	κ	2×10^{-5}	m^2/(MPa s)
Shear modulus	G	6000	MPa
Drained Poisson's ratio	ν	0.2	
Undrained Poisson's ratio	ν_u	0.33	
Skempton's coefficient	B	0.62	
Bulk modulus, solid	K_s	36000	MPa
Bulk modulus, fluid	K_f	3000	MPa
Porosity	η	0.19	
Fluid viscosity	μ	10^{-9}	MPa s

Schrefler, Secchi, Simoni, 2006

Hydraulic fracturing

Fracture propagation

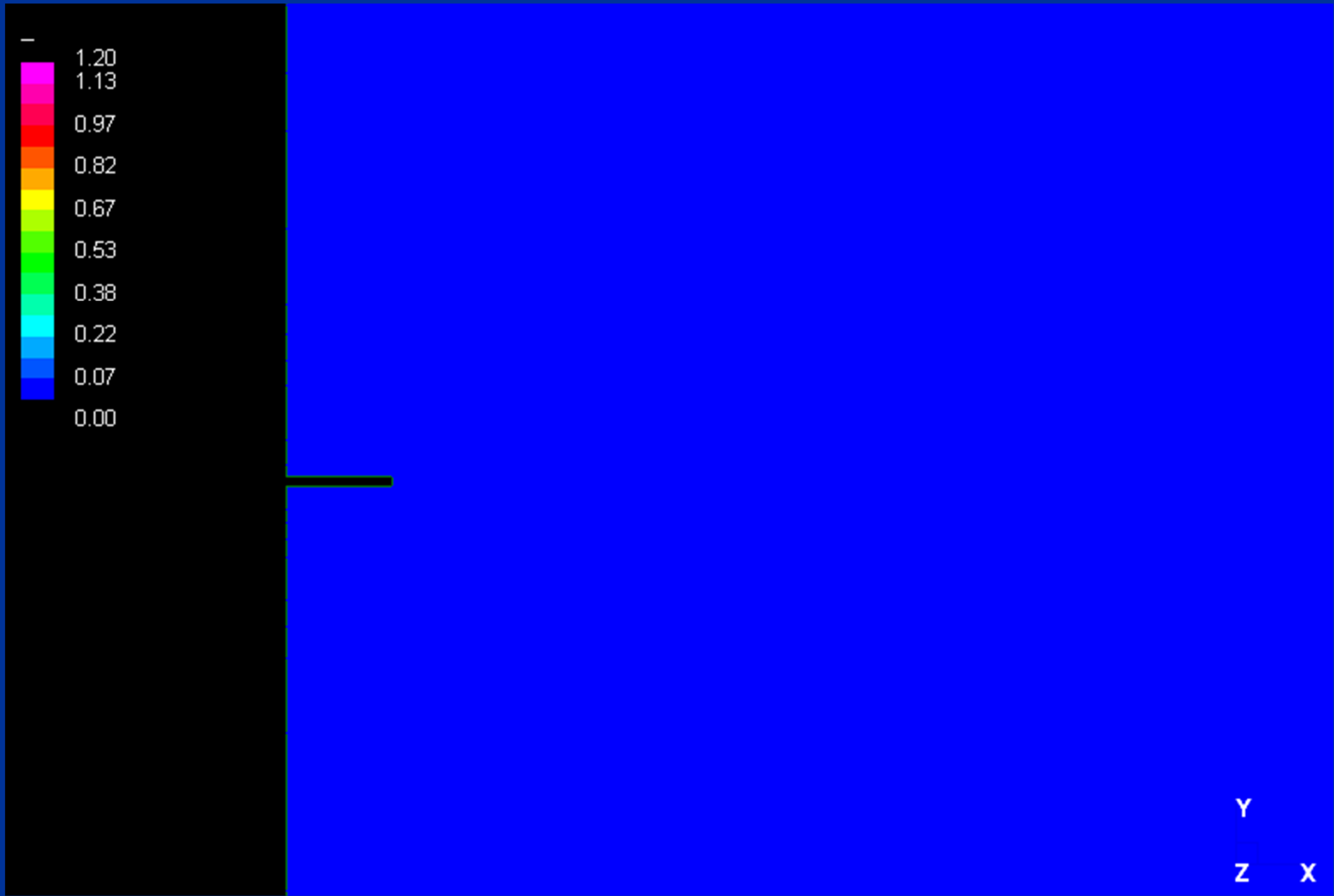

Mouth pressure

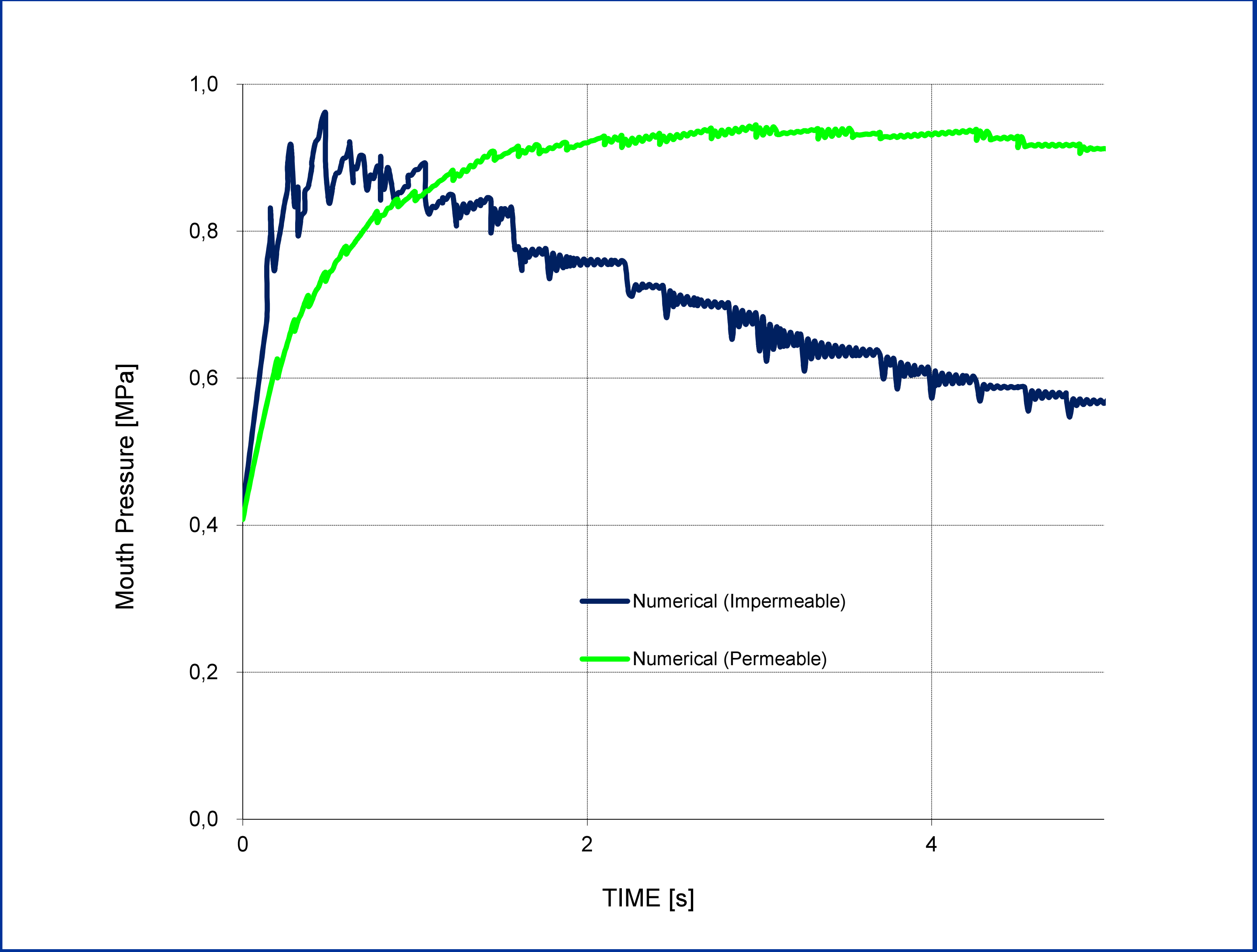

Effect of Viscosity

Pressure [MPa]
t = 10 s

Lower viscosity ($1x10^{-11}$ MPa s) ***Higher viscosity ($1x10^{-9}$ MPa s)***

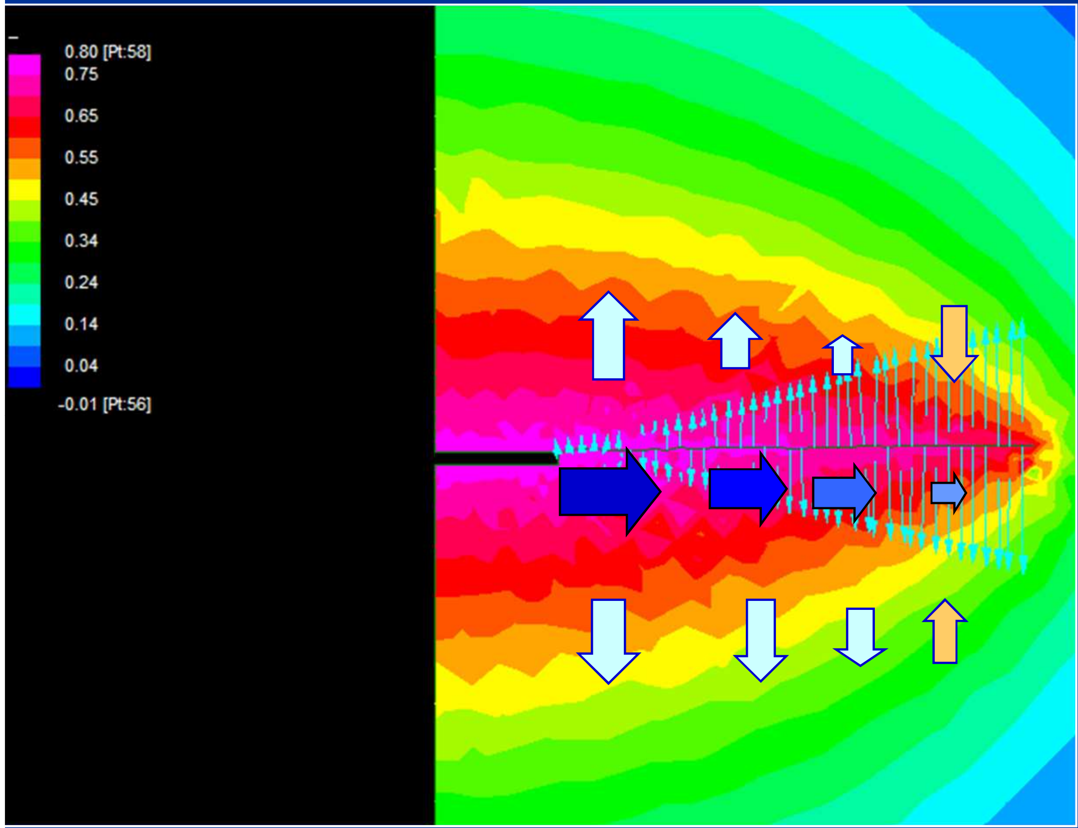

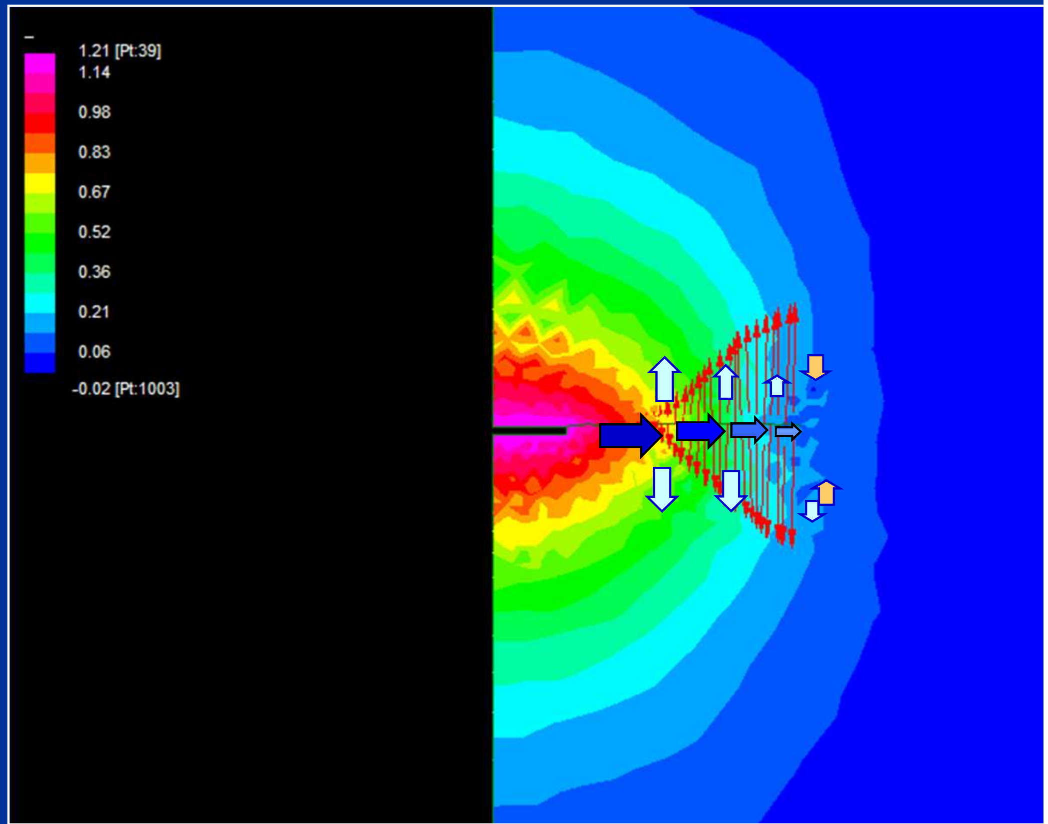

Effect of Viscosity and Injection Rate

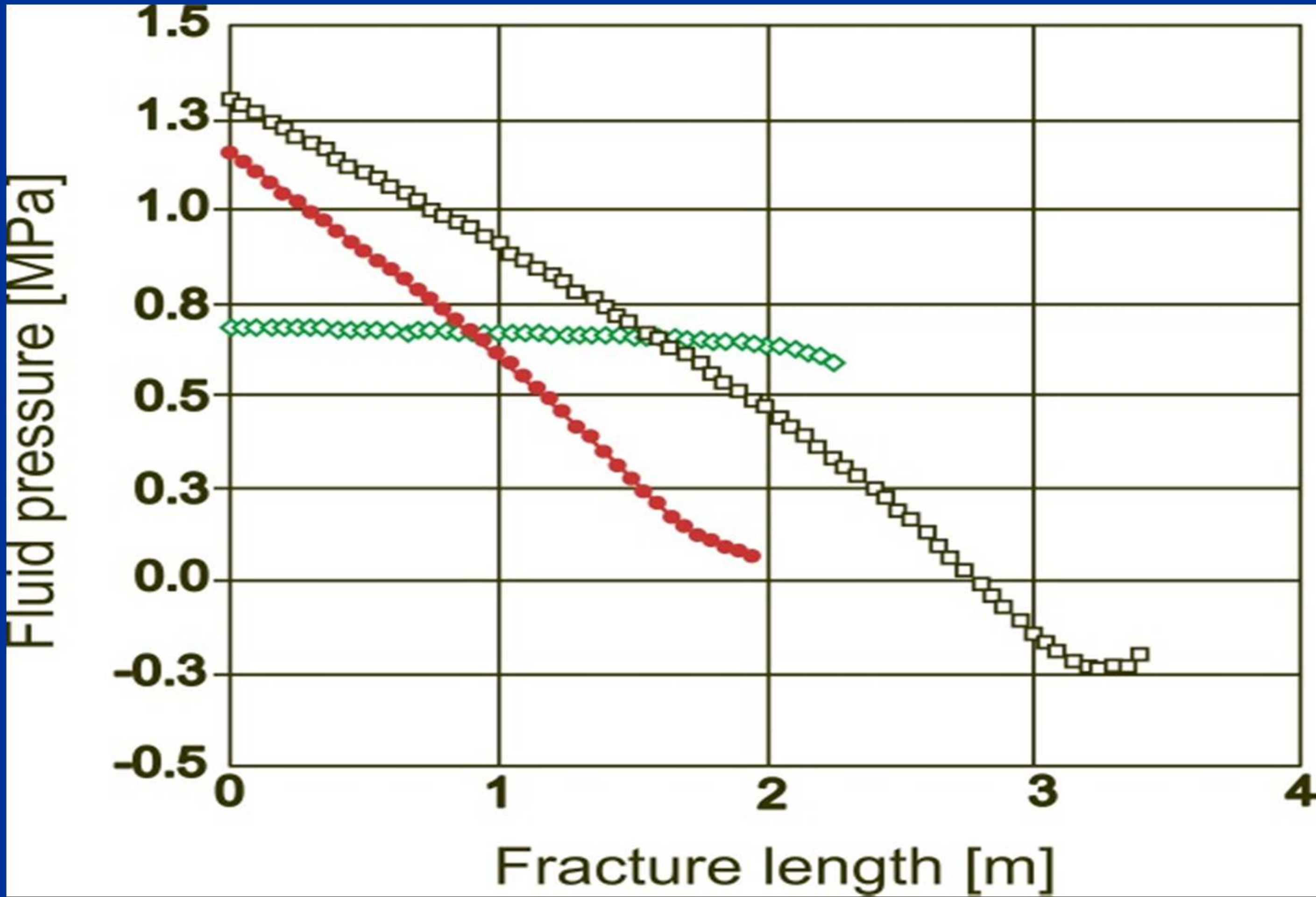

Distribution of the fluid pressure over the fracture length at time station 10 min for different permeabilities and pumping rates

Crack length/time

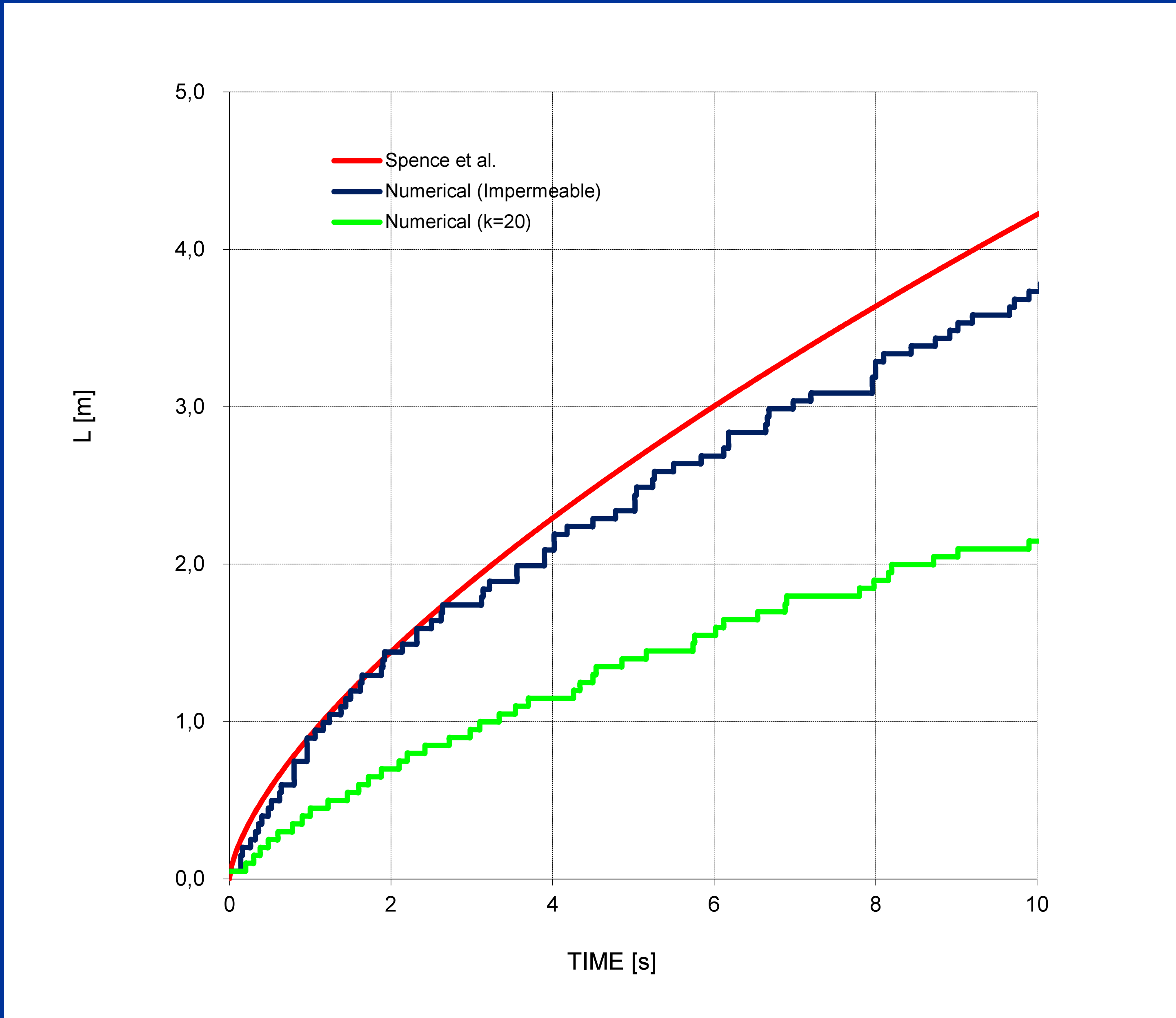

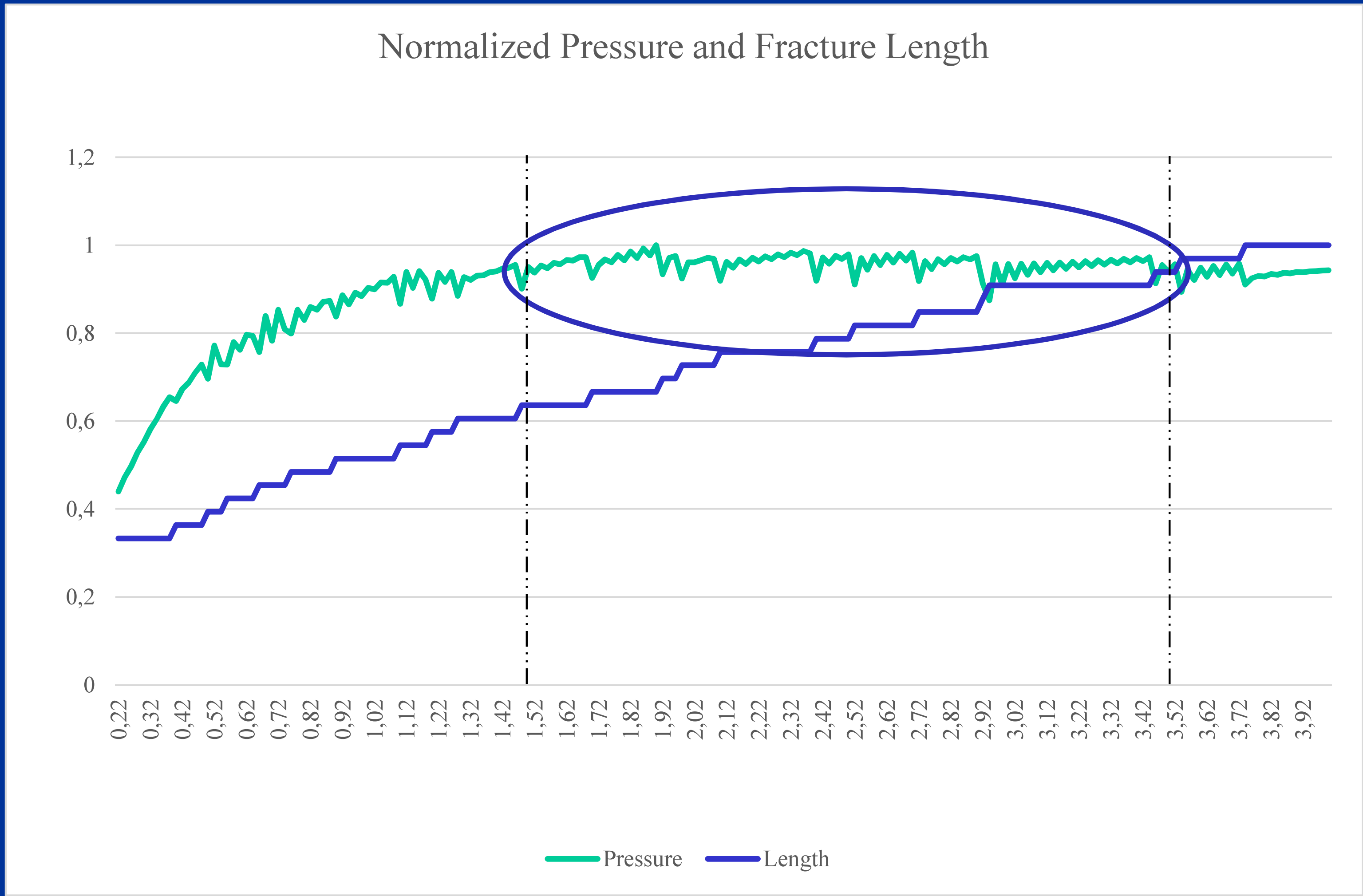

Pressure drop

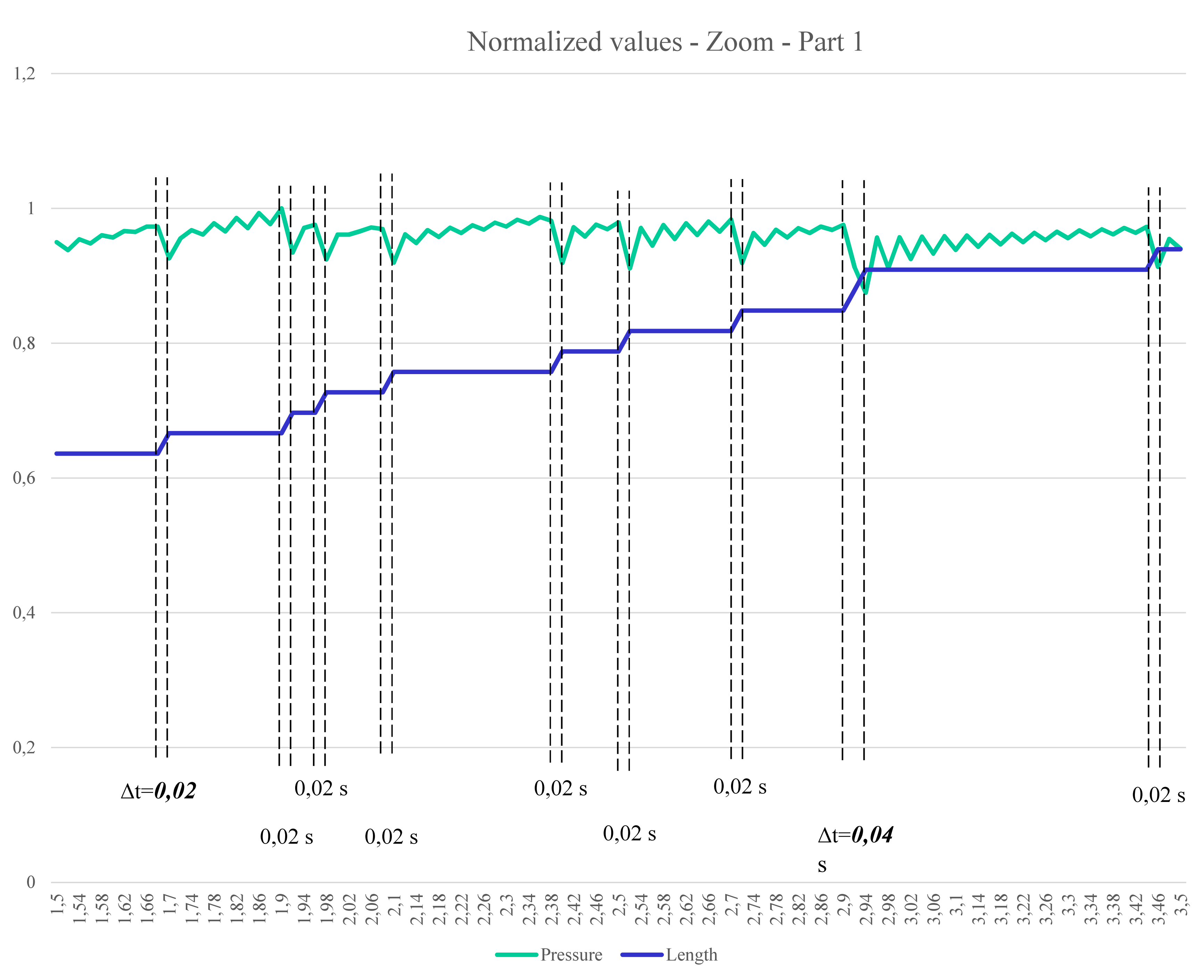

Normalized values - Zoom - Part 1
1,2
1
0,8
0,6
0,4
0,2
0
Δt=0,02
0,02 s
0,02 s
0,02 s
0,02 s
0,02 s
0,02 s
Δt=0,04 s
0,02 s
1,5
1,54
1,58
1,62
1,66
1,7
1,74
1,78
1,82
1,86
1,9
1,94
1,98
2,02
2,06
2,1
2,14
2,18
2,22
2,26
2,3
2,34
2,38
2,42
2,46
2,5
2,54
2,58
2,62
2,66
2,7
2,74
2,78
2,82
2,86
2,9
2,94
2,98
3,02
3,06
3,1
3,14
3,18
3,22
3,26
3,3
3,34
3,38
3,42
3,46
3,5
Pressure
Length

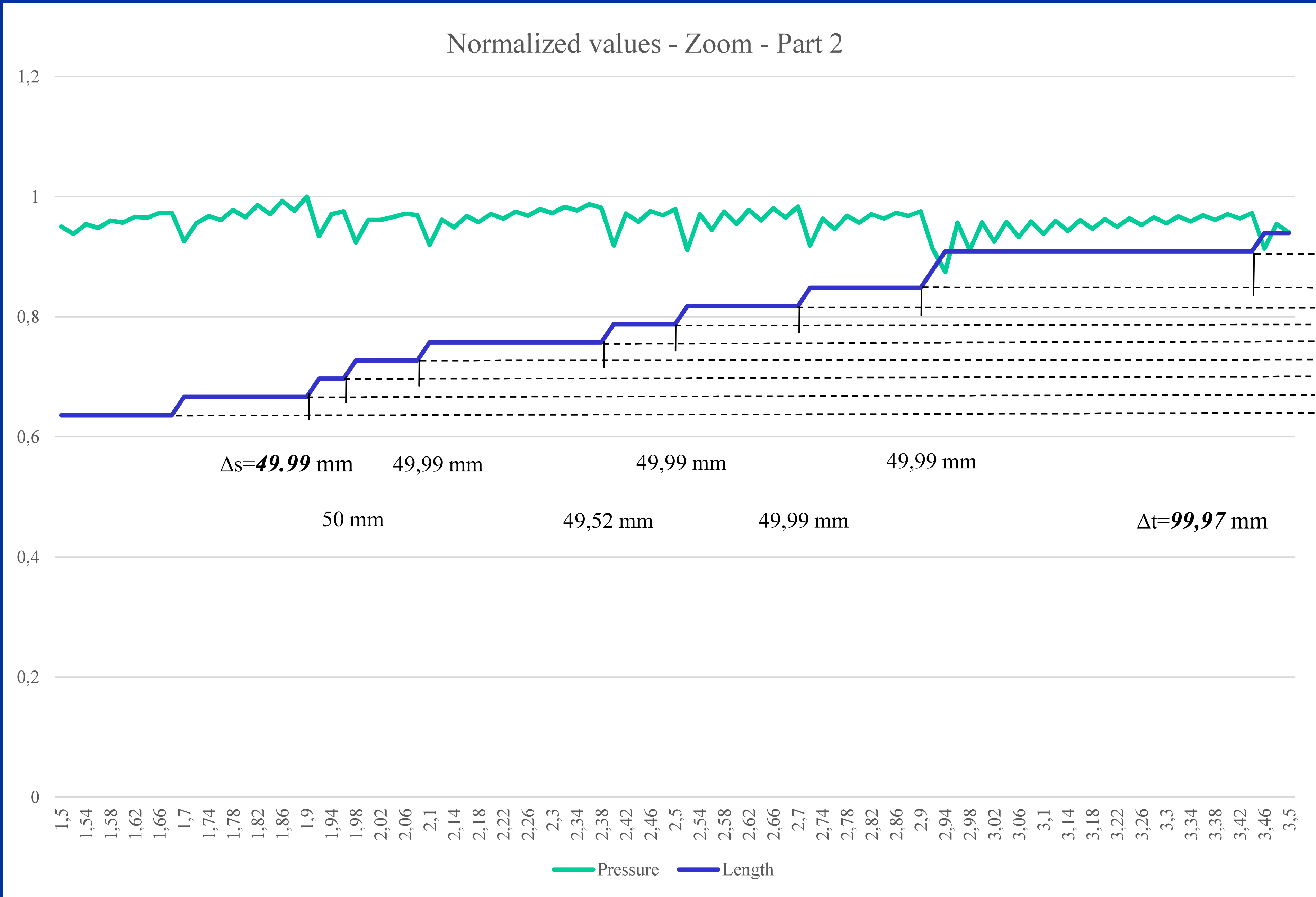

More tip advancements per time step (at least two)

Mesh Size Dependence

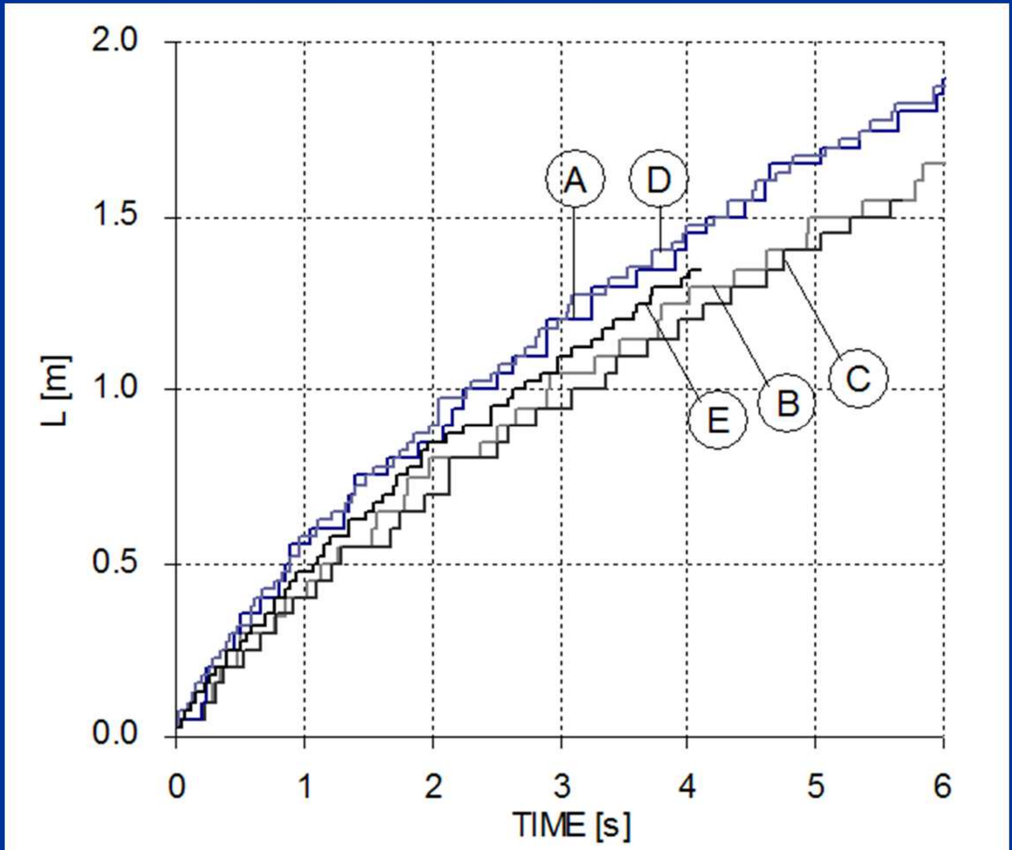

A: Δt=0.05 s, Δs=50 mm

B: Δt=0.02 s, Δs=50 mm

C: Δt=0.01 s, Δs=50 mm

D: Δt=0.02 s, Δs=25 mm

E: Δt=0.01 s, Δs=25 mm

About 30 elements needed along the process zone to get «mesh independent» results

XFEM Mohammadnejad & Khoei, FEAD2013

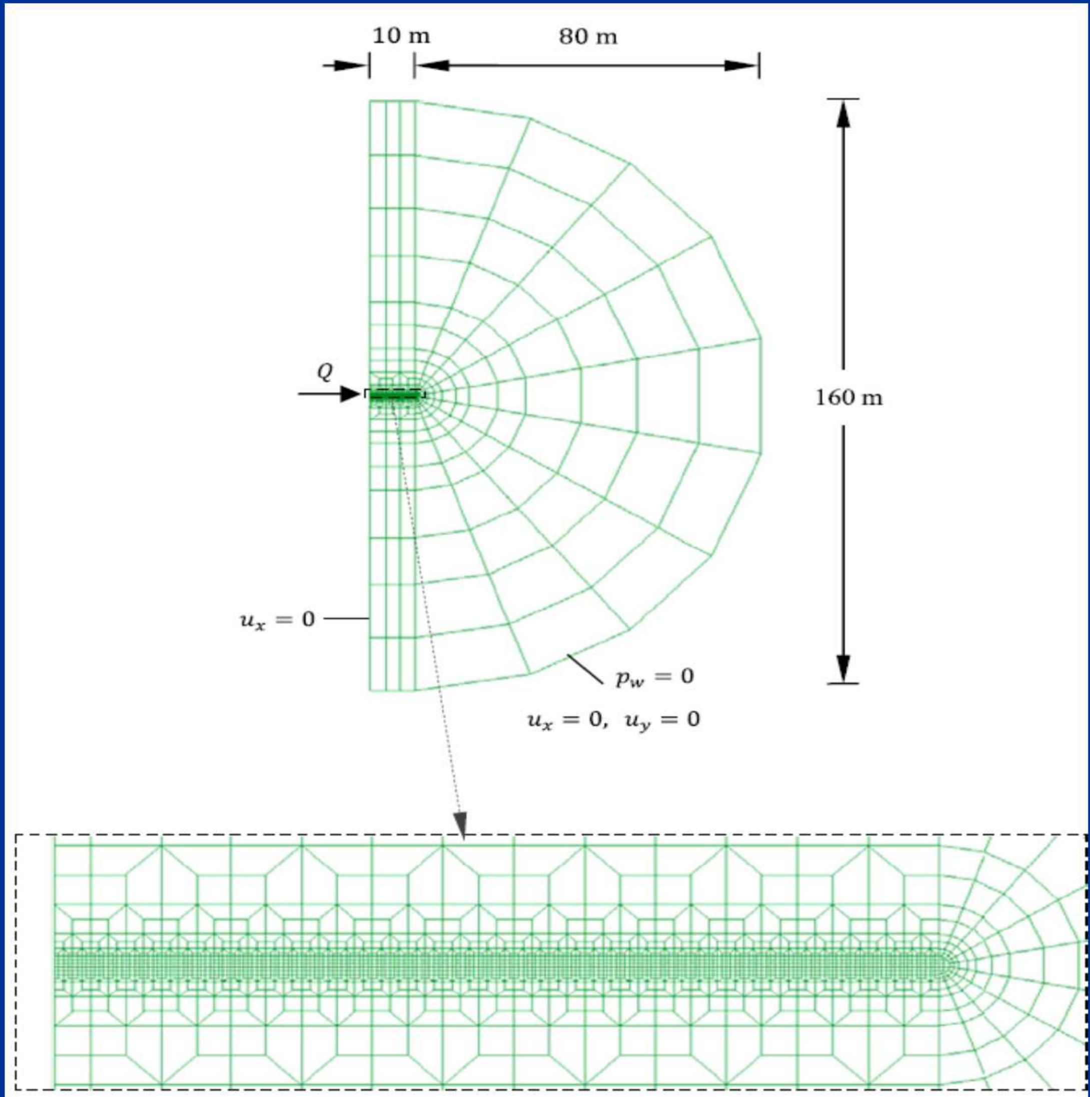

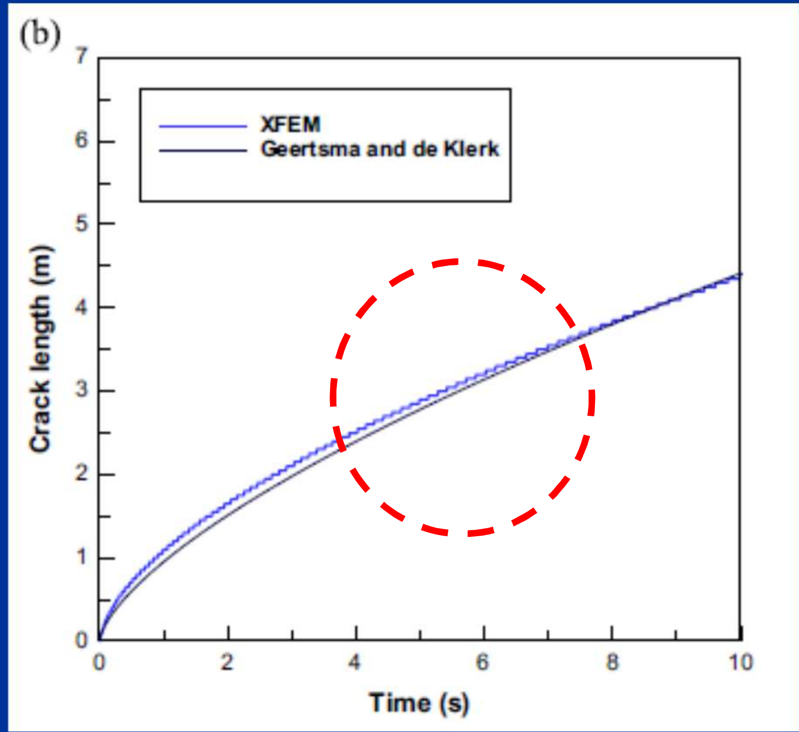

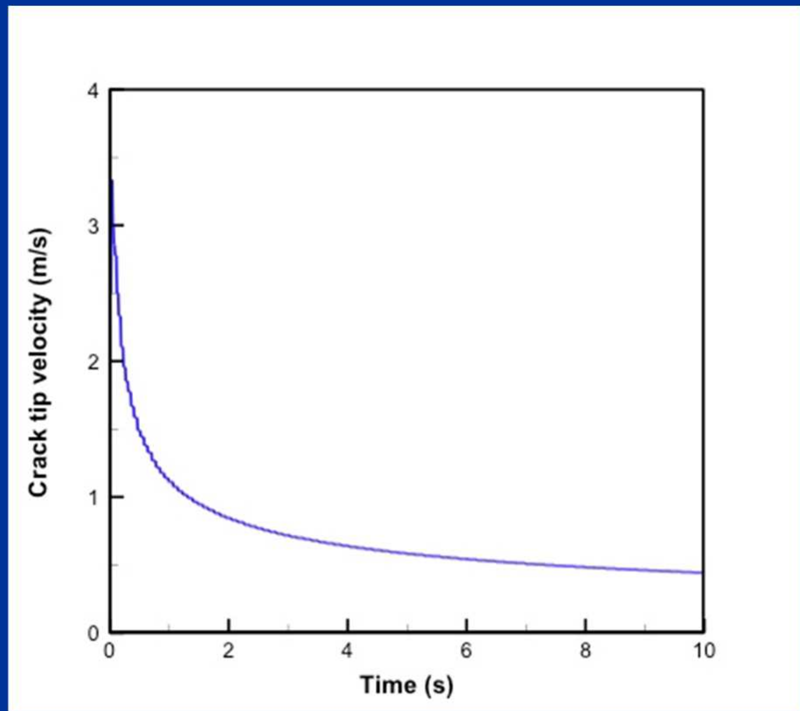

The crack tip velocity at the beginning is roughly 3.3 m/s, then it shows a sudden drop and subsequently approaches a value of .45 m/s at t=10 s. The element size is .05 m, **the elapsed time steps for the crack to pass through one element increases from roughly 1.5 time steps at the beginning to roughly 11 time steps at t=10 s.**

XFEM Mohammadnejad & Khoei, FEAD2013

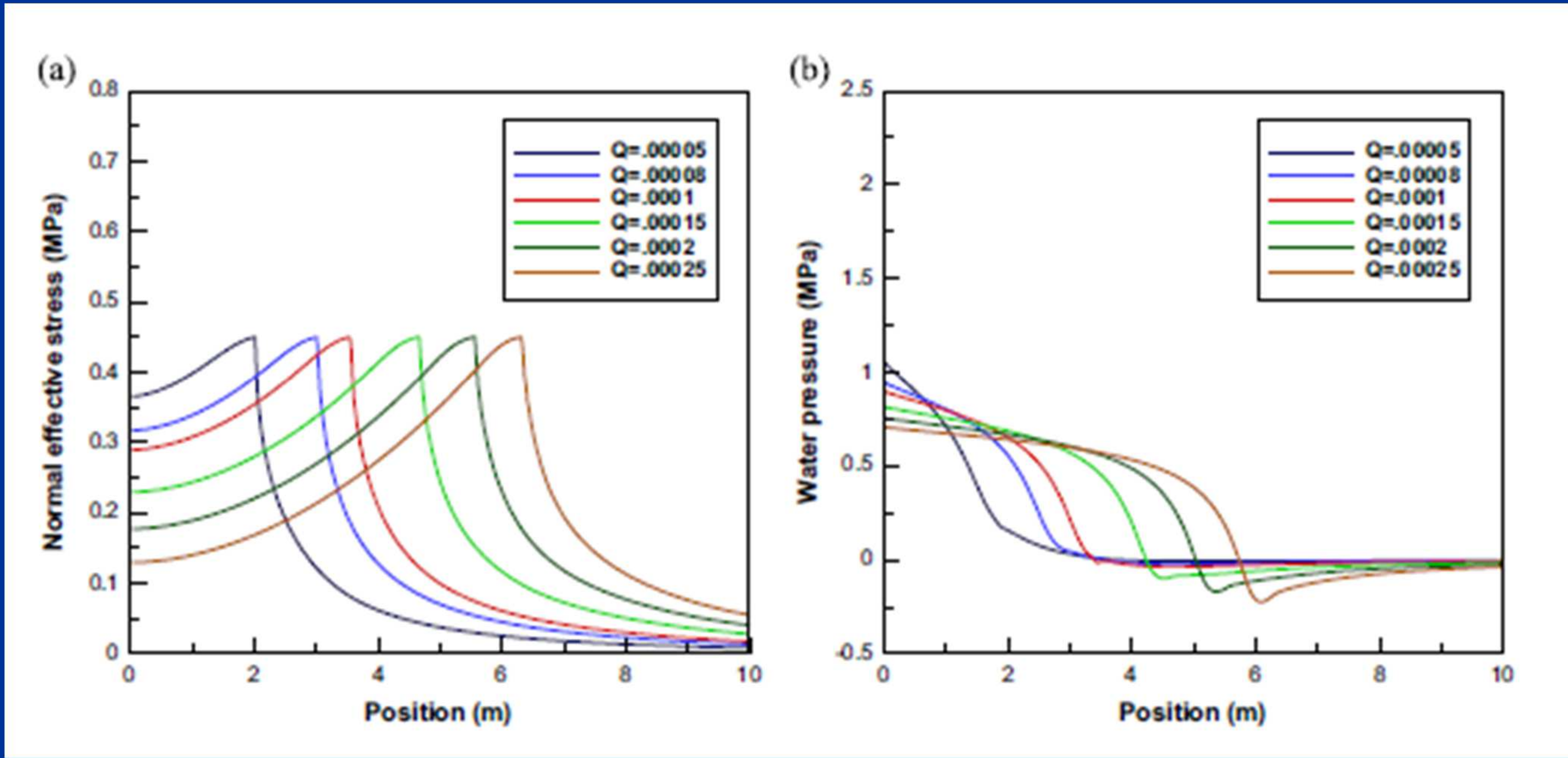

Normal effective stress distribution and water pressure distribution in the direction of the hydraulic fracture propagation at time = 10 s for different injection rates

2D Cohesive fracture in concrete dam

Benchmark ICOLD (homogeneous)

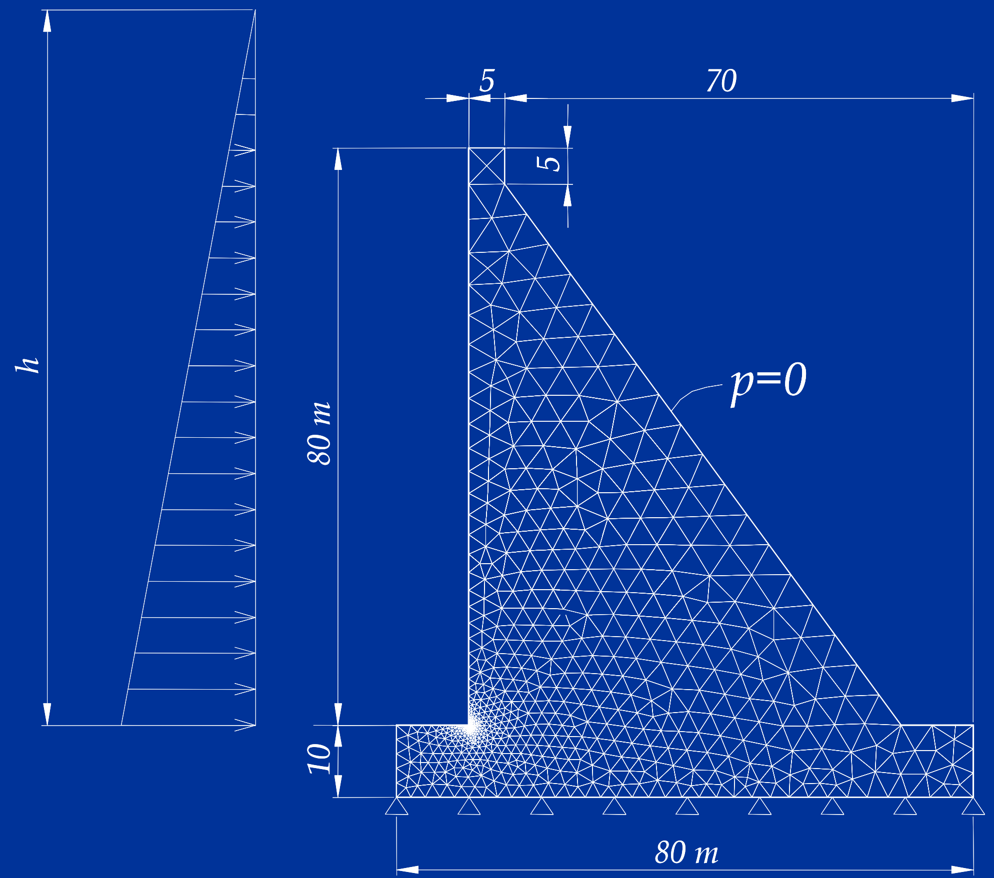

Material data

$\rho = 2400 \ kg/m^3$

$E = 24000 \ MPa$

$\nu = 0.15$

$\sigma_u = 1.3 \ MPa$

$w_c = 0.23 \ mm$

$G_f = 150 \ N/m$

2D Cohesive fracture in concrete dam

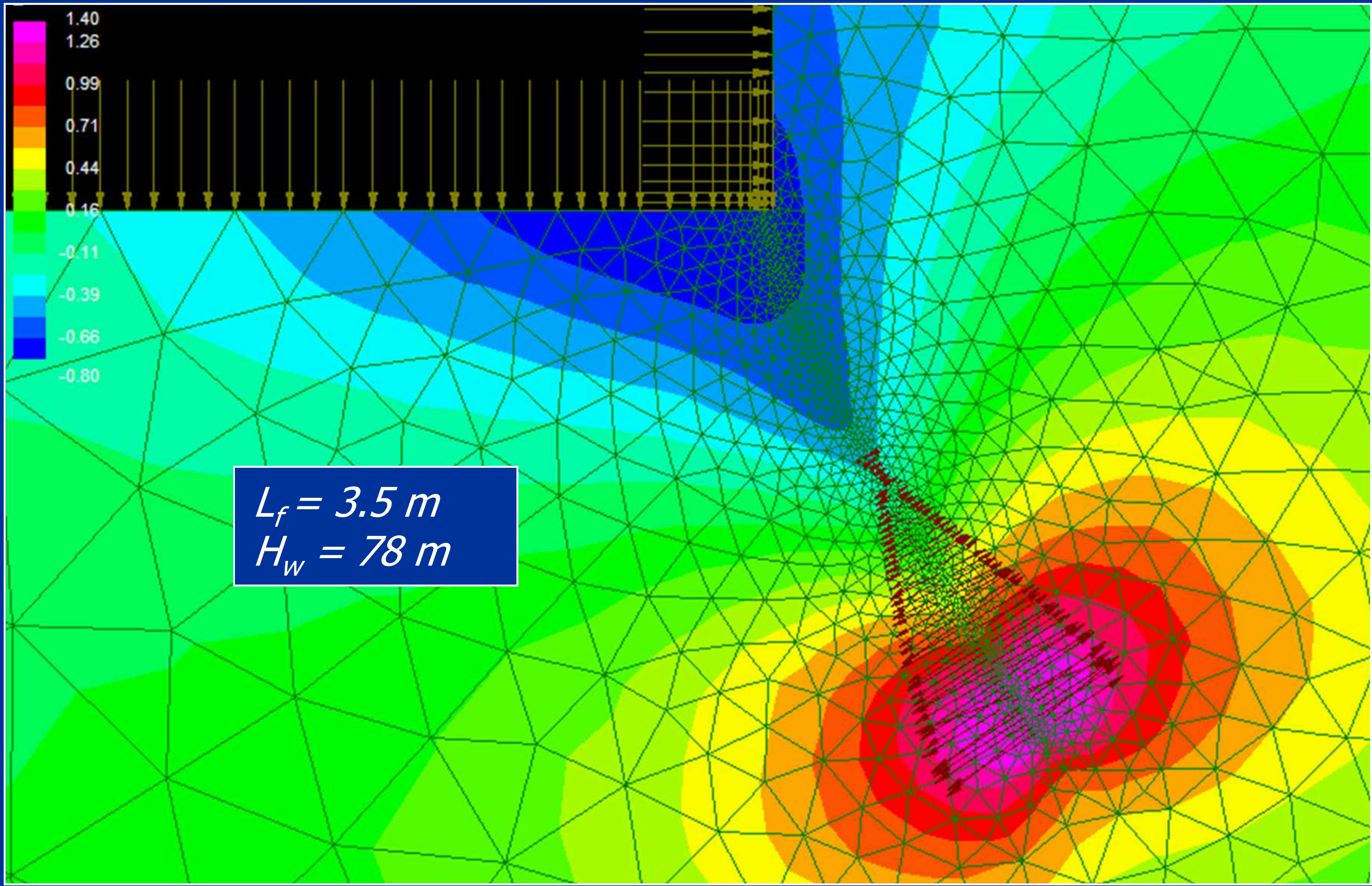

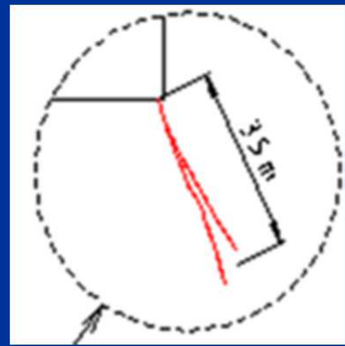

Zoom for the principal stress near the fracture

2D Cohesive fracture in concrete dam

Zoom for the pressure inside the fracture

Horizontal displacements

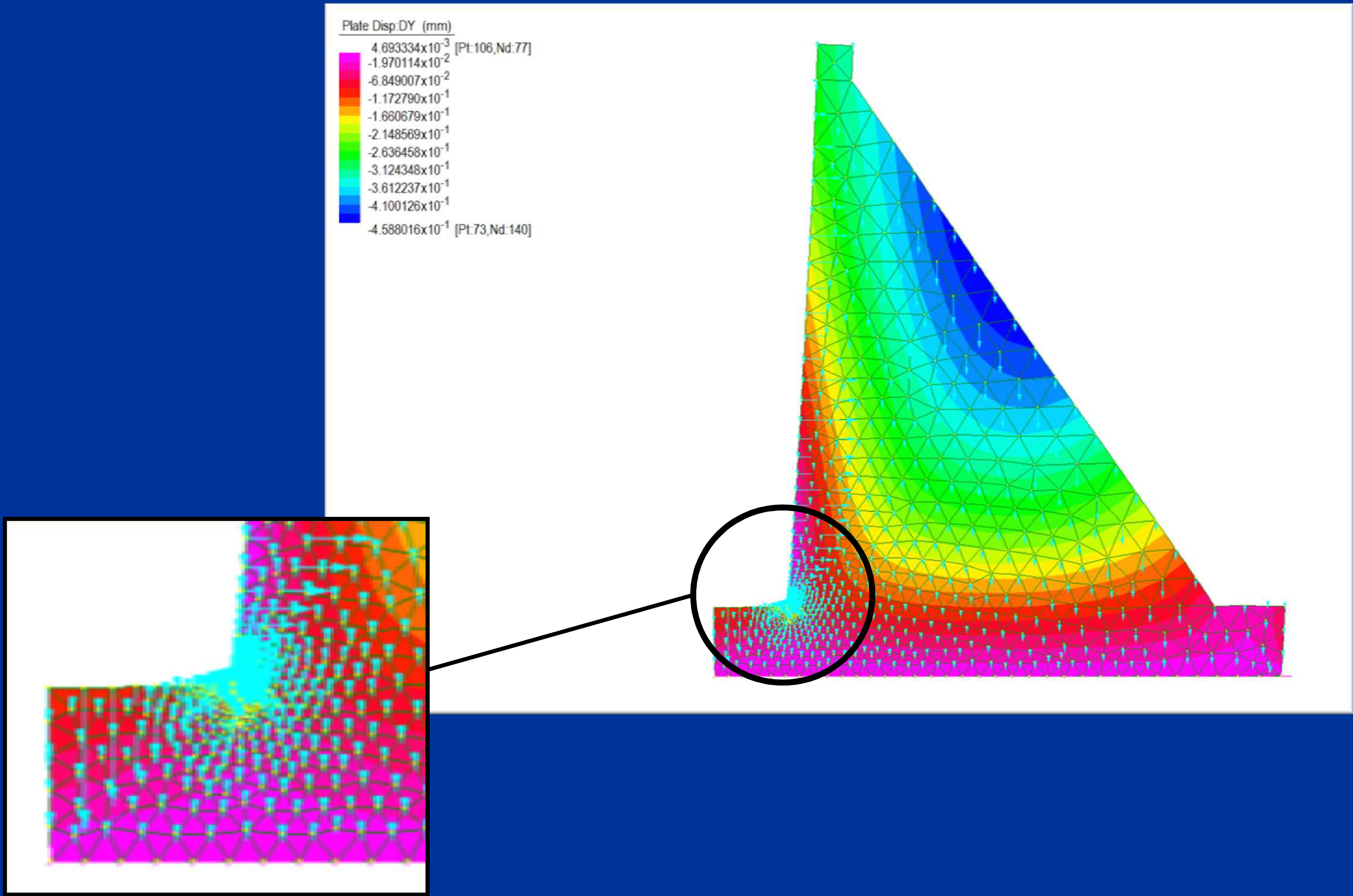

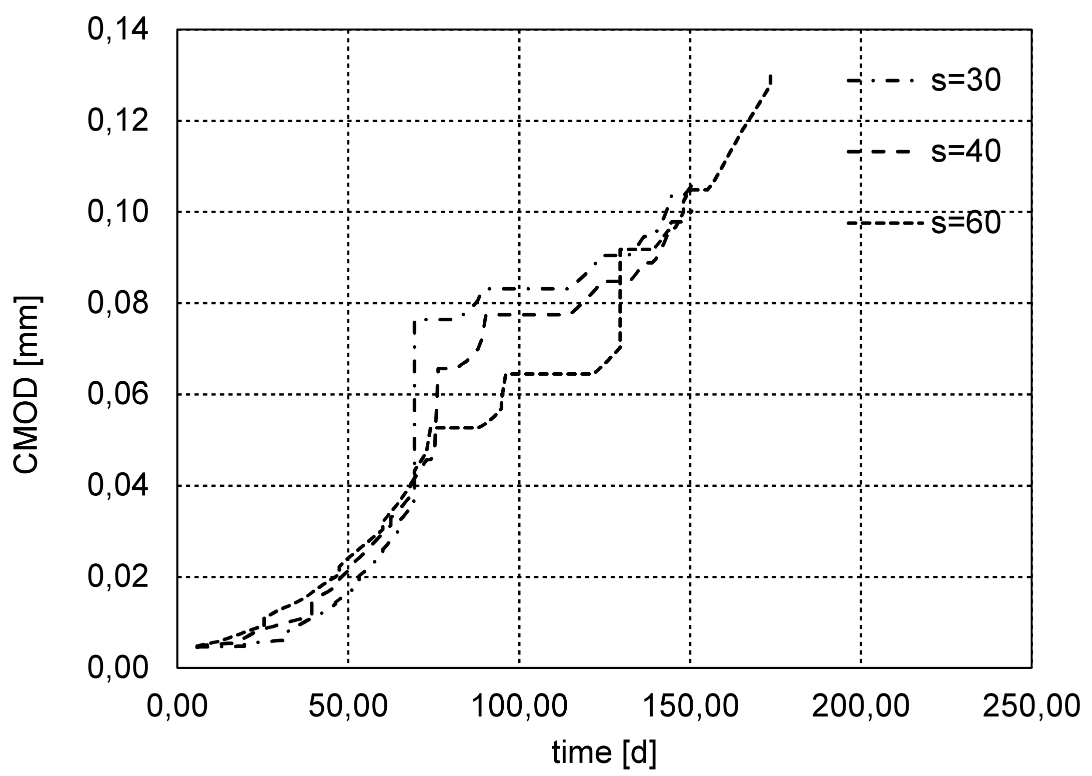

Crack mouth opening displacement versus time (days) for different values of the crack tip advancement s [mm].

3-D example of hydraulic fracturing in a dam

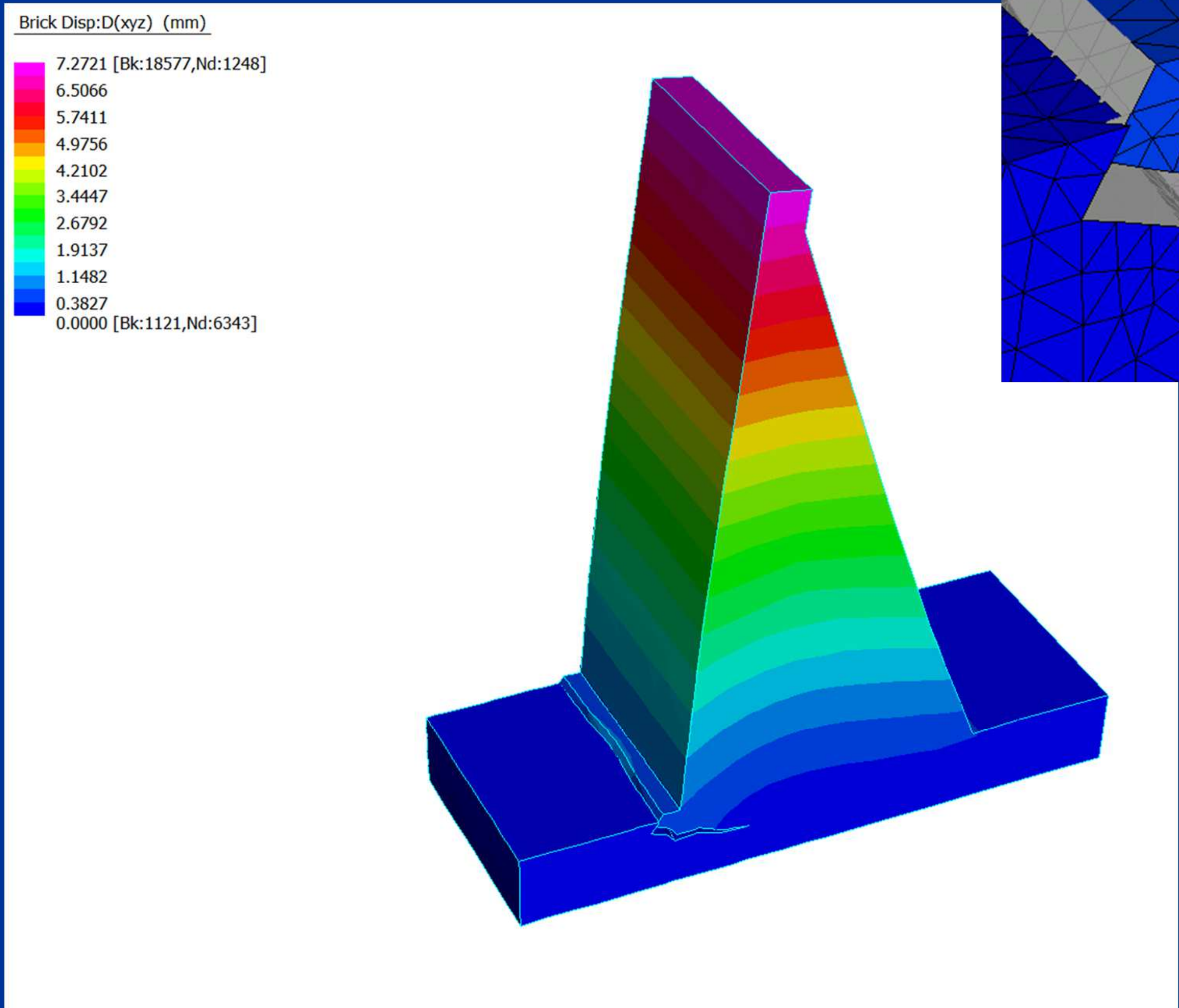

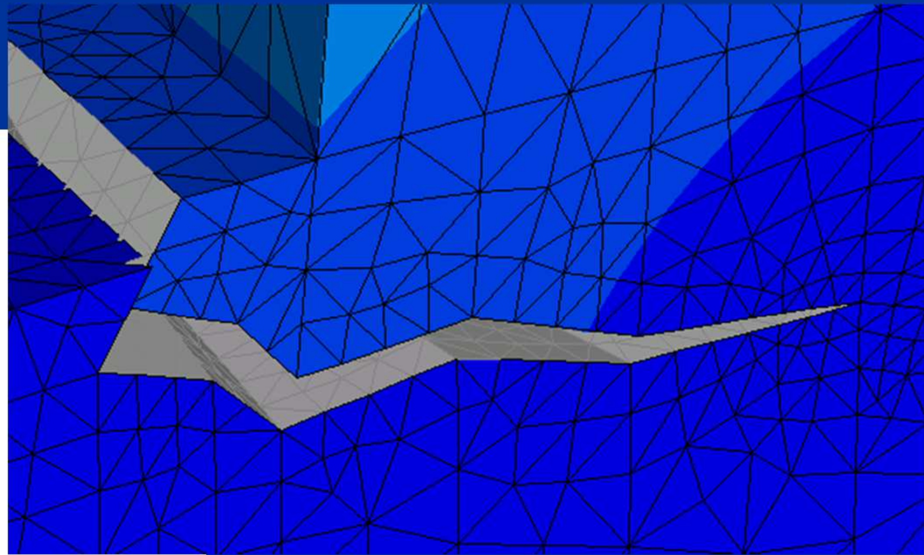

3-D example of hydraulic fracturing in a dam

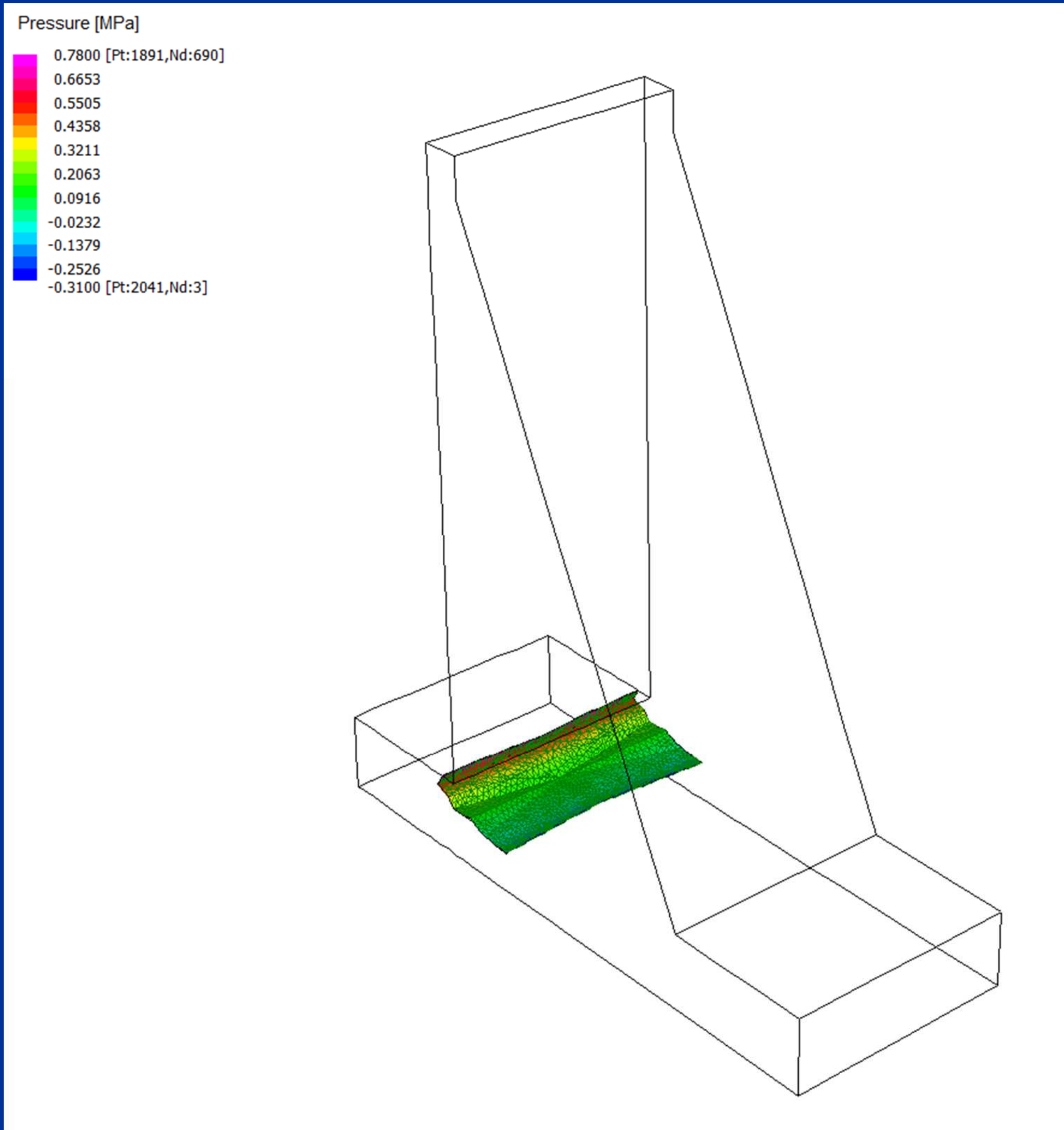

3-D example of hydraulic fracturing in a dam

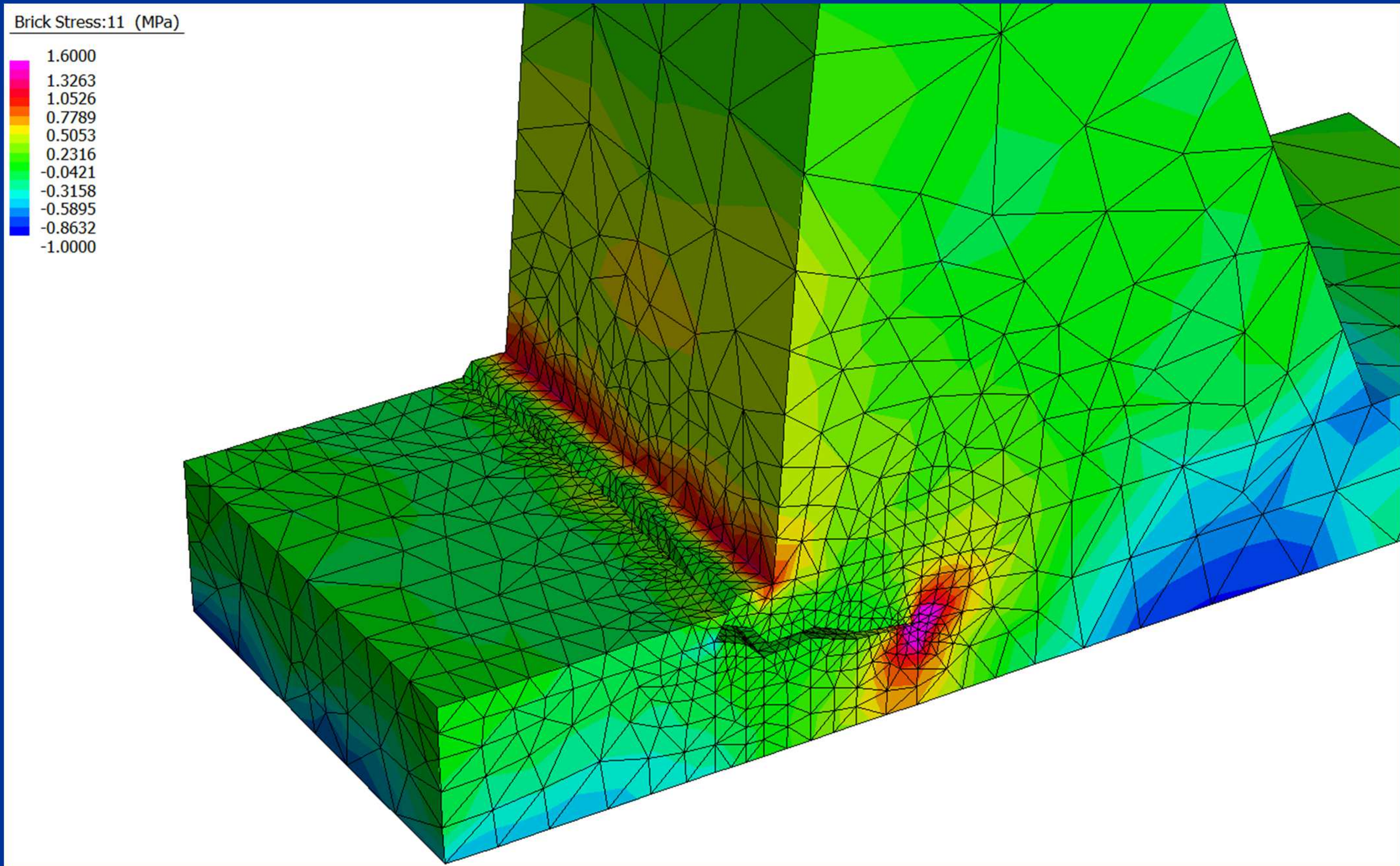

Horizontal displacements of the top

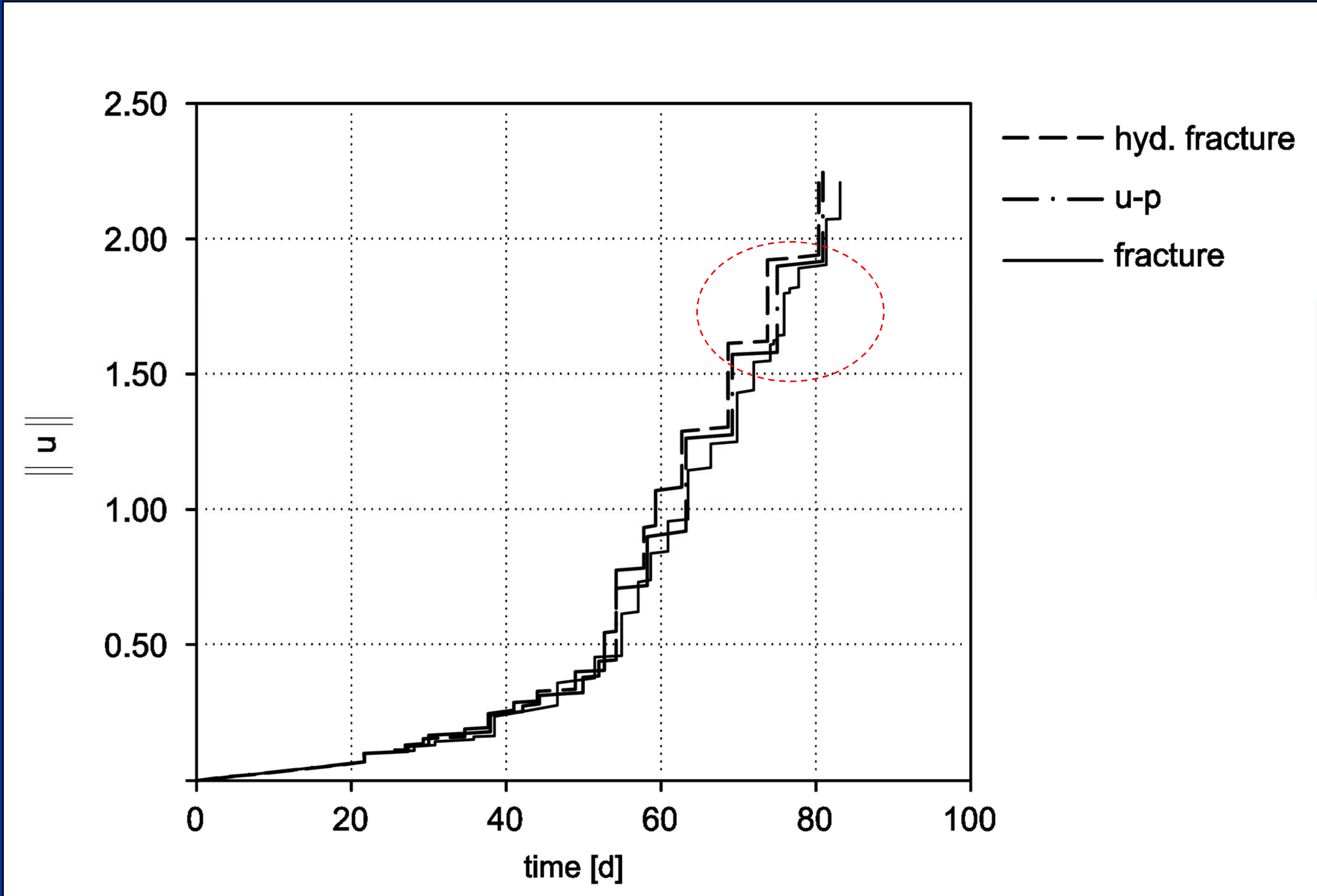

$$\|u\| = \left(\frac{u_i}{u_{el}} - 1 \right) \cdot 100$$

Pressure and stress fluctuations at the crack tip

XFEM

XFEM

General features

Why X-FEM? Which advantages?

- Discontinuities can be extended or added at any moment and in any direction
- No *remeshing*
- The topology of the FE mesh is not modified
- No alignment between elements and crack path is required
- Relatively coarse meshes can be used
- Cohesive constitutive models can be used

TU/e Technische Universiteit Eindhoven University of Technology

General features

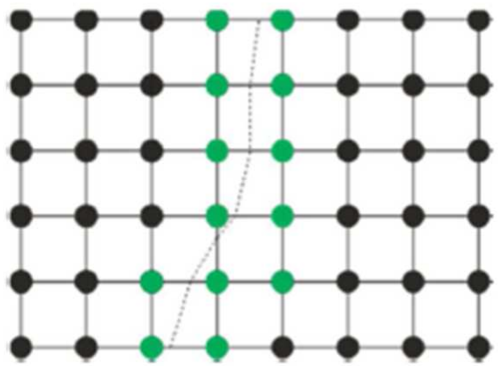

Jump in the displacement field:

$$\vec{u}(\vec{x},t) = \underline{\hat{\vec{u}}(\vec{x},t)} + \underline{\boxed{\mathcal{H}_{\Gamma_d}}(\vec{x})\tilde{\vec{u}}(\vec{x},t)}$$

Heaviside step function

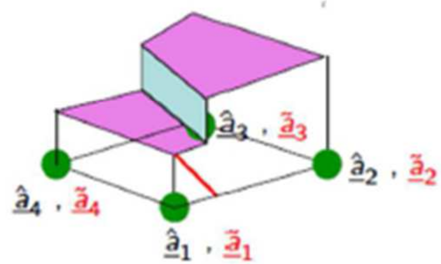

Technische Universiteit Eindhoven University of Technology

Governing equations: local momentum balance

Local momentum balance

Stress continuity over the crack surface reads:

$$\boldsymbol{\sigma} \cdot \vec{n}^{+} = \vec{t}_d - p\vec{n}^{+}$$

Described with a cohesive law

Governing equations: local mass balance

Local mass balance:

- Fluid flow from the formation into the crack:

$$\vec{q}^{+}_{\Gamma_d} \cdot \vec{n}^{+} + \vec{q}^{-}_{\Gamma_d} \cdot \vec{n}^{-} + [\dot{\vec{u}}]_n - \frac{1}{12\mu}[u]_n^3 \frac{\delta}{\delta s}\frac{\delta p_c}{\delta s} = 0$$

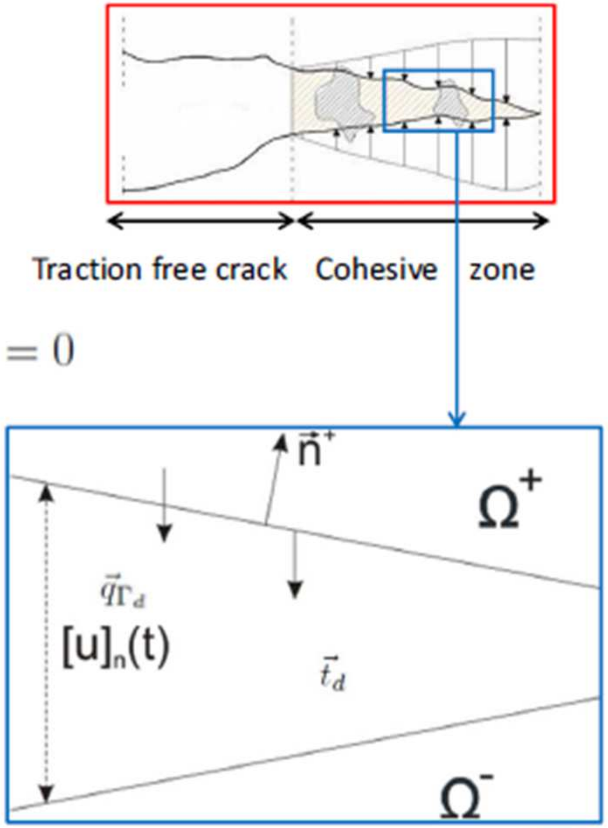

TU/e Technische Universiteit Eindhoven University of Technology

Peel Test with XFEM

❖ *Peel test*

- ❖ *Linearity displacements - time*
- ❖ *Geometry*
- ❖ *Boundary conditions*

Long side: 60 m
Short side: 25 m
Long side: 30 m
Short side: 3 m

Number of elements :
- Rough: 3844
- Medium: 5262
- Smooth: 10148

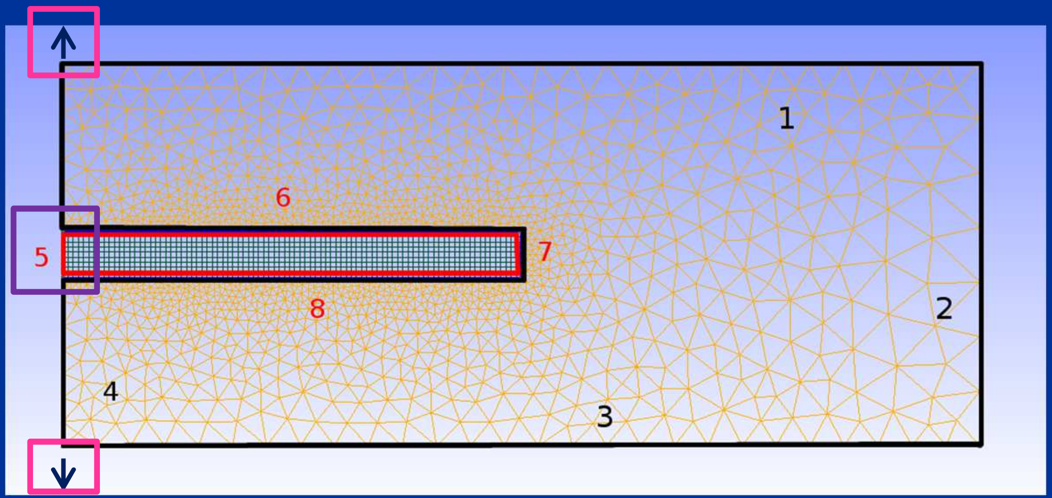

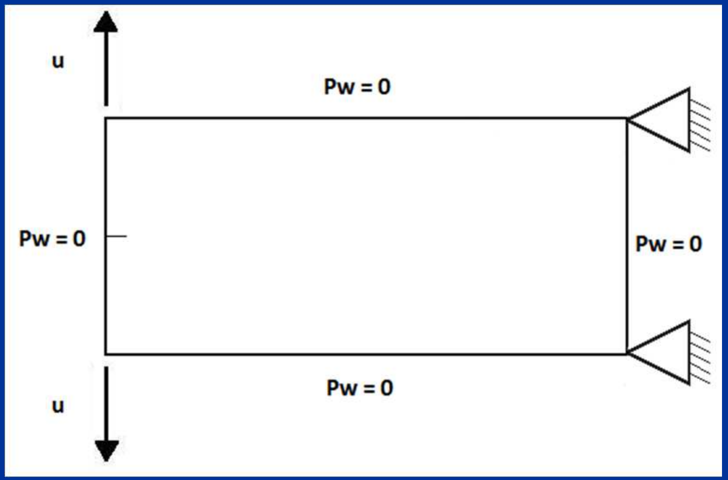

Università degli Studi di Padova

P. Rizzato, 2014

TU/e Technische Universiteit Eindhoven University of Technology

Materials

Peel test

Sedimentary rock: n°1

- $E = 18$ GPa
- $\nu = 0.275$
- $K = 10^{-12}\ mm^2$

Hydraulic Fracturing

Sedimentary rock: n°2

- $E = 37.5$ GPa
- $\nu = 0.275$
- $K = 10^{-11}\ mm^2$

(Mechanical properties taken from: Pariseau, 2006 & Bazant, 2014)

Sandstone

Shale

Università degli Studi di Padova

Technische Universiteit Eindhoven University of Technology

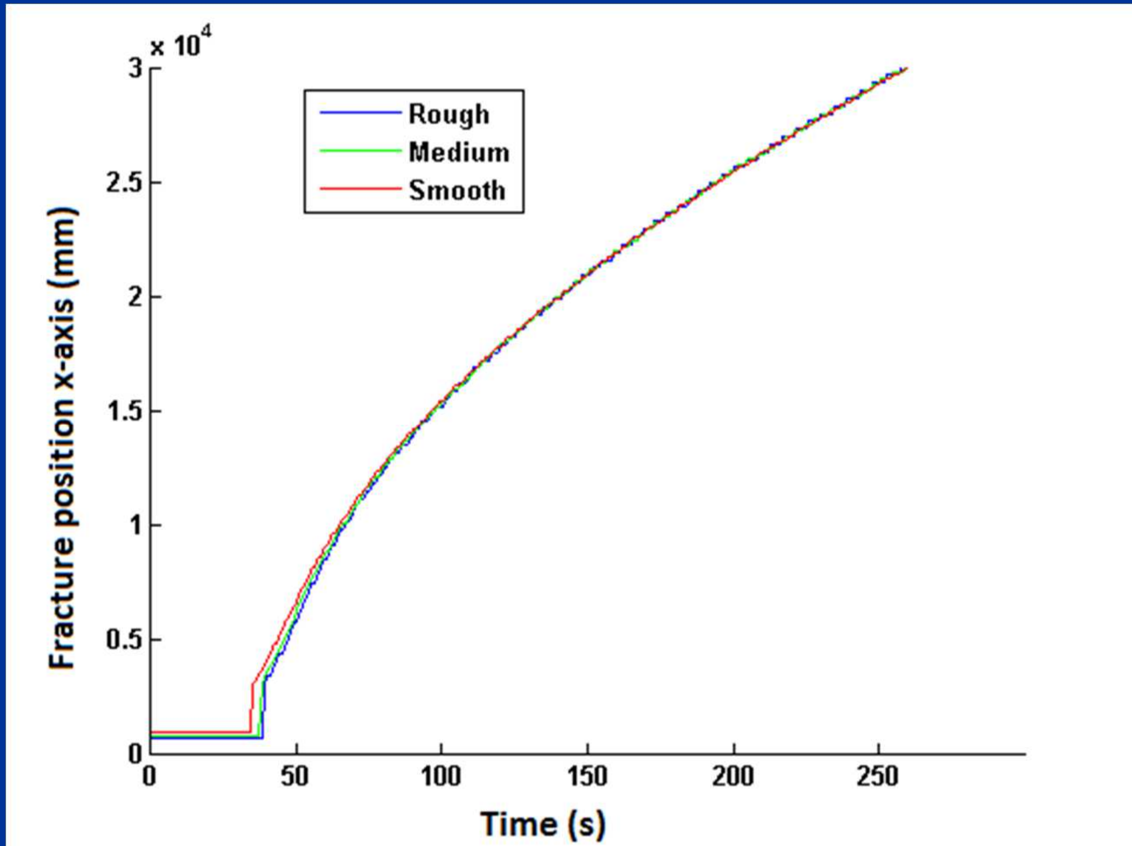

Number of elements :
- Rough: 3844
- Medium: 5262
- Smooth: 10148

- *Apparent mesh independence:*
  - *Initial differences between the 3 meshes, then same trend*
  - *Same fracture tip position for the 3 meshes*
  - ***But rough mesh shows regular steps, fine mesh not***

Università degli Studi di Padova

P. Rizzato, 2014

Technische Universiteit Eindhoven University of Technology

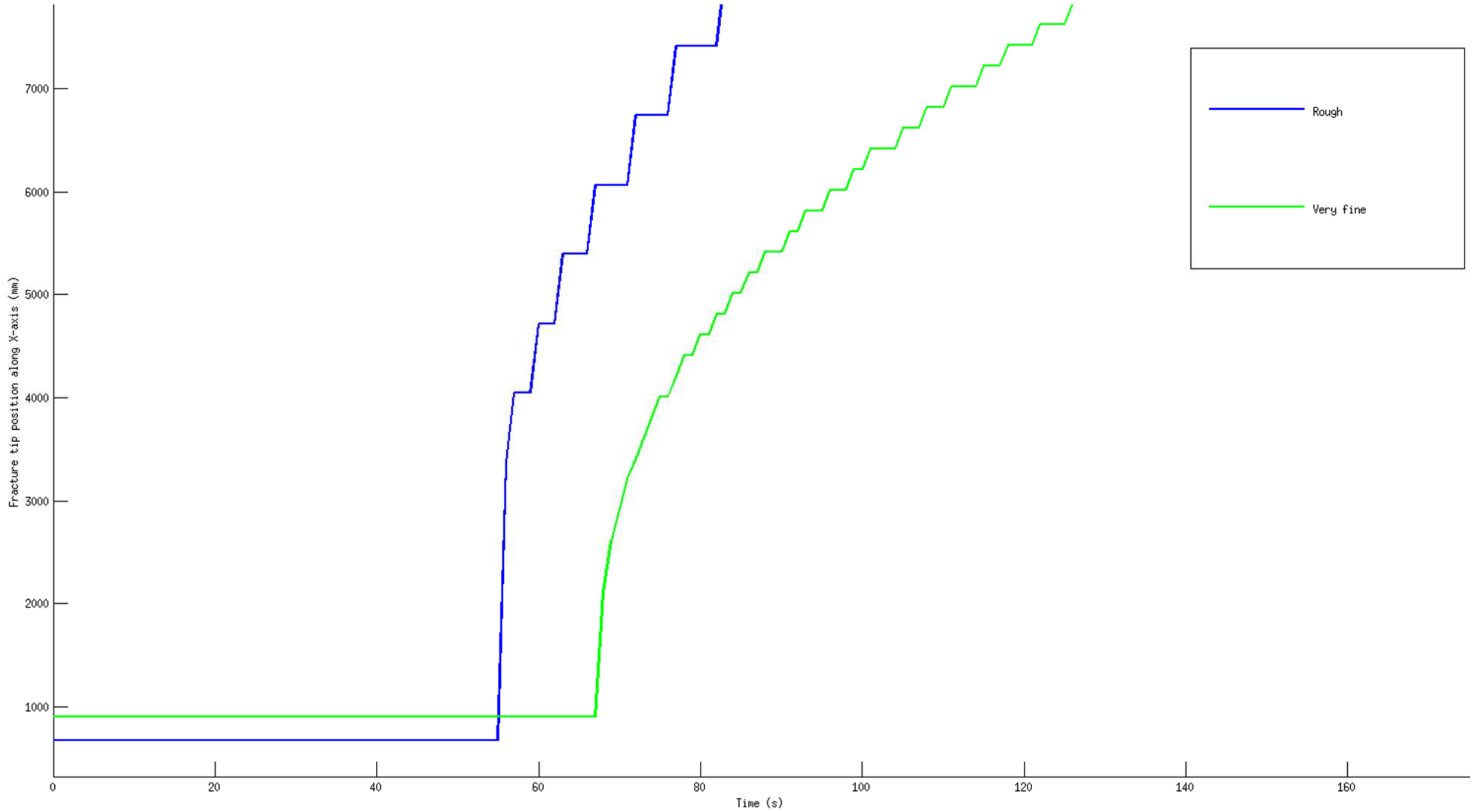

Rough
Very fine
Fracture tip position along X-axis (mm)
Time (s)
1000
2000
3000
4000
5000
6000
7000
0
20
40
60
80
100
120
140
160

❖ Pressure "fluctuation" $\lambda=0.01$

- *mesh: 3844 elements,*
- *Several time steps are elapsed before the fracture passes from one element to the next*
- *Pressure jumps when the fracture passes from one element to the next one*

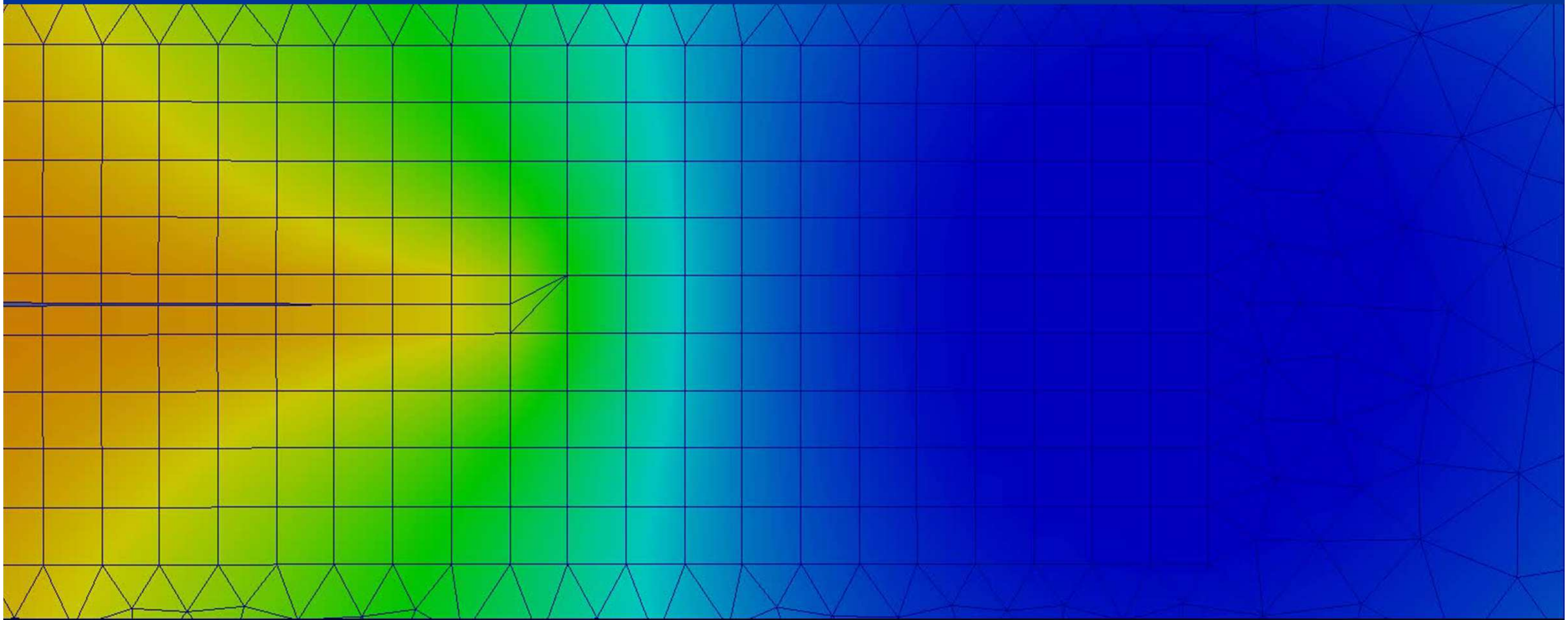

Fluid pressure (MPa)

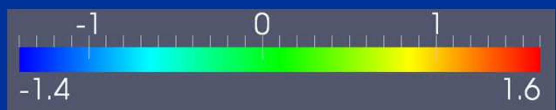

• *Coarse Mesh – standard* XFEM

- Each time there is a flicker a time step is elapsed
- Fracture can only propagate from one element side to the other, i.e. cracks can only fully penetrate elements: the jumps are numerical.
- There is clearly **interference with the crack tip advancement velocity**: everything is blurred

XFEM Mohammadnejad & Khoei, NAG2013

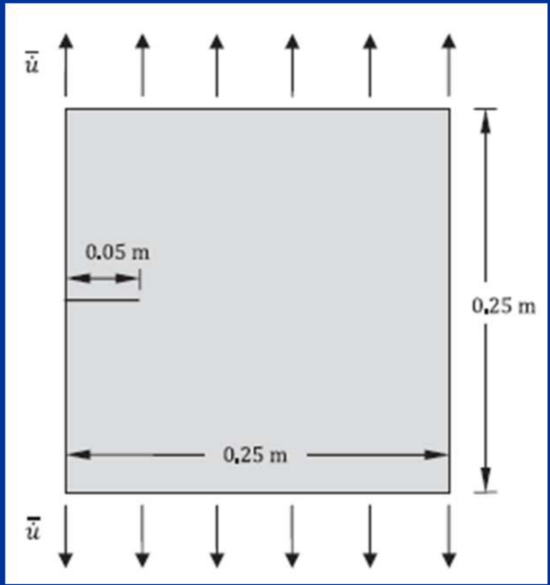

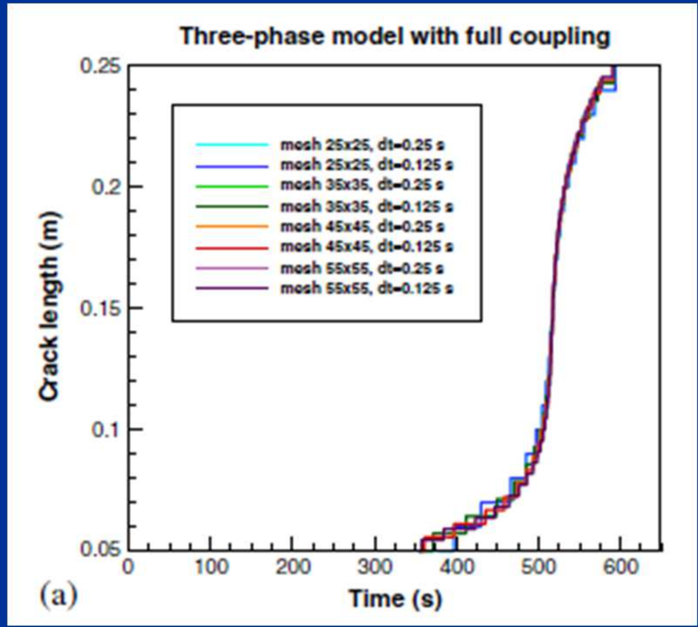

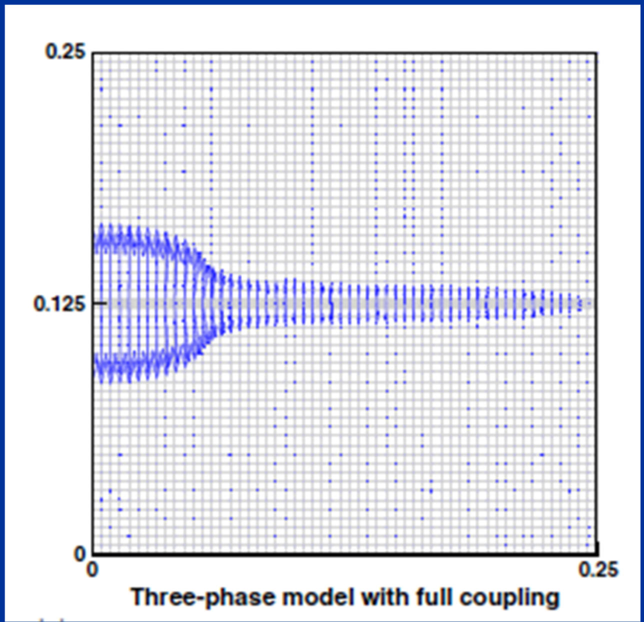

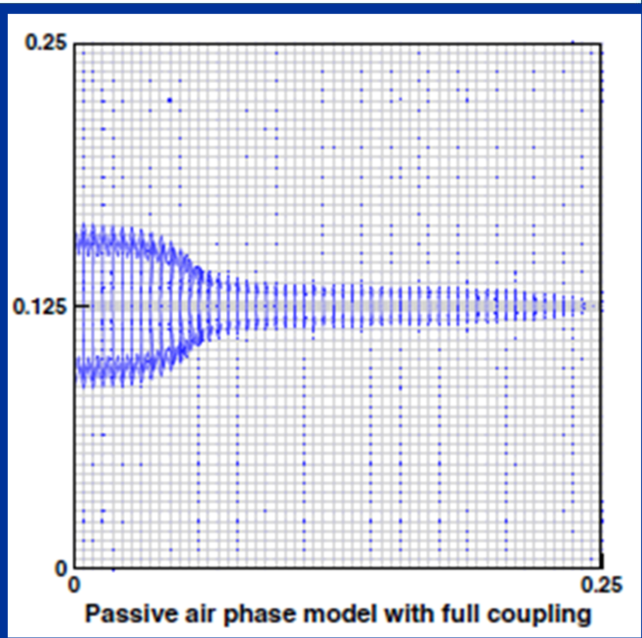

Water pressure gradient distribution

XFEM Mohammadnejad & Khoei, NAG2013

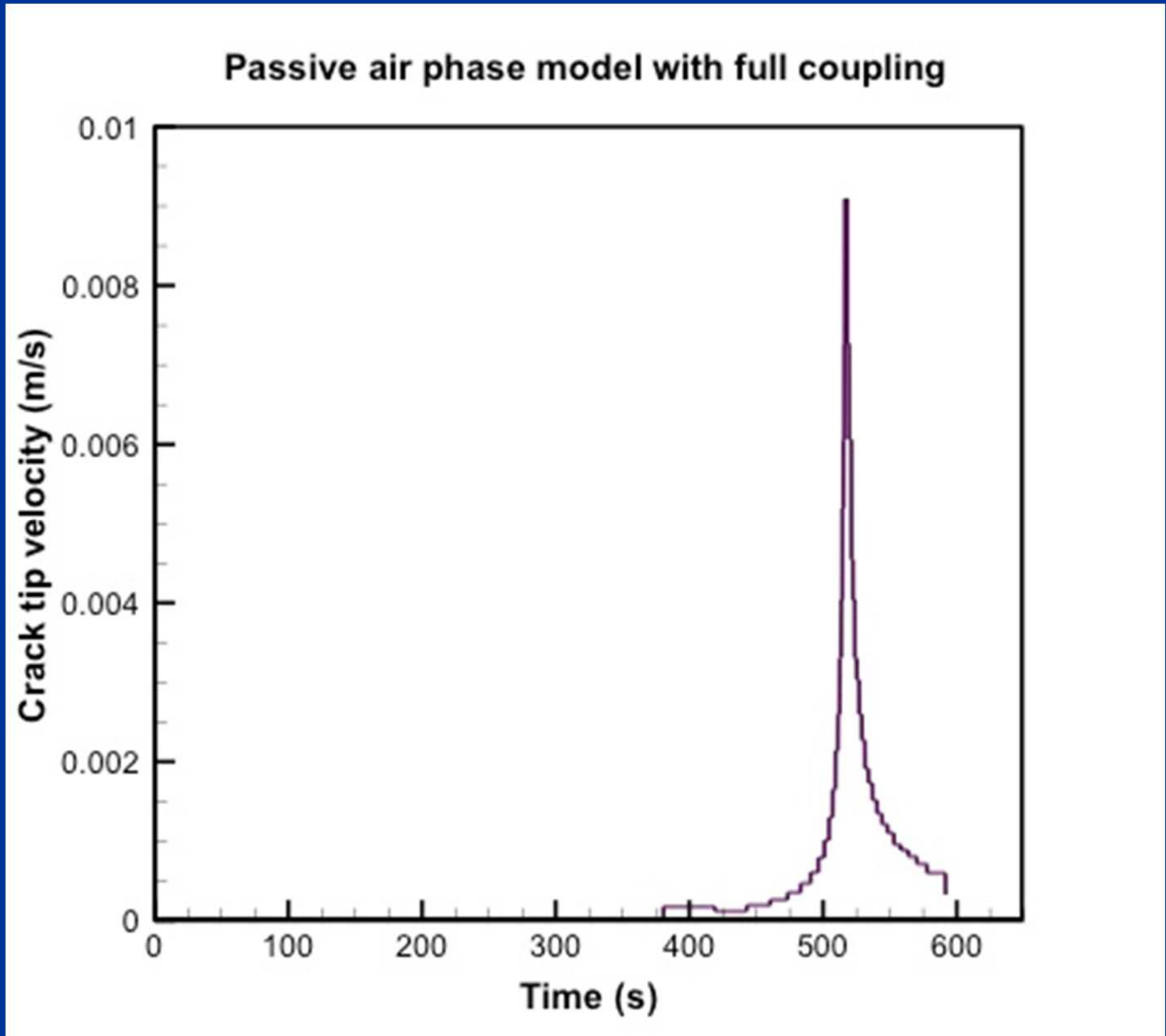

For 55x55 mesh (3025 elements) and time increment of 0.125 s, **minimum and maximum number of time steps needed for the crack to cross one element is 4 and 308 time steps, respectively**

Mohammadnejad, personal com.

❖ Pressure fluctuation λ=0.01

- *mesh: 17702 elements*,
- *Fracture advancement through multiple elements in one time step*
- *Stepwise advancements: fracture advances when tip stress satisfies Rankine criterion after load transfer from fluid*

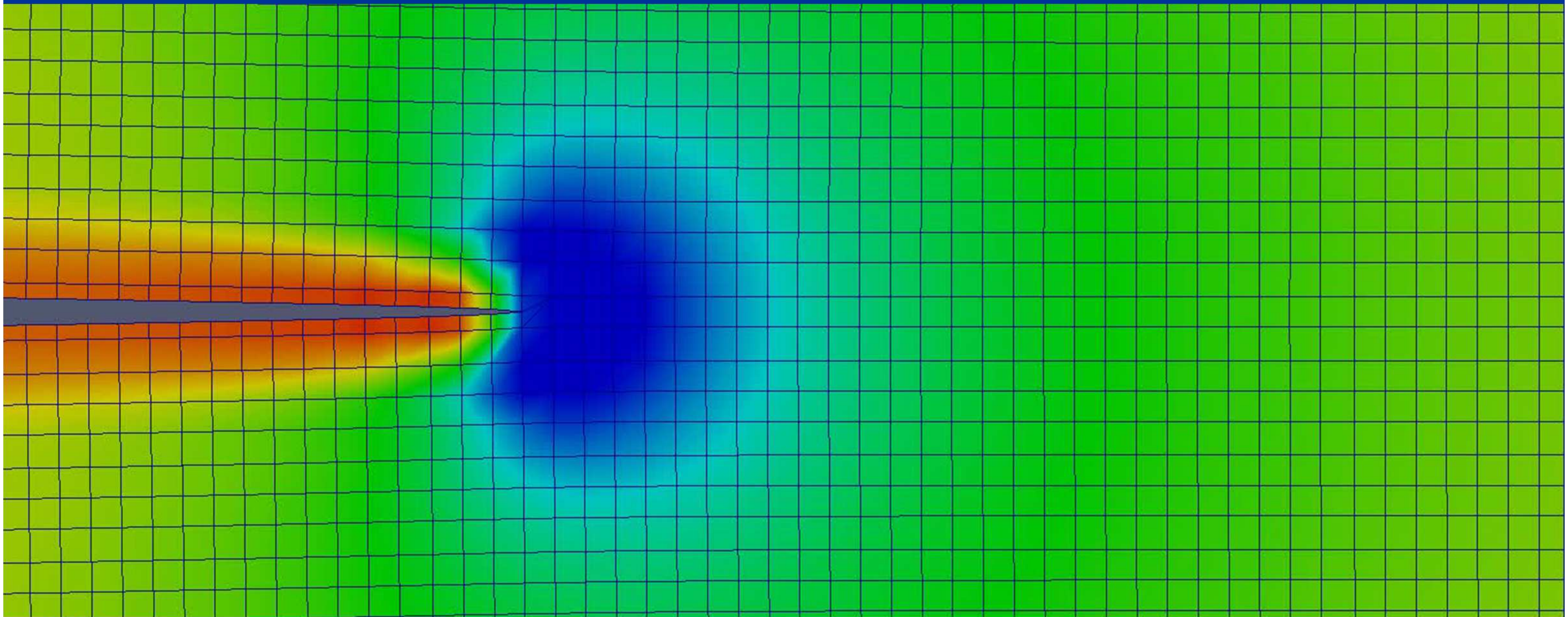

Fluid pressure (MPa)

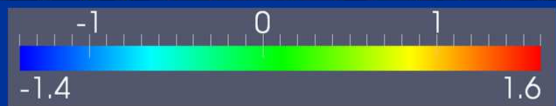

Principal tensile stress fluctuation $\lambda=0.01$

- *mesh: 17702 elements,*
- *Fracture advancement through multiple elements in one time step*
- *Stepwise advancements: fracture advances when tip stress satisfies Rankine criterion after load transfer from fluid*

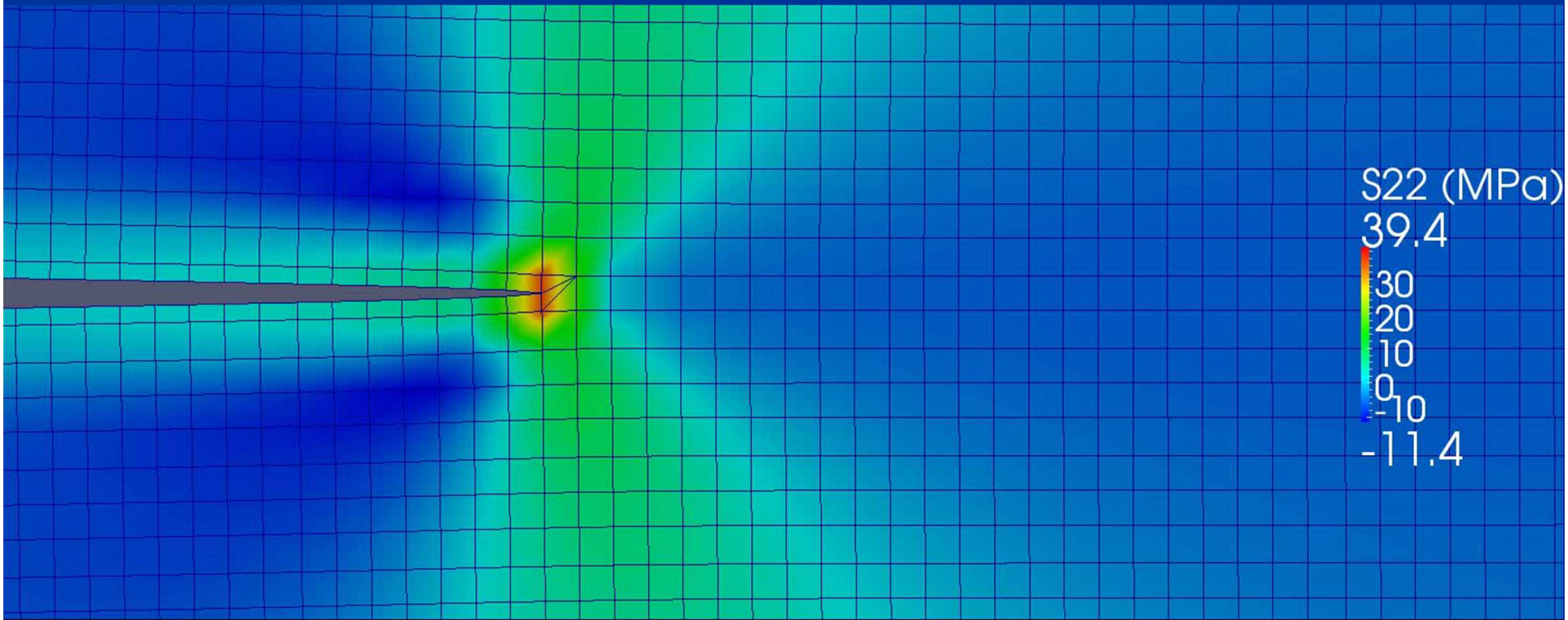

• *Very fine mesh*

- During the “quiescent” period, where fracture does not advance but time runs, consolidation comes into play reducing pressure and increasing the stress; after this period the fracture usually advances over more than one element
- The fracture is free to do what it wants during a time step: **no interference with crack tip advancement speed**, (captures hints of SOC?)
- Pressure and stress distribution is clearly defined

Before the jump

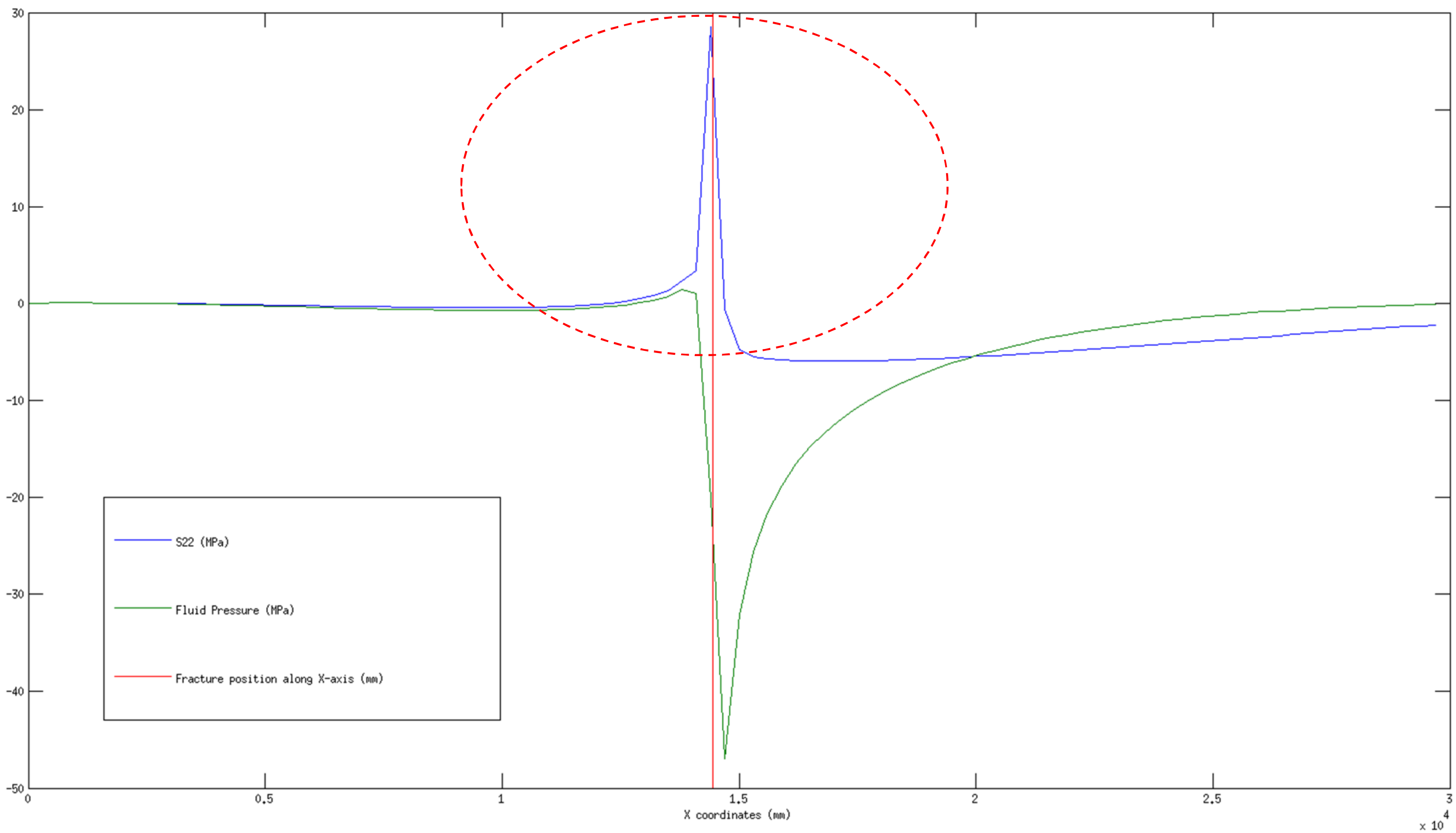

- **Cavitation!**

After the jump

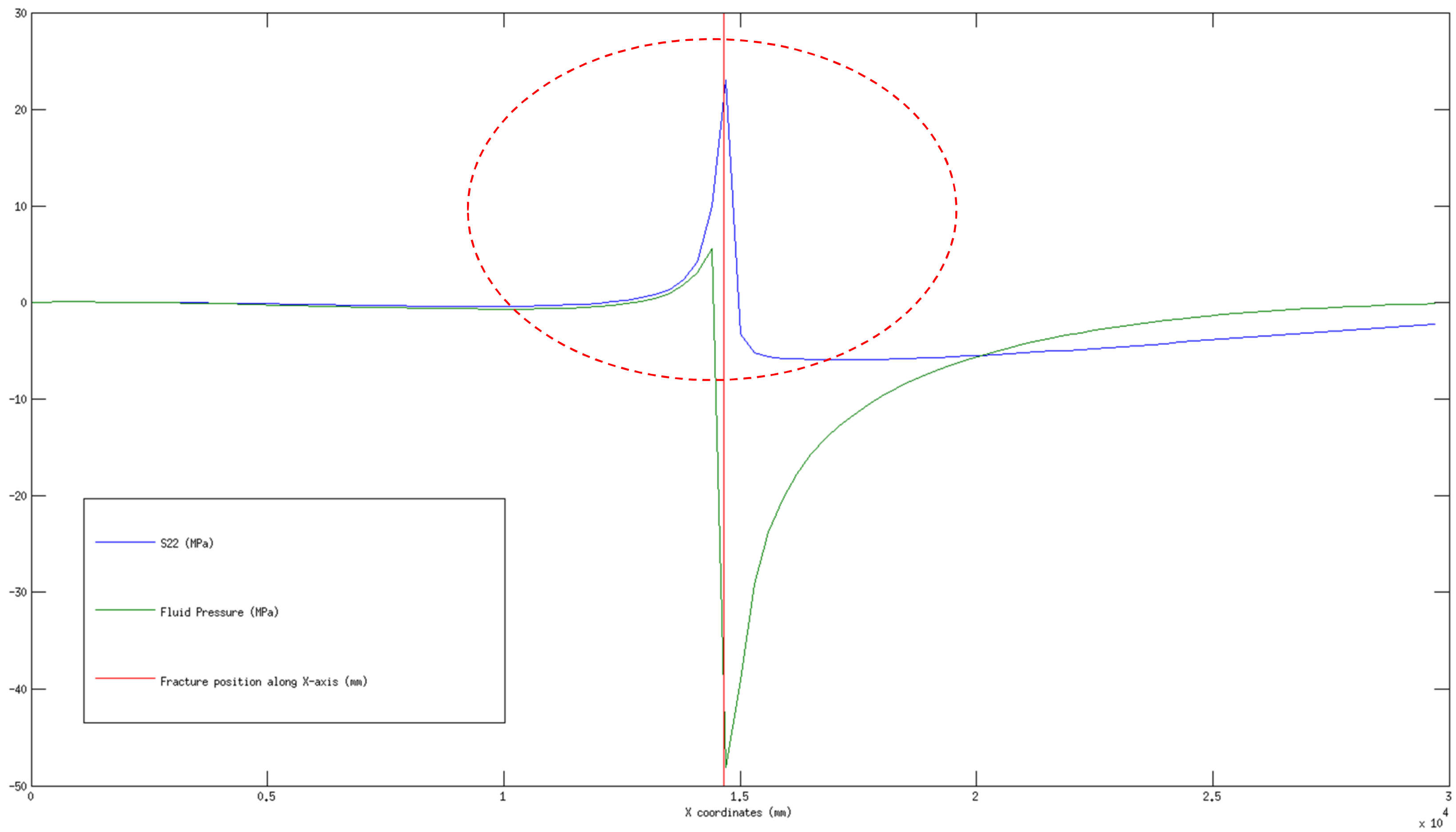

Case study and numerical simulations

- ***Hydraulic Fracturing***
- *Constant fluid inflow*
- *Same geometry of Peel test*
- *Different boundary conditions*

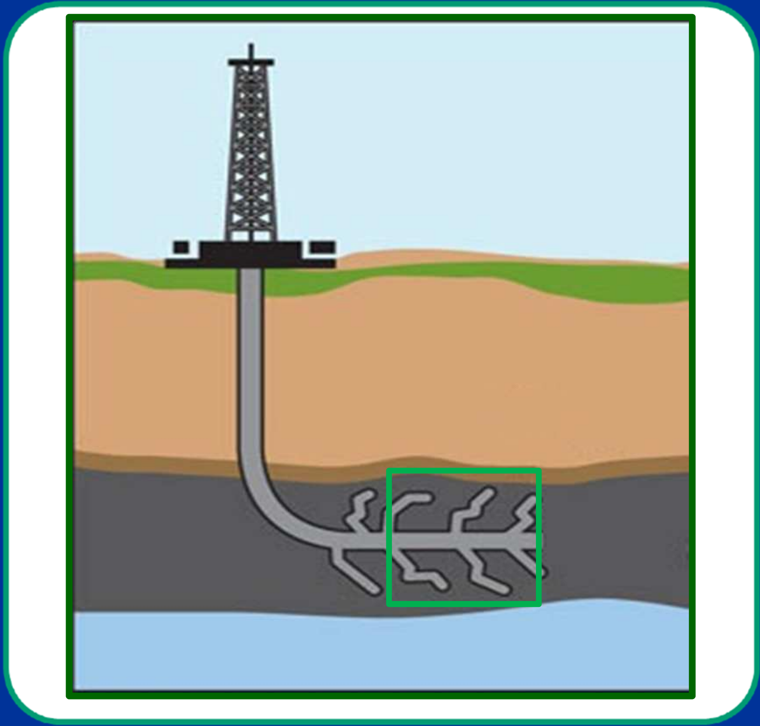

Long side: 60 m
Short side: 25 m
Long side: 30 m
Short side: 3 m

Elements number :
- *Rough: 3844*
- *Medium: 5262*
- *Smooth: 10148*

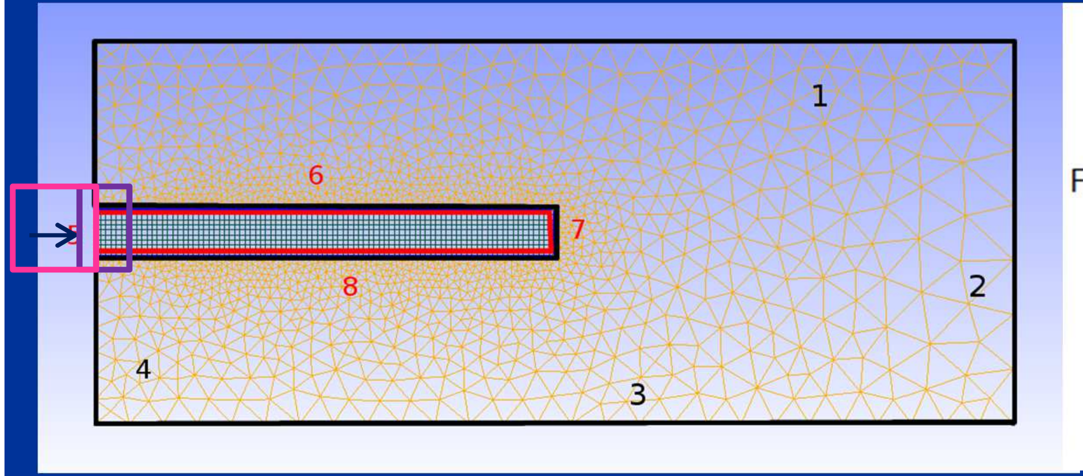

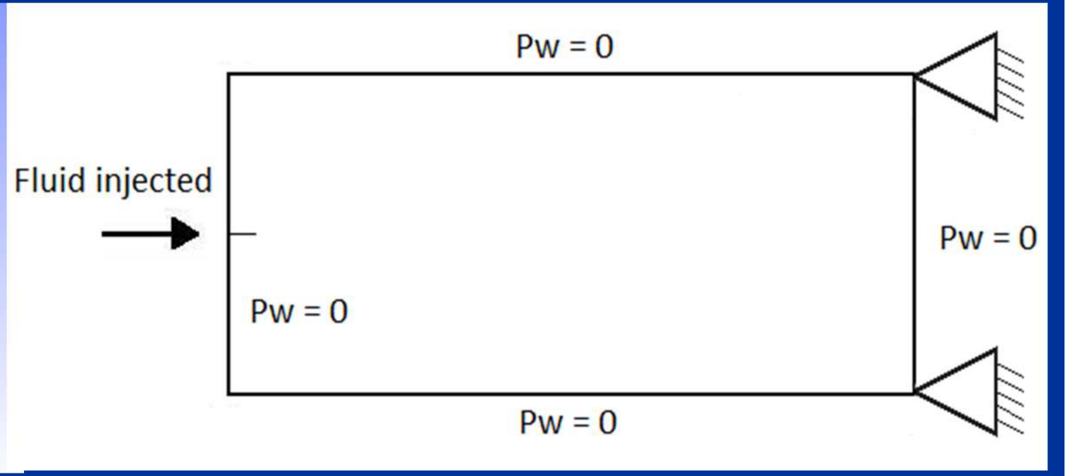

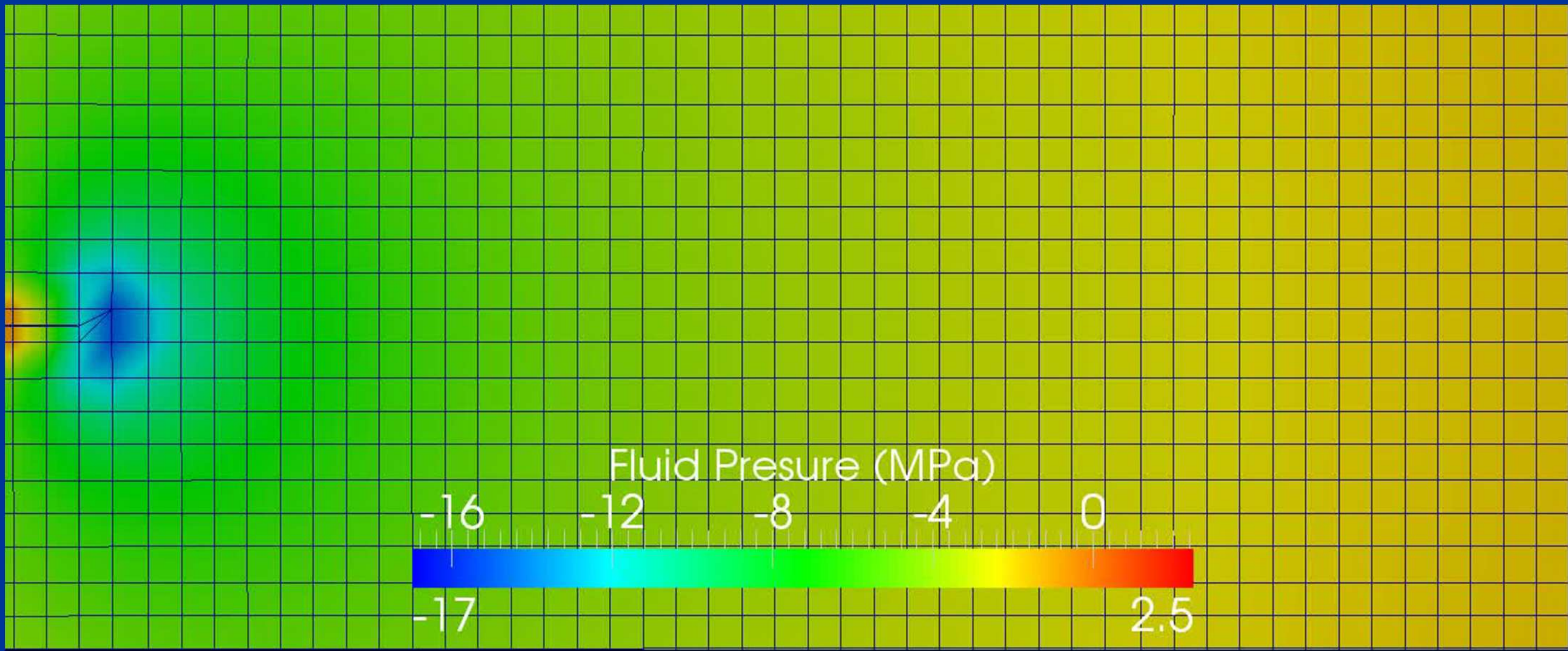

Fluid Presure (MPa)
-16
-12
-8
-4
0
-17
2.5

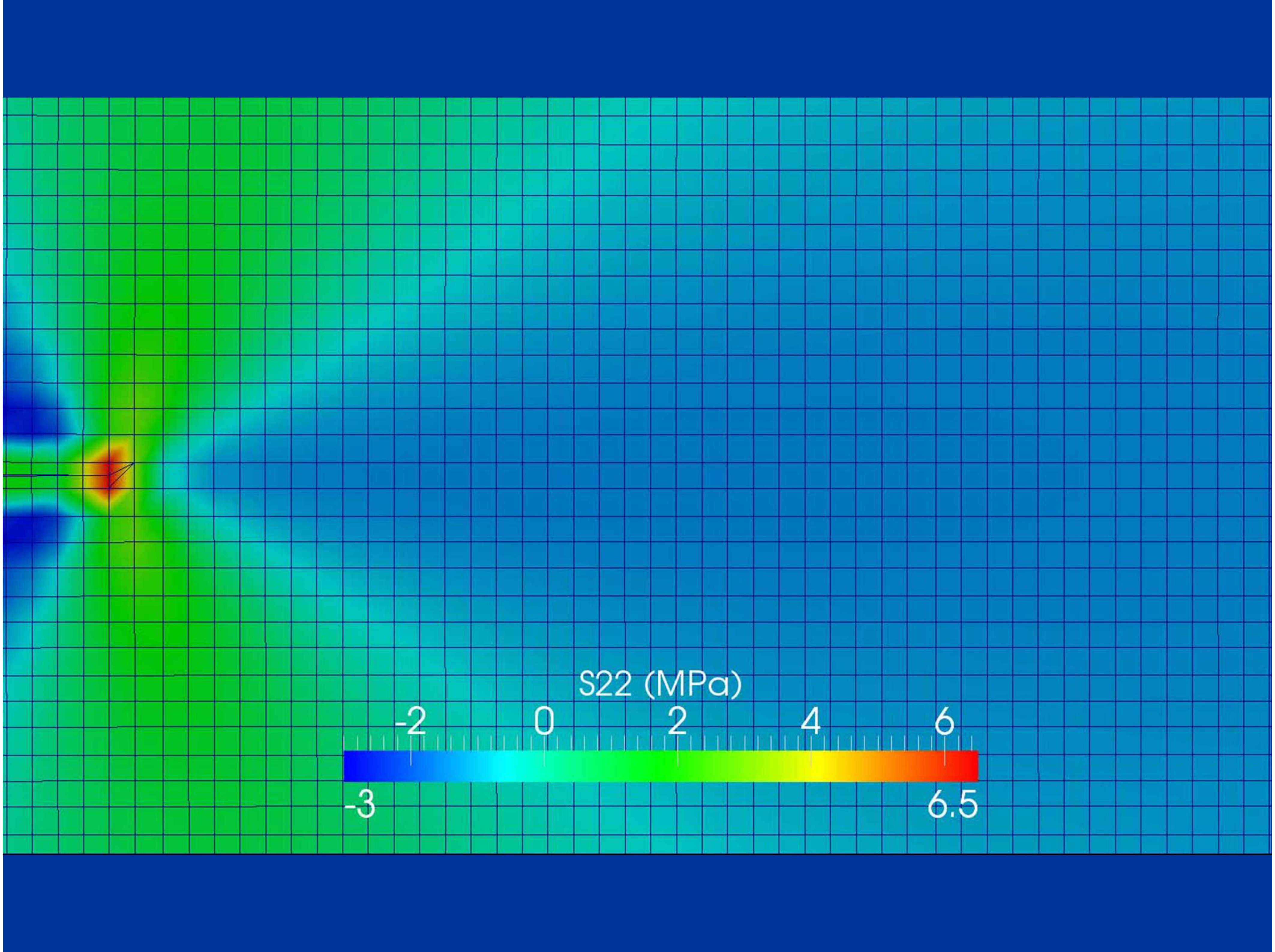
S22 (MPa)
-2
0
2
4
6
-3
6.5

Before the jump

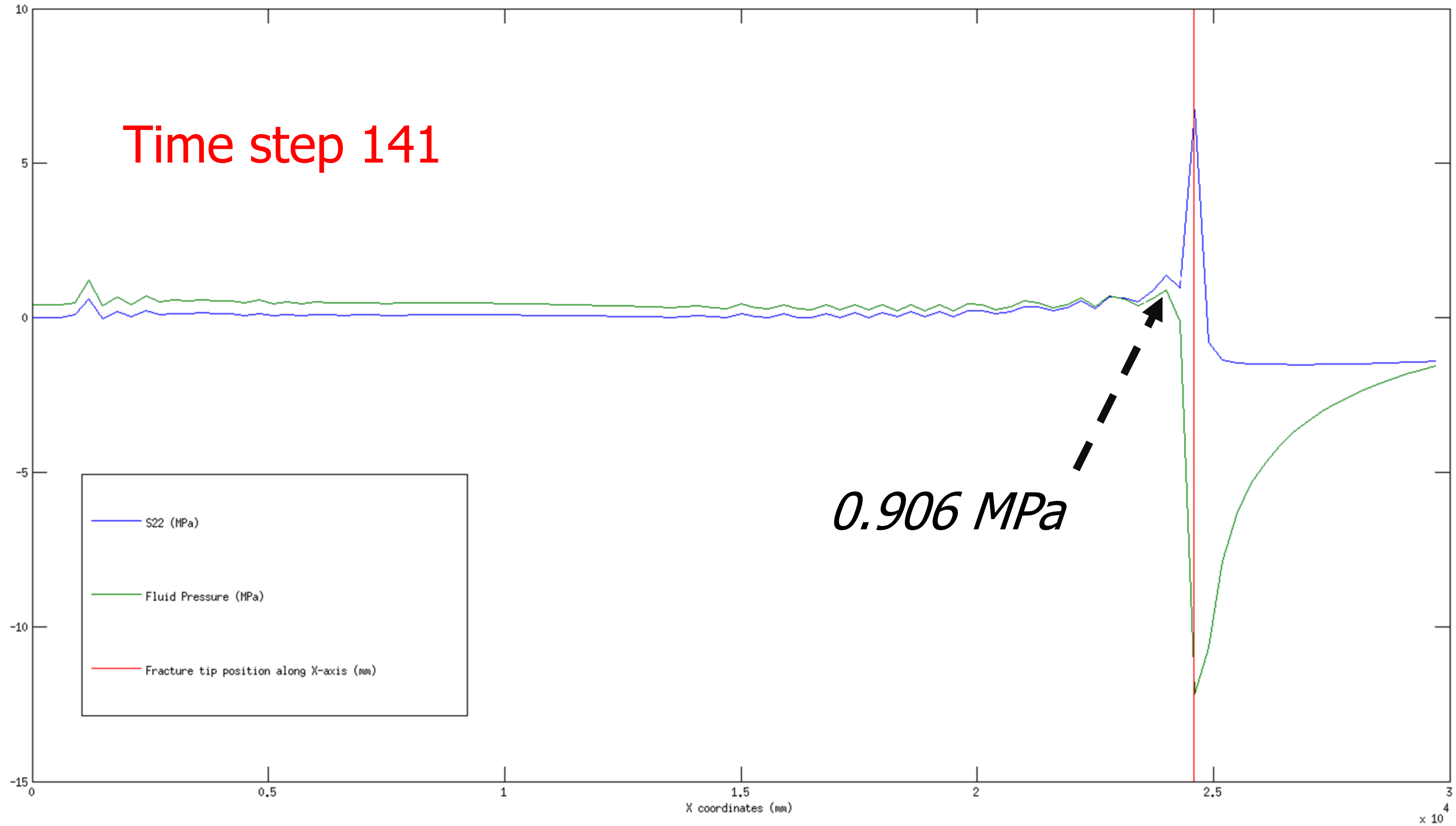

After the jump

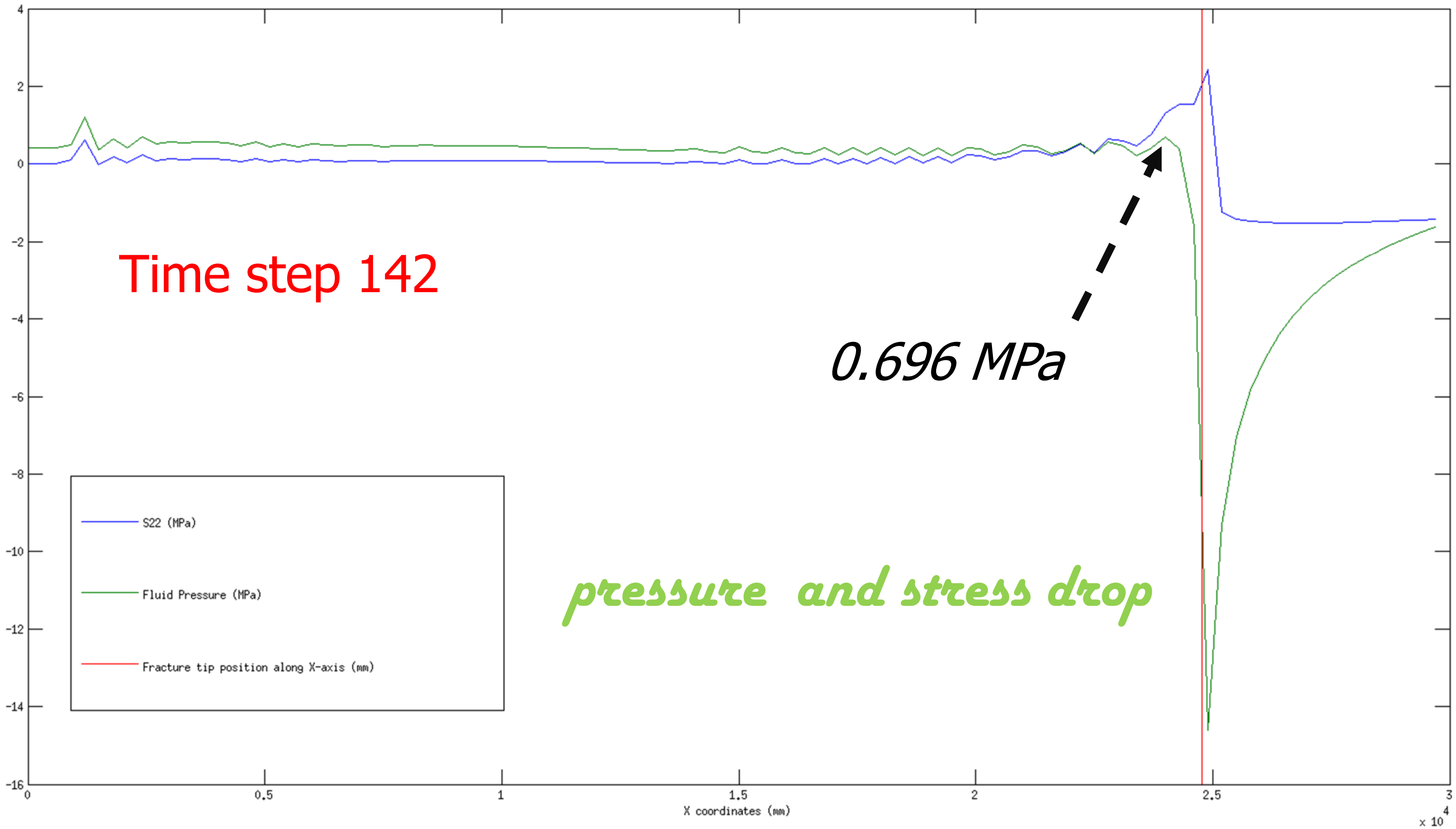

Conclusions 1

- *We have given a clear explanation of stepwise advancement, pressure rise or pressure drop based on meso- and macromechanics. Before there were only partial and sometimes strange explanations around.*
- *Irregular steps are most probably a signature of the real physical behaviour (interaction of three velocities…)**
- *Regular steps seem numerical and are probably linked to the time/crack discretization scheme of XFEM and others*
- *Pressure rise/drop and irregular steps are obtained naturally with SGFEM and appropriate crack advancement algorithm and by XFEM by reducing drastically the element size which downplays the effect of the time/crack discretization scheme .*
- *Large negative pressure peaks are still obtained with XFEM which would require cavitation modeling (two phase flow). But are they always real?*
- *XFEM would require a better enrichment scheme both for solid and fluid fields*

* *"the most elaborate nesting of length scales arises in hydraulic fracturing" (Pearson 1999)*

Conclusions 2

- *To obtain proper stepwise advancement and pressure rise/drop at crack advancement there has to be no interference between the crack advancement speed and the time stepping algorithm: the algorithm has to allow for jumps.*
- *These physical fluctuation are **not** obtained with more time steps per element (usual in XFEM, PUFEM…).They are actually only obtained with XFEM if extremely small elements are used such that the crack can propagate through more elements per time step (jumps) as in SGFEM.*
- *XFEM, PUFEM… are perfectly adapted for engineering problems where the overall picture matters but not so much for problems where new physical insight should be gained (e.g. interfaces).*
- *Next: dynamics and phase change (cavitation) needed.*

Is step-wise advancement relevant for earthquakes? (time scales)

Thank you for your attention